

**PARAGLACIAL REWORKING OF LATERAL MORaine SLOPES,
SHARP-CRESTED LATERAL MORAINES AND ALLUVIAL FANS
BUTTRESSED BY LATERAL MORAINES**

by
Kenneth T. Ash

A thesis submitted in fulfillment of the
requirements of GEOL 4550

for the Degree of Bachelor of Science (Honours)

Department of Geology
Saint Mary's University
Halifax, Nova Scotia, Canada

© K.T. Ash, 2020

April 27, 2020

Members of the Examining Committee:

Dr. Philip Giles (Supervisor)
Department of Geography and Environmental Studies
Saint Mary's University

Dr. Jacob Hanley
Department of Geology
Saint Mary's University

Abstract

Paraglacial Reworking of Lateral Moraine Slopes, Sharp-Crested Lateral Moraines and Alluvial Fans Buttressed by Lateral Moraines

by

Kenneth T. Ash

The ongoing retreat of alpine glaciers has exposed large quantities of glacial sediments prone to paraglacial geomorphic processes. Lateral moraines are key features of these glacial landscapes. Studies on the paraglacial reworking of lateral moraines are rare; consequently, their transformation is relatively undocumented. However, as deglaciation in alpine regions increases the requirement for a fuller understanding of paraglacial response increases as well. This is due to a need to understand the complex geomorphological responses to deglaciation. To document typical examples, analyze the morphological setting and provide an analysis of lateral moraine paraglacial reworking in deglaciating regions of the United States, Canada, Asia, Afghanistan, Argentina and Switzerland, analysis ready data from GIS software packages was utilized. Paraglacial adjustment is evident through the development of gullying, primarily on the proximal moraine slope. Gully slope and length increase with moraine height. The proximal slope had a steeper angle of repose compared to the distal slope. The erosional activity as well as the more or less in activity is a reflection of slope stability. Sharp-crested lateral moraines were defined within the context of slope profile and captured within selected regions. Extensive paraglacial modification by debris flows was limited to sections of the glacial valley where valley wall slopes gradients are steep. The slope profile of moraines, with a gentler lower slope, an intense gullied upper section and a sediment deposit at the bottom of the proximal slope was more prevalent towards the glacier terminus. There, moraines are either devoid of vegetation colonization or vegetation colonies are well established. Up-glacier moraines have little or no distal slope and are devoid of vegetation on both slopes. The general form of the moraines establishes that there are many feedbacks, between position and geomorphic activity on a moraine, that influence the paraglacial process.

April 27, 2020

Acknowledgements

First and foremost, I hereby greatly thank and express my special regards to Dr. Philip Giles (Supervisor), Professor, Department of Geography and Environmental Studies, for providing me with this opportunity. Furthermore, I express my gratitude for his help and engagement in helping me write this thesis and for introducing me to this very interesting topic.

Additionally, I would like to thank Dr. Jacob Hanley (second examiner), Chairperson, Department of Geology, for stepping forward in the eleventh-hour to take on the position of second examiner, during such a troubling time.

I would like to thank Dr. Steven Smith, Dean of Science, Dr. Pierre Jutras and Jacob Hanley, Geology Departmental Chairpersons and Dr. Philip Giles, Professor, for their collaborative spirit which allowed me to pursue this thesis. This cooperative mindset provided the supportive environment that was essential not only to my success, but to the success of Saint Mary's University as a whole.

Last but not least I would like to express my sincere appreciation to my family. My spouse Marlene for her patience and support. My son Ryan for his deep appreciation of the English language and my daughter Natalie for her deep appreciation for working with technical documents in Microsoft Word.

Table of Contents

| | |
|---|-----|
| Abstract | ii |
| Acknowledgements | iii |
| List of Tables | v |
| List of Figures | vi |
| | |
| Chapter 1 Introduction..... | 1 |
| Chapter 2 Description of Study Sites and Data | 19 |
| Chapter 3 Paraglacial Reworking of Lateral Moraines | 33 |
| Chapter 4 Alluvial Fans and Debris Flow Fans Buttressed by Lateral Moraines | 54 |
| Chapter 5 Conclusion | 69 |
| | |
| List of References | 74 |
| | |
| Appendix Images of Study Sites | 77 |

List of Tables

| | |
|---|----|
| Table 2.1: Initial 59 Sites Identified for Possible Inclusion | 21 |
| Table 2.2: Sites and Preliminary Data | 23 |
| Table 2.3: Image Data..... | 26 |
| Table 2.4: Study Sites | 32 |
| | |
| Table 3.1: Moraine Profiles | 36 |
| Table 3.2: Moraine Site Particulars | 37 |
| Table 3.3: Morphological Details of Gullies | 40 |

List of Figures

| | |
|--|----|
| Figure 1.1: Global Alpine Glacier Annual Mass Balance | 1 |
| Figure 1.2: Photo of Glaciers in Southern Alaska and Canada | 3 |
| Figure 1.3: Example of an Asymmetrical Lateral Moraine | 5 |
| Figure 1.4: Examples of Lateral Moraines | 6 |
| Figure 1.5: Typical Fan Deposits Buttressed by a Lateral Moraine | 7 |
| | |
| Figure 2.1: Mercator Map with Shaded Relief of Site ID 051 (Donjek Glacier) Created using CALTOPO Software | 28 |
| Figure 2.2: Example of the Trimble SketchUp File for a Section of Study Site ID 007 (Otter Glacier)..... | 29 |
| Figure 2.3: Examples of the Output Data from CALTOPO for Study Site ID 004 (Glacier Creek) | 30 |
| | |
| Figure 3.1: Moraine Setting Graphic Illustration | 39 |
| Figure 3.2: Moraine Morphological Features | 41 |
| Figure 3.3: Moraine Lateral Slope vs. Glacier Lateral Slope | 42 |
| Figure 3.4: Lateral Moraine Profiles (Up-Glacier, Mid-Glacier and Down Glacier) for Study Site ID 029 – Roovers Glacier, BC | 43 |
| Figure 3.5: Lateral Moraine Profiles (Up-Glacier, Mid-Glacier and Down Glacier) for Study Site ID 033 – Mount Waddington, BC | 44 |
| Figure 3.6: Cross Valley Asymmetry in the Down Glacier Section on Study Site ID 055 – Easton Glacier Proximal Side | 45 |
| Figure 3.7: Gully Length vs. Moraine Height | 47 |
| Figure 3.8: Gully Slope vs. Moraine Height..... | 48 |
| Figure 3.9: Gully Width vs. Moraine Height | 49 |
| Figure 3.10: Photos Capture in Google Earth, of the Gullied Lateral Moraine of Study Site ID 057 (Vadret da Tschierva, Grisons) | 51 |
| Figure 3.11: Increased Gully Activity at a Change in Lateral Morainic Trough Path from Study Site ID 048 (Nagong, China) | 52 |
| Figure 3.12: Ecosystem Engineering and Unbound Solifluction Processes Dominant from Study Site ID 007 (Otter Glacier) | 53 |

| | |
|---|----|
| Figure 4.1: Example of a Glacial Valley with Alluvial Fans and Debris Flow Fans Buttressed by a Lateral Moraine Study Site ID 032 (Dorothy Glacier)..... | 55 |
| Figure 4.2: Example of Fans Buttressed by the Lateral Moraine from Study Site ID 041 (Afghanistan) | 56 |
| Figure 4.3: Example of a Fan Buttressed by the Lateral Moraine from Study Site ID 041 (Afghanistan) | 57 |
| Figure 4.4: Example of a Fan Buttressed by the Lateral Moraine from Site ID 046 (Shkuk Yoz Glacier) | 57 |
| Figure 4.5: Photos of Study Site ID 051 (Donjek Glacier)..... | 59 |
| Figure 4.6: Example of a Disconnected Section of the Lateral Moraine in way of a Debris Flow from Study Site ID 054 (Findelengletscher Glacier) | 61 |
| Figure 4.7: Example of an Engulfed Section of the Lateral Moraine in way of a Debris Flow from Study Site 050 (Tiedemann Glacier) | 62 |
| Figure 4.8: Example of a Fans buttressed by the Lateral from Study Site ID 041 (Afghanistan) | 63 |
| Figure 4.9: Example of a Fan Buttressed by the Lateral Moraine with Incised Gullying from Study Site ID 048 (Nagong, China)..... | 64 |
| Figure 4.10: Example of the Earlier Stages of Gullying Prior to Vegetation Colonization from Study Site ID 046 (Shkuk Yoz Glacier) | 65 |
| Figure 4.11: Example of the Fluvial Component of a Debris Flow from Study Site ID 041 (Afghanistan) | 65 |
| Figure 4.12: Example of a Stagnant Pool at the Base of a Fan Cone from Study Site ID 041 (Afghanistan) | 66 |
| Figure 4.13: Example of Incised Gullying at a Restriction in the Lateral Morainic Trough from Study Site ID 048 (Nagong, China) | 67 |
| | |
| Figure A.1a: Study Site ID 022 (Exploradores Glacier) Mercator Map | 78 |
| Figure A.1b: Study Site ID 022 (Exploradores Glacier) Photos | 79 |
| Figure A.2a. Study Site ID 021 (Ventisquero Grosse) Mercator Map | 80 |
| Figure A.2b: Study Site ID 021 (Ventisquero Grosse) Terrain Models and Photos | 81 |
| Figure A.3a: Study Site ID 007 (Otter Glacier) Mercator Map | 82 |
| Figure A.3b: Study Site ID 007 (Otter Glacier) Mercator Map and Terrain Models | 83 |
| Figure A.4a: Study Site ID 009, 010, and 011 (Mantanuska) Mercator Map | 84 |

| | |
|--|-----|
| Figure A.4b: Study Site ID 009, 010, and 011 (Mantanuska) Terrain Models and Photos | 85 |
| Figure A.5a: Study Site ID 004 (Glacier Creek) Mercator Map | 86 |
| Figure A.5b: Study Site ID 004 (Glacier Creek) Mercator Map and Terrain Models | 87 |
| Figure A.6a: Study Site ID 006 (Fairweather Glacier) Mercator Map | 88 |
| Figure A.6b: Study Site ID 006 (Fairweather Glacier) Terrain Models | 89 |
| Figure A.7a: Study Site ID 055 (Easton Glacier) Mercator Map | 90 |
| Figure A.7b: Study Site ID 055 (Easton Glacier) Terrain Model and Photos | 91 |
| Figure A.8a: Study Site ID 033 (Mount Waddington A) Mercator Map | 92 |
| Figure A.8b: Study Site ID 033 (Mount Waddington A) Terrain Models and Photos | 93 |
| Figure A.9a: Study Site ID 050 (Tiedemann Glacier) Mercator Map | 94 |
| Figure A.9b: Study Site ID 050 (Tiedemann Glacier) Terrain Models | 95 |
| Figure A.10a: Study Site ID 051 (Donjek Glacier) Mercator Map | 96 |
| Figure A.10b: Study Site ID 051 (Donjek Glacier) Photos | 97 |
| Figure A.11a: Study Site ID 028 (Bell Glacier) Mercator Map | 98 |
| Figure A.11b: Study Site ID 028 (Bell Glacier) Terrain Model and Photo | 99 |
| Figure A.12a: Study Site ID 029 (Roovers Glacier) Mercator Map | 100 |
| Figure A.12b: Study Site ID 029 (Roovers Glacier) Terrain Models and Photo | 101 |
| Figure A.13a: Study Site ID 030 (Geddes Glacier) Mercator Map | 102 |
| Figure A.13b: Study Site ID 030 (Geddes Glacier) Terrain Model | 103 |
| Figure A.14a: Study Site ID 032 (Dorothy Glacier) Mercator Map | 104 |
| Figure A.14b: Study Site ID 032 (Dorothy Glacier) Terrain Model and Photo | 105 |
| Figure A.15a: Study Site ID 048 (Nagong, China) Mercator Map | 106 |
| Figure A.15b: Study Site ID 048 (Nagong, China) Terrain Models | 107 |
| Figure A.16a: Study Site ID 034 (Mount Everest) Mercator Map | 108 |
| Figure A.16b: Study Site ID 034 (Mount Everest) Terrain Models and Photos | 109 |
| Figure A.17a: Study Site ID 056 (Mount Everest - 2) Mercator Map | 110 |
| Figure A.17b: Study Site ID 056 (Mount Everest - 2) Terrain Models and Photo | 111 |
| Figure A.18a: Study Site ID 012 (Tamdykul Mountain) Mercator Map | 112 |
| Figure A.18b: Study Site ID 012 (Tamdykul Mountain) Mercator Map and Photos | 113 |
| Figure A.19a: Study Site ID 041 (Afghanistan) Mercator Map and Terrain Model | 114 |

| | |
|---|-----|
| Figure A.19b: Study Site ID 041 (Afghanistan) Terrain Models | 115 |
| Figure A.20a: Study Site ID 046 (Shkuk Yoz Glacier) Mercator Map | 116 |
| Figure A.20b: Study Site ID 046 (Shkuk Yoz Glacier) Terrain Models | 117 |
| Figure A.21a: Study Site ID 036 (Karakoram Range) Mercator Map | 118 |
| Figure A.21b: Study Site ID 036 (Karakoram Range) Terrain Model | 119 |
| Figure A.22a: Study Site ID 040 (Karakoram Range - 2) Mercator Map | 120 |
| Figure A.22b: Study Site ID 040 (Karakoram Range -2) Terrain Models | 121 |
| Figure A.23a: Study Site ID 045 (Lupghar Yaz Glacier) Mercator Map | 122 |
| Figure A.23b: Study Site ID 045 (Lupghar Yaz Glacier) Terrain Models and Photo | 123 |
| Figure A.24a: Study Site ID 054 (Findelengletscher Glacier) Mercator Map | 124 |
| Figure A.24b: Study Site ID 054 (Findelengletscher Glacier) Terrain Models and Photos | 125 |
| Figure A.25a: Study Site ID 057 (Vadret da Tschierva, Grisons) Mercator Map | 126 |
| Figure A.25b: Study Site ID 057 (Vadret da Tschierva, Grisons) Terrain Models and Photos | 127 |
| Figure A.26a: Study Site ID 052 (Fee Glacier) Mercator Map | 128 |
| Figure A.26b: Study Site ID 052 (Fee Glacier) Terrain Models | 129 |
| Figure A.27a: Study Site ID 053 (Tsidjiore Nouve). Mercator Map and Photo | 130 |
| Figure A.27b: Study Site ID 053 (Tsidjiore Nouve) Terrain Models | 131 |
| Figure A.28a: Study Site ID 058 (Vadret Pers dams) Mercator Map | 132 |
| Figure A.28b: Study Site ID 058 (Va dret Pers dams) Terrain Models and Photos | 133 |
| Figure A.29a: Study Site ID 059 (Vadret da Tschierva, Grisons) Mercator Map | 134 |
| Figure A.29b: Study Site ID 059 (Vadret da Tschierva, Grisons) Terrain Models | 135 |

Chapter 1

Introduction

1.1 Trend Towards Deglaciation

The World Glacier Monitoring Service (WGMS) tracks changes in alpine glaciers worldwide. The WGMS mass balance behavior provides a global index for alpine glacier terminus behavior. Figure 1.1 shows mass balance of over 40 reference glaciers each year since 1980 (grey bars), along with the total mass loss over time (red line). According to the Arndt (2019), the mean annual glacier mass balance was -951 mm for all glaciers monitored in 2017.

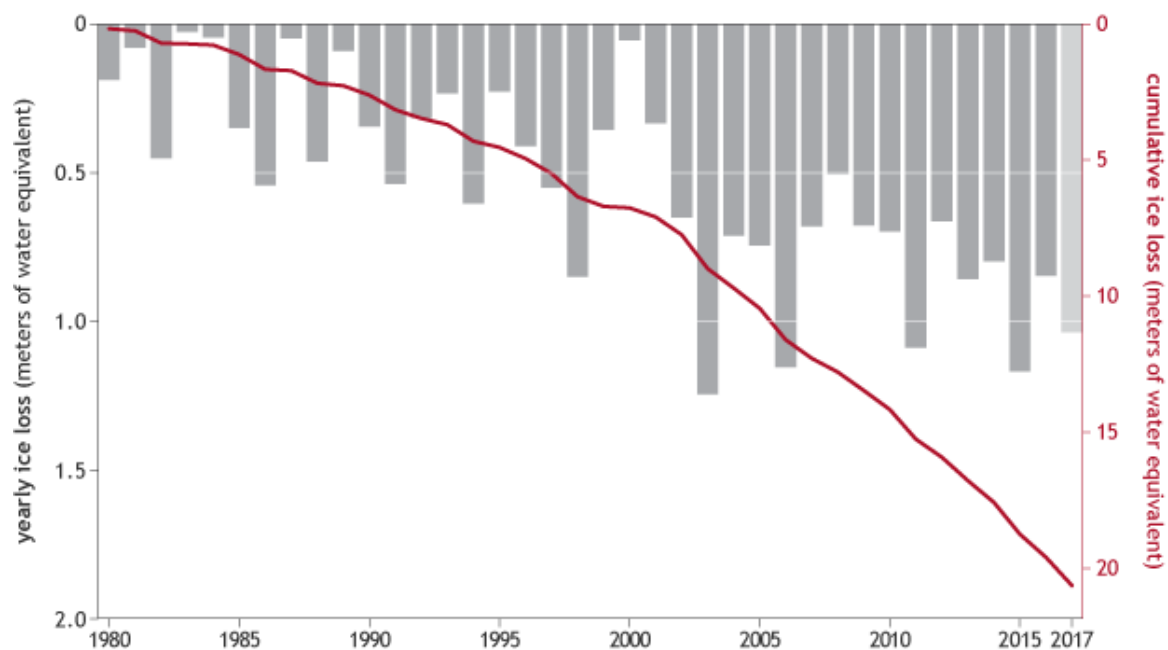


Figure 1.1: Global Alpine Glacier Annual Mass Balance.
Reproduced from State of the Climate in 2018. Bulletin American Meteorological Society.

The cumulative mass balance from 1980 to 2018 was -21.7 m. The decadal mean annual mass balance was -228 mm yr^{-1} in the 1980s, -443 mm yr^{-1} in the 1990s, -676 mm yr^{-1} for the 2000s, and -921 mm yr^{-1} for 2010–18. This reveals that alpine glacier retreat has been dominant for several decades and that the melting and subsequent retreat of glaciers has accelerated since

2000. Zemp et al. (2020) suggested that glacier retreat reflects sustained negative mass balances in recent years. Pelto (2018) suggested that the increasing rate of glacier mass loss during a period of retreat indicates that alpine glaciers are not approaching equilibrium and retreat will continue to be the dominant terminus response. This distinct trend toward glacier retreat offers an opportunity to study the landform modifications as the exposed landscapes of deglaciation become susceptible to new patterns of remobilization in their new conditioning environment.

1.1.1 Paraglacialiation in Terms of Geomorphology

The storage and flux of sediments represent an increasingly important subject for contemporary geomorphological study. This heightened geomorphological activity is termed *paraglacial*. Church and Ryder (1972, p. 3059) defined this term as: ‘nonglacial processes that are directly conditioned by glaciation’. Ballantyne (2002, p. 1938) proposed a broader definition of paraglacial: ‘nonglacial earth-surface processes, sediment accumulations, landforms, land systems and landscapes that are directly conditioned by glaciation and deglaciation’. This revised definition captures both the processes and the resultant landforms, landscapes and land systems. Figure 1.2 is a photo of a typical deglaciating landscape that is exemplary of this revised definition of paraglacial. Investigation of the paraglacial response to deglaciation in alpine environments is relatively understudied. However, as deglaciation in alpine regions increases the requirement for a more complete understanding of paraglacial response becomes necessary. This is due to both a need to understand the complex responses to deglaciation and to assess any potential impacts on, or from, human activities in alpine areas. Knight and Harrison (2009, p.

230) state that ‘paraglaciation will become the most significant process controlling sediment supply and landscape change in the mid to high-latitudes over the next few hundred years’.



Figure 1.2: Photo of Glaciers in Southern Alaska and Canada. The Steele Glacier, the horizontal feature in the center of the image, and the Donjek Glacier in the lower right. Retrieved from <https://earthobservatory.nasa.gov/blogs/fromthefield/files/2014/07/Steele-720x537.jpg>.

1.1.2 Paraglacial Adjustment

Paraglacial means unstable conditions caused by a significant relaxation time in processes and geomorphic patterns following glacial climates (Ballantyne, 2002). The term paraglacial addresses the specific morphodynamics including their development over time within a deglaciated landscape (Ballantyne, 2002). The geomorphic response to deglaciation has been conceptualized in paraglacial geomorphology. Encompassing spatial and temporal changes in

the activity of geomorphic processes, slope instability, and the build-up and depletion of sediment storage landforms. Several authors have explained the response of geomorphic processes and sediment fluxes to deglaciation, as the reaction to a disturbance (Church and Ryder, 1972; Ballantyne, 2002). These models describe how morphodynamics and sediment transfer change over time. They demonstrate the transitional character of the response to deglaciation as topography adjusts. The response to deglaciation occurs on different temporal and spatial scales. From decades, at the hillslope scale (Curry et al., 2006) to millennia, at the catchment scale (Church and Slaymaker, 1989), and differs between deglaciated environments (Ballantyne 2002).

1.1.3 Lateral Moraines

Perhaps the most visually obvious manifestation of glacial sediment storage, release, and redistribution within deglaciating alpine environments are the large lateral moraines that flank deglaciated landscapes throughout alpine regions. The ridges of debris that laid adjacent to the sides of a valley constitute the lateral moraines. An alpine glacier erodes the valley side walls while it moves down valley. Additionally, debris is added to the glacier surface as rubble falls or slides from the valley walls and collects on the periphery of the moving glacier. During glacial retreat, an accumulation of debris flanks the lateral perimeter of the previously glaciated site. Following glacier retreat, paraglacial processes, including debris flows, rework lateral moraine slopes (Ballantyne, 2002). However, the details of lateral moraine formation and their internal structure remain incompletely understood.

Lateral moraines are typically asymmetrical (Curry et al., 2009) in cross-profile, as depicted in Figure 1.3. The moraines are prominent features of glaciated landscapes in high-mountain environments. They are primarily piles of till with relatively uniform distal slopes and

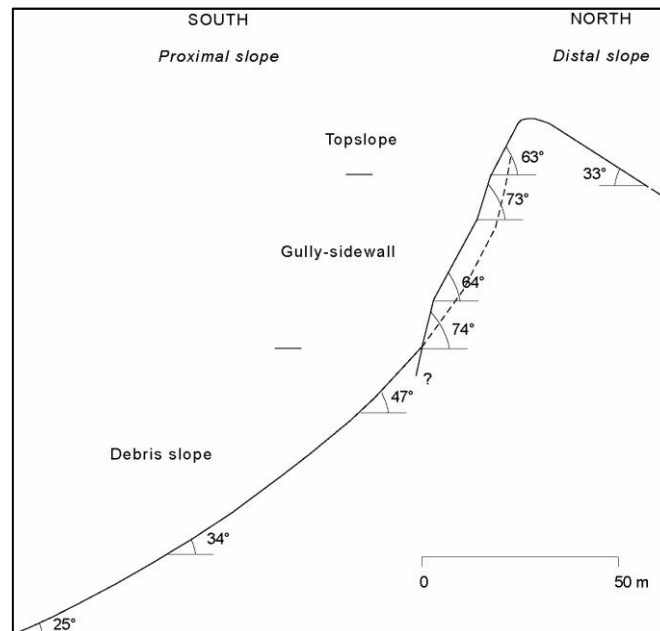


Figure 1.3: Example of an Asymmetrical Lateral Moraine. Reproduced from: Curry et al., (2009). Geotechnical controls on a steep lateral moraine undergoing paraglacial slope adjustment. *Geological Society, London, Special Publications*, 320, (181-197) (Fig.4).

much steeper proximal slopes. The distal side of the lateral moraine, between the moraine and the mountain side, may contain a depression of variable depth. Historically, this depression has been called the ‘ablation valley’ (Oestreich, 1906), ‘paraglacial valley’ (Burrows, 1973) and more recently the ‘lateral morainic trough’ (Hambrey et al., 2009). In this study the later term ‘lateral morainic trough’ will be adopted. The depth of the trough depends on the amount of alluvium from mountain torrents, avalanche detritus, debris flows, and screes falling from steep slopes above. The distal side can be virtually free of debris fill and the outer face of the moraine can make visible contact with bedrock, in some cases. The formation and development of gullies or gully-like channels may develop on either the distal slope or the proximal slope (Curry et al.,

2006; 2009). Figure 1.4 depicts an example of a lateral moraine in Grisons, Switzerland. Lateral moraines with unconsolidated glacial till provide the combination of steep slopes, loose material and missing or only sparse vegetation cover. This facilitates the reworking of the sediments by geomorphic processes. Their geomorphic forms are detectable from aerial observations and are characterized especially by incised gullies and debris cones.

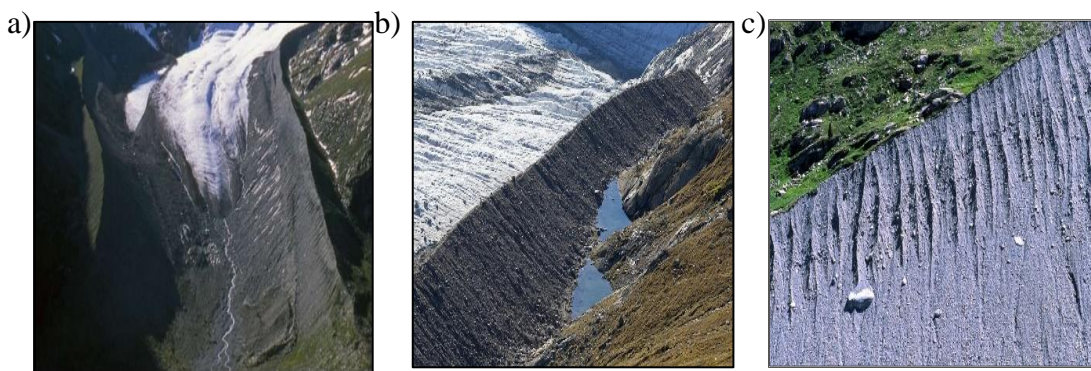


Figure 1.4: Examples of Lateral Moraines.

a) A pair of lateral moraines, Vadret da Tschierva, b) right lateral moraine of Vadret Pers dams small lakes below Munt Pers, Vadret da Morteratsch, c) Gully development on lateral moraine, Vadret da Tschierva.

Über SwissEduc (n.d). *Glaciers online*. Retrieved from: a)

<https://www.swisseduc.ch/glaciers/glossary/lateral-moraine-tschierva-en.html>, b)

<https://www.swisseduc.ch/glaciers/morteratsch/2011-2012/index-en.html?id=4>, c)

<https://www.swisseduc.ch/glaciers/glossary/fluted-lateral-moraine-en.html>. Accessed on 18 09 2019.

1.1.4 Alluvial Fans and Debris Flow Fans

Alluvial and debris flow fans are probably amongst the most widespread landforms produced by paraglacial reworking of sediment. Recent paraglacial cones are generally much smaller than their mature counterparts, reflecting the more limited availability of sediment following the recent glacial advances (Ballantyne 2001; Lukas et al., 2012). Typical fan depositions buttressed by a lateral moraine is illustrated in Figure 1.5. Environmental conditions affecting fans change more or less continuously during their formation time. Their formation is

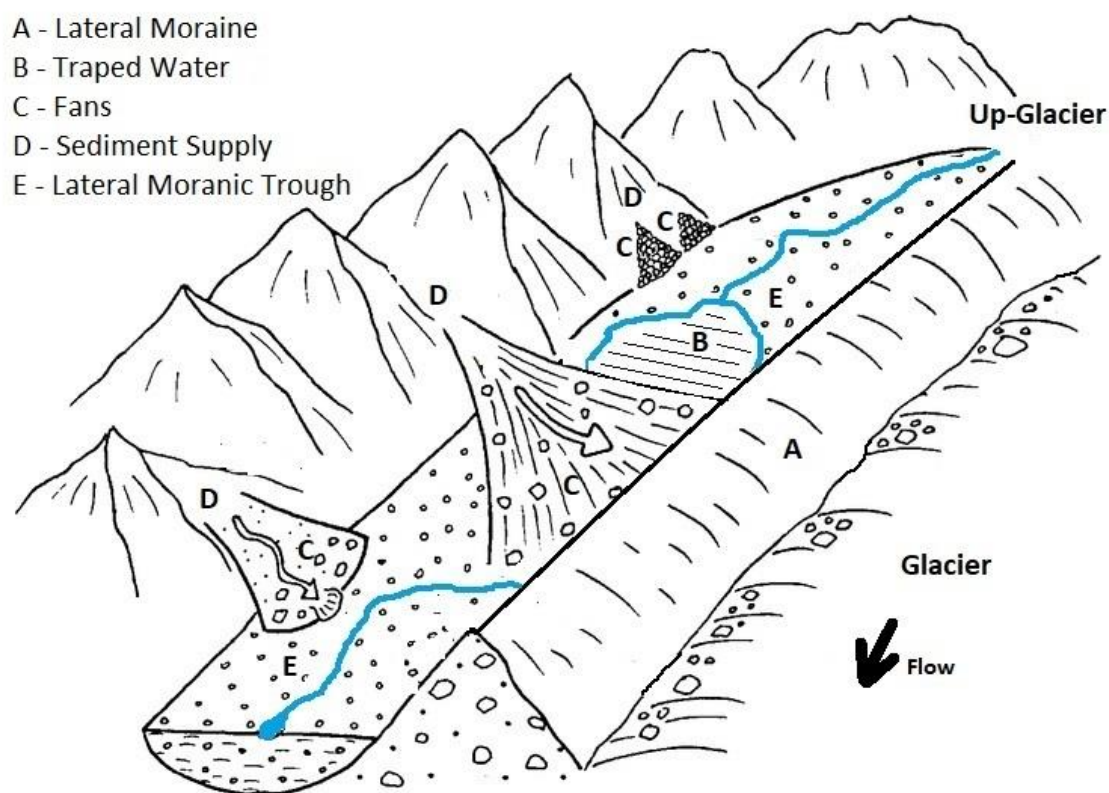


Figure 1.5: Typical Fan Deposits Buttressed by a Lateral Moraine.

particularly favored where sediment loads are high (National Research Council, 1996). They occur where sediment transport is triggered by the collapse of an accumulation of weathered rock, soil, or sediment in a steep source region (National Research Council, 1996). A fan is landform deposit shaped like a simple cone emanating from a single, well-defined apex, in the

simplest case. A stream follows more-or-less radial paths down the cone, in the case of alluvial fans (National Research Council, 1996). The contours on the map of such fans are convex down slope. Fans merge with the smoother depositional topography of the lateral moraine at their down slope margins along the glacier. The lateral morainic trough may be small, shallow or non-existent.

Fans grow with the deposition of eroded sediment. The thickness generally increases at the slope transition formed at the fan toe as it is progressively buried (National Research Council, 1996). Deposits up slope towards the apex are redeposited farther down the fan, on and below the fan toe, in the lateral morainic trough. Deposition propagates both up the fan toe and distal slope of the lateral moraine, where the slope typically diminishes. Eventually, deposition breaches the crest of the lateral moraine. Infills of lateral morainic trough tend to be more complete up-glacier. There lateral morainic troughs are smaller and slope processes more effective at supplying material to the trough.

1.2 Study

The purpose of the project is to define sharp-crested lateral moraines, to analyze the paraglacial reworking of lateral moraines, and the paraglacial reworking of alluvial fans and debris fans flows deposits at the buttress of the lateral moraine, by:

1. Defining the term sharp-crested lateral moraine.
2. Documenting typical examples of paraglacial adjustment of lateral moraines.
3. Describing the typical setting and morphology of lateral moraines.
4. Providing a quantitative comparative analysis of the description and observations of moraine.

5. Documenting typical examples of paraglacial adjustment of alluvial and debris flow fans deposits buttressed by lateral moraines.
6. Describing the typical setting and morphology of alluvial and debris flow fans buttressed by lateral moraines.
7. Providing a qualitative analysis of the description and observations of the alluvial and debris flow fan buttressed by lateral moraines in the context paraglacial reworking of lateral moraine slopes.

1.3 Definition

Terms such as ‘abnormally steep slopes’ (Whalley, 1975), ‘steep, sediment-mantled slopes’ (Curry et. al., 2006), ‘steep moraine slopes’ (Curry et. al., 2009) and ‘large lateral moraines’ (Lukas et al., 2012) are used at times in the literature to refer to lateral moraines that are unusually higher and/or have an unusually steeper angle of repose on the upper proximal slope. According to Beakawi, et.al. (2018) the angle of repose of earth is 30° - 45° . Whalley (1975), Curry et. al. (2006), Curry et. al. (2009) and Lukas et al. (2012) collectively imply that the height, steep gullied upper proximal slope and gentler distal slope are a departure from the conventional lateral moraine geometry. The term ‘sharp-crested lateral moraine’ is introduced by this paper to define those lateral moraines that are a departure from the conventional moraine’s geometry. The term has not been used in any of the literature reviewed for the study. Generally, Whalley (1975), Curry et. al. (2006), Curry et. al. (2009) and Lukas et al. (2012) are referring to lateral moraines that are greater than 80 meters in height and/or have an angle of repose on the upper proximal slope that is greater than 45° and a distal slope with a gentler angle of repose. The working definition of the term ‘sharp-crested lateral moraine’ introduced here in

recognition that these moraines are a special case in the response to paraglacial adjustment, is a lateral moraine that has:

1. An upper proximal slope with an angle of repose greater than 45° .
2. A distal slope with an angle of repose that is less than the maximum angle of repose of the upper proximal slope.
3. Have a height of more than 80 meters measured on the proximal side.

1.4 Literature Review

Many glaciated areas in alpine regions are characterised by a rapid deglaciation since the end of the Little Ice Age (LIA). The paraglacial process has received increased attention in recent years because of the geomorphological consequences of deglaciation becoming ever more pronounced. Research interest in the resultant impacts on sediment reworking is likely to become further enhanced with deglaciation in alpine regions continuing. This will likely add to the growth of interest in paraglacial geomorphology identified by Ballantyne (2002). A comprehensive review of published literature was required to ascertain the depth of research currently completed on the paraglacial reworking of the landform and identify data sources that other researchers have used. The review provides insight on what aspects of lateral moraine geomorphology have been investigated, defined how others have addressed and measured key concepts and provided evidence to support the findings of this study.

1.4.1 Lateral Moraines as Sediment Stores

One kind of sediment stores are lateral moraines. Their geomorphic forms are clearly detectable from satellite imagery and are characterised especially by incised gullies. The combination of steep slopes, loose material and minimal vegetation cover facilitates the

reworking of sediments by geomorphic processes like debris flows. Studies on reworking rates of moraine slopes were carried out by Ballantyne and Benn (1994), and Curry (1999), in western Norway. Curry et al. (2006) examined erosion rates on lateral moraines in the central Swiss Alps. They concluded that gullies on lateral moraines reached their maximum dimension after approximately 50 years, and a stabilisation of the gully system was reached 80–140 years after deglaciation.

1.4.2 Development of Lateral Moraines

Early theories of lateral moraine formation generally assumed that sub-aerial processes were primarily responsible for accumulation of sediment at the ice margin, with additional contribution of sediment from englacial sources. Later theories cite processes of repeated stacking of debris flows at the glacier margins, with sedimentary stratification, gently sloping distal morphology. However, substantial subglacial and glaciofluvial sediments observed within lateral moraines at Findelengletscher, Switzerland, contrast with observations made elsewhere. This signifies the potential importance of sediment transfer via englacial pathways (Lukas et al., 2012). More recent geophysical investigations indicate ice-marginal moraine depositional history and evidence of polygenesis (Tonkin et al., 2017). These observations combined, indicate the potential genetic complexity of lateral moraine features.

1.4.3 Factors Affecting Reworking of Lateral Moraines

Irrespective of the precise modes of formation, it is clear that lateral moraine complexes have the potential to be extensively reworked and redistributed during deglaciation. The extent to which any given slope unit is reworked will depend on multiple factors. This may include slope geotechnical properties such as lithology and degree of consolidation (Curry et al., 2009; Lukas et al., 2012), topographic setting (Barr and Lovell, 2014) and geomorphological processes

(Curry, 1999; Curry et al., 2006). Lateral moraines are more commonly located away from highly dynamic proglacial fluvial systems. Hence, they are more usually dissected, reworked and modified on a recurring basis. This occurs through the operation of debris flow activity, facilitated by, for example, extreme precipitation events or spring thaw (Lukas et al., 2012).

Paraglacial response to deglaciation is complex. Different land systems will respond at differing rates and spatial scales (Ballantyne, 2002). Lateral moraine slopes in deglaciating environments demonstrate the attributes of both primary and secondary paraglacial systems. Primary paraglacial system is when sediment release is directly conditioned by glaciation. Secondary paraglacial system is when rate of sediment release is additionally controlled by reworking of paraglacial sediment stores (Ballantyne, 2002). Paraglacial reworking of lateral moraines frequently causes dissection of moraine slopes, formation of gullies and redistribution of sedimentary materials. (Curry et al., 2006, 2009; Lukas et al., 2012). Despite their apparent stability, the presence of lateral moraines is a potentially important conditioning factor for paraglacial slope modification (Curry et al., 2009).

1.4.4 Erosion Processes of Lateral Moraines

Paraglacial modification of lateral moraine slope form takes place through a variety of processes. This includes: debris flow, stream action, solifluction and snow avalanching (Ballantyne, 2002; Curry et al., 2006). Such processes are largely responsible for the characteristic paraglacial landscapes of gullied lateral moraines (Ballantyne and Benn, 1994; Ballantyne, 1995, Curry, 1999; Curry et al., 2006). It is clear that extensive paraglacial modification of slope form through gullying, for example, can take place within of a few decades (Ballantyne and Benn, 1994). This debris flow activity is one of the prime agents responsible for the slope form and sediment redistribution. However, the precise controls on the extent and

effectiveness of debris flowage and other paraglacial hillslope activity represent a relatively under studied aspect of deglaciation terrain (Curry, 2000). Curry et al. (2006) found the upper part of the lateral moraine is often intensely gullied. Indicating that erosion takes place at these locations and identifying debris flows as being the most important sediment transport. Ballantyne (2002) found this to be the case in many sediment-mantled slopes in recently glaciated terrain.

If the moraine is ice cored, the ice can play an important role in releasing mass movements. The melting of the underlying ice reduces the strength of the overlying material. However, 83% of failures are still caused by rainfall, where only 14% is possibly caused by buried ice melt (Ballantyne, 2002). The probability of lateral moraine's susceptibility to debris flow erosion is not only dependent on the climatic shifts that cause melting. Curry et al. (2000) suggests that steep moraine gradients of over 30° are necessary to create a heavily gullied moraine where extensive erosion can happen. After reworking the exposed moraines, the terrain often ends up with a steep gullied upper part. The original slope is completely lost, and a lower zone that consists of mainly reworked debris forms. This lower part mostly consists of coalescing cones, which sometimes merge into one large talus slope (Ballantyne, 2002).

1.4.5 Lateral Moraine Steep Slope Stability following Deglaciation

The extent of any slope unit to release sediment will relate, in part, to the overall geomorphic stability of that unit. Lateral moraines may be particularly important in this respect, due to their ability, in many cases, to stand stably at extreme angles. Many lateral moraines exhibit very steep proximal slopes that appear to retain stable form, despite ongoing paraglacial reworking (Curry et al., 2006, 2009). The material properties and mechanisms that permit some lateral moraines to stand stably at extreme angles (Lukas et al., 2012) remains incompletely understood. Recent work conducted in the European Alps highlights the importance of processes,

such as overconsolidation (Lukas et al., 2012). Slope stability does not necessarily mean that sediments are held in storage. They are potentially available for release and reworking as evidenced by the presence of gullies. This characteristic of many lateral moraines is important in the context of deglaciation dynamics, irrespective of the source of sediment (Lukas et al., 2012).

The geotechnical properties of lateral moraine sediments offer one avenue of investigation towards a more complete understanding of lateral moraine stability. Whalley (1975) characterized various mechanical aspects of lateral moraines at Feegletscher, Switzerland. Calculated a friction angle of 45° and suggested that soil suction may have a role to play in enhancing slope strength and therefore stability. Curry et al. (2009) suggested that a suction effect of the inter-gully slopes potentially enhances surface crust formation. This may assist in slope stabilization with limited impact on long-term stability. A comprehensive sedimentological study carried out at Findelengletscher, Switzerland (Lukas et al., 2012) provides further information on lateral moraine mechanics and resultant factors that may influence slope stability. Lukas et al. (2012) suggested that rather than a dominant supraglacial source for lateral moraine sediments, subglacial and glaciofluvial sediments are dominant. Deposited by debris flows once material had been transferred from the bed to the ice surface via englacial pathways. The key, however, to proximal slope stability is the process of over consolidation according to Lukas et al. (2012). Suggesting that this overconsolidation arises through a combination of glaciotectonisation of pre-existing sediments and incremental plastering of till onto the proximal slopes. The resulting overconsolidation is suggested to be an important factor in enhancing slope stability, retarding paraglacial slope modification and, consequently, enhancing preservation potential. It may offer an explanation for slope stability and the extreme slope angles of up to 80° , as observed at Findelengletscher (Curry et al., 2009; Lukas et al., 2012).

The stability and steepness of proximal lateral moraine slopes often gives rise to cross-sectional asymmetry, with distal slopes exhibiting lower slope angles. Although, it should be noted that cross-sectional asymmetry is not a ubiquitous observation. Lower-angled distal slopes, in contrast to steep proximal slopes, usually represent depositional fan surfaces resting at the angle of repose (Ballantyne, 2002). Suggesting that they are generally less prone to intense paraglacial modification and the formation of gullies. Thus, they tend to become more readily stabilized by vegetation cover. Ballantyne (2002) suggest that vegetation colonization acts to decrease geomorphological activity and stabilize slope form. Conversely, at sites in Norway and the central Swiss Alps, Curry et al. (2006) suggest that progressive vegetation colonization on active proximal lateral moraine slopes is a response to slope stabilization. The role of vegetation therefore adds further complexity to the functioning of lateral moraines.

The very steep proximal slope of the lateral moraine (Lukas et al., 2012) may be susceptible to rock fallout from the glacially oversteepened moraine, that develops talus accumulations below. Much material remains on the adjacent slopes as talus debris and is reworked by secondary processes (Lukas et al., 2012). Examples of these processes are wet flows, avalanches and solifluction processes. The loose valley slope sediment consists of course boulders and rocks, but also of finer grained material, Hence, small slumps may change into debris flows that, because of the course material, can entrain bed material and grow in size substantially (Lukas et al., 2012). Snow avalanches are also capable of transporting this loose material. Wet snow avalanches have often not enough shear strength to erode the bedrock, but are an important process in distributing the sediment from these temporary storage sites (Lukas et al., 2012).

1.4.6 Indicators of Paraglacial Slope Modification and Time

Studying the paraglacial modification of glaciogenic slope sediments in western Norway, Curry (2000) utilizes gully density as a surrogate indicator of paraglacial modification. Similar to other studies, debris flow activity emerges as a dominant paraglacial process. However, a relative lack of paraglacial slope modification, even in high relief areas, demonstrates a clear need for a more complete understanding of the detailed constraints on paraglacial activity (Curry, 2000). The Church and Ryder (1972) model emphasizes time as the key variable. Their model dictates paraglacial sediment supply, release and reworking, with maximum sediment supply occurring shortly after deglaciation. Then steadily declining as glacier shrinkage continues. Indeed, Curry (1999) suggests that upslope sediment availability is a likely control on slope stabilization. The delivery of sediments from ice-marginal hillslopes, itself, ensures a continuously diminishing supply of sediment and longer-term stability. With debris flowage delivering material to the slope foot, progressively burying upper slope units, reducing slope gradient, reducing upslope sediment supply and potentially facilitating slope stability, with vegetation colonization furthering stability (Curry, 1999).

1.4.7 Fan Formation

Alluvial and debris flow fans are fan-shaped landforms created over time by the deposition of eroded sediment. During their formation time, environmental conditions affecting fans change more-or-less continuously. Several explanations regarding the location and triggering of fans have been proposed in literature. Fans develop where debris flows emerge from steep reaches where they are confined to relatively straight and narrow channels (National Research Council, 1996). These conditions develop where there are major breaks in gradient or channel confinement. This allows both deposition of sediment and the lateral movement of

channels to spread the sediment into a fan-shaped landform. Debris flow fans occur where sediment transport is triggered by collapse of an accumulation of weathered rock, soil, or sediment in a steep source region. This creates a steep accumulation of sediment, with or without a fluvial component (National Research Council, 1996). Ballantyne, (2002) suggest that glacial valleys are particularly prone to alluvial and debris flows and that their occurrence is associated with glacier retreat. For other authors the topography of slope is the sole cause. Church (2005) suggest it is favoured by a change in the profile of the slope, especially a break in a convex slope.

1.4.7.1 Surface Morphology and Age

Christenson and Purcell (1985) grouped debris fans into three age classes: young (Holocene), intermediate (Pleistocene), and old (from late to middle Pleistocene). They prescribe that young fans, less than 10,000 to 15,000 years, have a stream incision typically less than one meter. In contrast, intermediate-age fans, 10,000 to 700,000 years, have a dendritic to parallel drainage pattern and a major channel incision of about 1 to 10 meters with undissected interfluves. Old fans, older than 500,000 years, retain little of their original surface morphology, have stream incision greater than about 10 m, and typically are cut off from their original source areas.

Chapter 2

Description of Study Sites and Data

2.1 Introduction

The studied glaciers are situated in some of the more remote mountainous regions on Earth. Among the most visible changes in these regions is glacier retreat, a result of climatic shift (Zemp et al., 2020). Glacier retreat that started in the second half of the nineteenth century, after the end of a cold phase called the “Little Ice Age” (LIA), has been accelerating. Glaciers worldwide have been shrinking significantly, from these positions. There were strong glacier retreats in the 1940s, stable or growing conditions around the 1920s and 1970s, and again increasing rates of ice loss since the mid 1980s (Zemp et al., 2020). This retreat results in the exposure of formerly glaciated terrain to subaerial conditions, with an impact on geomorphic processes. The geomorphic response to deglaciation has been conceptualized in paraglacial geomorphology (Ballantyne, 2002). The response includes spatial and temporal changes in the activity of geomorphic processes, such as the development of lateral moraines, slope instability, and the build-up and depletion of sediment storage landforms.

This study focuses on the more remote mountainous regions of Earth where alpine glaciers showcase the subsequent geomorphological consequences of deglaciation. Specifically, it focuses on the mountainous regions of the United States (Washington and Alaska), Canada (British Columbia and Yukon), Tajikistan, Asia, Afghanistan, Argentina and Switzerland.

2.2 Initial Selection of Sites

The geomorphological landforms studied in this project are situated in some of the most remote regions on Earth. Attempts to conduct field studies in these regions are not logistically or economically feasible, as a result, within the context of this project. Typically, no large-scale

maps are available for the vast majority of these regions. However, satellite digital images, from platforms such as Google Earth, are obtainable. Google Earth satellite digital imagery is an effective means for identifying and obtaining information about geomorphological landforms in relatively unexplored areas. Resolution and clarity of the digital imagery is a limiting factor. Hence, digital images offer the opportunity of limited study of the distribution and morphological characteristics of geomorphological landforms from a remote location.

Google develops and freely distributes two widely used data visualization platforms: Google Maps and Google Earth. Both are, essentially, simplified GIS software packages. The programs permit the viewing of satellite digital imagery for almost any point on the earth's surface in two or three dimensions (Google, 2019). Digital images dating as far back as 1984, of varying resolution and clarity, are available for remote regions in Google Earth. The digital imagery is collected from a variety of sources and pieced together to make up a mock continuous digital image of the globe (Google, 2019). Digital images on Google Earth are obtained from both commercial satellite operators and government agencies (Google, 2019). The majority of the images are obtained from either MAXAR (formerly DigitalGlobal), USGS / NASA Landsat satellite images or Copernicus / European Space Agency Sentinels satellite images. The resolution and clarity of the digital imagery hosted by Google varies widely. Remote areas receive updates far less often. Therefore, for some remote regions, the digital image often predates the image resolution and clarity compared to contemporary satellites. The level of detail provided in such digital imagery limits the accuracy of the available information and, in some cases it does not provide sufficient detail to merit any evaluation of a site.

Initially, based on the initial visual scan in Google Earth, 59 sites were identified for possible inclusion in the project. These sites are tabulated in Table 2.1. Each site has been

assigned a unique numeric identification (ID), their name, their location, and their geographic coordinates (latitude and longitude). Italicized glacier names in the tables are tentative designations assigned for practical convenience, because glacier names have not been established.

Table 2.1: Initial 59 Sites Identified for Possible Inclusion.

| ID | Name | Location | Coordinates | |
|-----|------------------------------|-------------|---------------|----------------|
| | | | Latitude | Longitude |
| 001 | Klutan Glacier | Yukon | 61°28'52.23"N | 140°34'25.95"W |
| 002 | Marvine Glacier | Alaska | 60° 3'8.29"N | 140°10'16.05"W |
| 003 | Sawyer Glacier | Alaska | 57°56'1.86"N | 133° 6'3.57"W |
| 004 | Glacier Creek | Alaska | 61°22'55.00"N | 142°10'16.66"W |
| 005 | Kluane Glacier | Yukon | 60°56'31.50"N | 139°17'17.84"W |
| 006 | Fairweather Glacier | Alaska | 58°52'56.30"N | 137°42'48.41"W |
| 007 | Otter Glacier | Alaska | 58°53'57.40"N | 137°46'11.57"W |
| 008 | North Crillon | Alaska | 58°37'53.81"N | 137°23'24.31"W |
| 009 | Matanuska Glacier | Alaska | 61°38'24.83"N | 147°40'5.82"W |
| 010 | Matanuska Glacier | Alaska | 61°38'39.77"N | 147°36'42.01"W |
| 011 | Matanuska Glacier | Alaska | 61°41'14.09"N | 147°37'10.22"W |
| 012 | Tamdykul MTN | Tajikistan | 39°28'31.89"N | 71° 9'55.79"E |
| 013 | Surkhnago Peak | Tajikistan | 39°14'16.10"N | 71°50'56.94"E |
| 014 | Tajikistan MTN | Tajikistan | 39° 0'9.96"N | 72°18'34.56"E |
| 015 | Tajikistan MTN | Tajikistan | 38°42'46.06"N | 72°30'12.72"E |
| 016 | Tajikistan MTN | Tajikistan | 38°42'14.17"N | 72°31'43.05"E |
| 017 | Tajikistan MTN | Tajikistan | 38°58'12.33"N | 72°14'49.94"E |
| 018 | Tajikistan MTN | Tajikistan | 39°25'12.66"N | 73° 5'19.87"E |
| 019 | Tajikistan MTN | Tajikistan | 39°19'27.38"N | 73° 7'10.13"E |
| 020 | Argentina | Argentina | 48°24'39.88"S | 73°17'30.25"W |
| 021 | Ventisquero Grosse | Argentina | 46°27'35.95"S | 73°19'21.91"W |
| 022 | Exploradores Glacier | Argentina | 46°31'46.37"S | 73°12'5.01"W |
| 023 | Baffin Island | Canada | 66°39'55.66"N | 62°25'56.66"W |
| 024 | Baffin Island | Canada | 66°31'56.11"N | 62°42'35.95"W |
| 025 | Baffin Island | Canada | 66°28'22.05"N | 64°33'37.75"W |
| 026 | Kaskawulsh Glacier | Alaska | 60°45'35.33"N | 138°42'28.37"W |
| 027 | Fairweather Glacier | Alaska | 58°50'41.21"N | 137°46'41.48"W |
| 028 | Bell Glacier | Canada | 51°26'28.39"N | 125°23'33.06"W |
| 029 | Roovers Glacier | Canada | 51°28'14.76"N | 125°22'28.40"W |
| 030 | Geddes Glacier | Canada | 51°25'43.84"N | 125°21'22.23"W |
| 031 | Mt. Waddington A | Canada | 51°26'38.42"N | 125°22'10.66"W |
| 032 | Dorothy Glacier | Canada | 51°23'49.49"N | 125°30'34.60"W |
| 033 | Mt. Waddington A | Canada | 51°29'15.75"N | 125°32'42.17"W |
| 034 | Mount Everest | China | 27°59'39.51"N | 87° 2'19.96"E |
| 035 | Karakoram Range | Asia | 34°23'58.06"N | 78°37'44.55"E |
| 036 | Karakoram Range | Asia | 34°33'8.66"N | 78°29'5.73"E |
| 037 | Karakoram Range -1 | Asia | 34°34'20.51"N | 78°19'7.96"E |
| 038 | Karakoram Range - 3 | Asia | 34°35'42.42"N | 78° 6'57.26"E |
| 039 | Karakoram Range - 4 | Asia | 34°37'37.01"N | 78° 6'40.77"E |
| 040 | Karakoram Range - 2 | Asia | 34°11'25.98"N | 78°36'43.98"E |
| 041 | Afghanistan | Afghanistan | 36°15'49.74"N | 75°38'4.17"E |
| 042 | Afghanistan - 1 | Afghanistan | 36°18'11.60"N | 75°25'22.91"E |
| 043 | Afghanistan - 2 | Afghanistan | 36°23'29.01"N | 75°22'55.64"E |
| 044 | Mulungutti Glacier | Afghanistan | 36°27'45.95"N | 75°13'2.86"E |
| 045 | Lupghar Yaz Glacier | Afghanistan | 36°27'35.34"N | 75° 1'3.13"E |
| 046 | Shkuk Yoz Glacier | Afghanistan | 36°45'32.36"N | 74°18'48.32"E |
| 047 | Jiangchacun, China | China | 29°45'46.12"N | 96°41'10.98"E |
| 048 | Nagong, China | China | 29°27'32.35"N | 96°25'52.92"E |
| 049 | Bogda, China | China | 43°49'15.11"N | 88°23'57.92"E |
| 050 | Tiedemann Glacier | Canada | 51°19'28.21"N | 124°59'20.39"W |
| 051 | Donjek Glacier | Canada | 61° 9'52.41"N | 139°33'8.34"W |
| 052 | Fee Glacier | Switzerland | 46° 1'42.72"N | 7°56'9.25"E |
| 053 | Tsidjiore Nouvelle | Switzerland | 46° 0'56.37"N | 7°27'43.66"E |
| 054 | Findelengletscher | Switzerland | 46° 0'42.60"N | 7°49'55.04"E |
| 055 | Easton Glacier | USA | 48°43'50.99"N | 121°49'49.20"W |
| 056 | Mount Everest_2 | China | 28° 1'27.97"N | 87° 9'41.07"E |
| 057 | Vadret da Tschierva, Grisons | Switzerland | 46°24'19.58"N | 9°51'56.61"E |
| 058 | Vadret Pers dams | Switzerland | 46°24'52.95"N | 9°55'43.20"E |
| 059 | Vadret da Tschierva, Grisons | Switzerland | 46°23'47.29"N | 9°50'32.13"E |

Further critiquing of these sites elucidated that some were not relevant to this project. The critique also elucidated that the resolution and clarity of the images was not adequate, in all cases, for complete analysis. Examples of these include:

1. The Google Earth panoramic imagery for Glacier Creek, Alaska was compiled based on data imagery available between 1984 and 2016. The magnified imagery was dated between 2012 and 2014. The resolution provided in either period permit the identification of a moraine at the site. However, the visual detail was not suitable for further analysis of the site.
2. The Google Earth panoramic imagery for the Otter Glacier was compiled based on data imagery available between 1984 and 2016. The magnified imagery was dated between 2015 and 2019. The resolution provided in the later of these periods was sufficient for the identification of distinguishing features of the site.
3. Similarly, the Google Earth panoramic imagery for the Donjek Glacier, Canada was compiled based on data imagery available between 1984 and 2016. The magnified imagery was dated 9/26/2002. The resolution provided in the later image was sufficient the identification of distinguishing features of the site.

Additionally, a general idea of the geomorphological form was established. Specifically, if a lateral moraine and/or fan buttressed by lateral moraines were present at the site and to obtain a general idea of the possible profile, i.e. slope angle, the height and the length.

This survey established that suitable Google Earth images of varying resolution and clarity were available for 31 of the 59 sites. The results of the preliminary analysis were tabulated in Table 2.2. The table records the ID, glacier name and a preliminary assessment of the slope angle, height and length. Additionally, both the lateral moraine and the fan were

qualitatively ranked numerical (1 - Poor, 2 – Fair, 3 – Good and 0 – Element not visible) together with a combined ranking.

Table 2.2: Sites and Preliminary Data.

| ID | Name | Location | Moraine Rank ¹ | Fan / Debris Rank ¹ | Combined Rank ² | Preliminary Assessment | | |
|-----|------------------------------|-------------|---------------------------|--------------------------------|----------------------------|------------------------|------------|------------------------|
| | | | | | | Slope Angle (Deg) | Height (m) | Length (Sections) (km) |
| 050 | Tiedemann Glacier | Canada | 3 | 3 | 6 | > or ~ 45 | > 100 | > 1 |
| 004 | Glacier Creek | Alaska | 1 | 0 | 1 | > or ~ 45 | > 50 < 100 | < 1 |
| 006 | Fairweather Glacier | Alaska | 2 | 0 | 0 | > 45 | ~ 100 | < 1 |
| 007 | Otter Glacier | Alaska | 2 | 0 | 0 | > or ~ 45 | ~ 50 | > 1 |
| 009 | Matanuska Glacier | Alaska | 2 | 2 | 4 | < 45 | < 50 | > 1 |
| 010 | Matanuska Glacier | Alaska | 1 | 3 | 4 | < 45 | < 50 | < 1 |
| 011 | Matanuska Glacier | Alaska | 2 | 1 | 3 | < 45 | < 50 | < 1 |
| 012 | <i>Tamdykul MTN</i> | Tajikistan | 2 | 1 | 3 | < 45 | >50 < 100 | < 1 |
| 021 | Ventisquero Grosse | Argentina | 3 | 0 | 0 | < 45 | < 100 | < 1 |
| 022 | Exploradores Glacier | Argentina | 2 | 1 | 3 | > or ~ 45 | >50 < 100 | < 1 |
| 028 | Bell Glacier | Canada | 3 | 1 | 4 | 35 - 45 | > 100 | > 1 |
| 029 | Roovers Glacier | Canada | 2 | 1 | 3 | < 45 | > 100 | > 1 |
| 030 | Geddes Glacier | Canada | 1 | 3 | 4 | < 45 | > 100 | > 1 |
| 032 | Dorothy Glacier | Canada | 2 | 2 | 4 | < 45 | > 100 | > 1 |
| 033 | Mt. Waddington A | Canada | 2 | 2 | 4 | < 45 | > 100 | > 1 |
| 034 | <i>Mount Everest</i> | China | 3 | 2 | 5 | < 30 | < 100 | < 1 |
| 036 | <i>Karakoram Range</i> | Asia | 1 | 0 | 1 | < 45 | < 100 | < 1 |
| 040 | <i>Karakoram Range</i> | Asia | 2 | 2 | 4 | < 30 | < 100 | < 1 |
| 041 | Virjerab Glacier | Afghanistan | 2 | 3 | 5 | < 30 | < 100 | < 1 |
| 045 | Lupghar Yaz Glacier | Afghanistan | 1 | 0 | 1 | < 30 | < 50 | > 1 |
| 046 | Shkuk Yoz Glacier | Afghanistan | 1 | 2 | 3 | ??? | ??? | > 1 |
| 048 | <i>Nagong, China</i> | China | 2 | 0 | 0 | > or ~ 45 | < 100 | < 1 |
| 051 | Donjek Glacier | Canada | 1 | 3 | 4 | < 30 | < 50 | > 1 |
| 052 | Fee Glacier | Switzerland | 2 | 3 | 5 | > or ~ 45 | < 50 | > 1 |
| 053 | Tsidjiore Nouve | Switzerland | 2 | 2 | 4 | > or ~ 45 | < 50 | < 1 |
| 054 | Findelengletscher | Switzerland | 3 | 0 | 0 | > or ~ 45 | < 100 | > 1 |
| 055 | Easton Glacier | USA | 3 | 0 | 0 | < 45 | < 100 | > 1 |
| 056 | <i>Mount Everest_2</i> | China | 2 | 0 | 0 | < 30 | < 100 | < 1 |
| 057 | Vadret da Tschierva, Grisons | Switzerland | 3 | 0 | 0 | > or ~ 45 | ~ 100 | > 1 |
| 058 | Vadret Pers dams | Switzerland | 3 | 2 | 5 | > or ~ 45 | < 100 | > 1 |
| 059 | Vadret da Tschierva | Switzerland | 3 | 0 | 0 | > or ~ 45 | ~ 100 | > 1 |

¹Rank - 1 - Poor, 2 - Fair, 3 - Good and 0 - Element not visible

²Combined Rank – Sum of the Moraine Ranking + the Fan / Debris Ranking

2.3 Data Used for Study

The assessment of paraglacial slope adjustment at selected sites required detailed geomorphological data of slope profiles. The acquired data needed to be sufficiently detailed for

documentation and description for providing a quantitative comparative analysis of the paraglacial adjustment of the study features. Further evaluation of the 31 remaining sites was conducted with the intent to gather information of detailed geomorphological data of slope profiles.

2.3.1 Satellite Imagery

The digital images, in some cases, can be complimented with contour maps produced by various government agencies and research institutions or generated with third party geographic information system software (GIS) packages, and data from field observations detailed in published papers. Today, some satellites obtain images at a level of detail that can identify objects less than 30 centimeters across. This is called the spatial resolution. It refers to the size of one pixel on the ground. For example, 10 meters means that one pixel on the image corresponds to a square of 10 by 10 meters on the ground. Google imagery is sourced from many different 3rd party partners. Google keeps the imagery current over populated places and areas of cultural significance. For much of the remote world, Google uses lower resolution satellite imagery. High resolution imagery is available for the areas users view the most including urban areas and culturally significant locations (Google, 2019). Companies such as Google provides imagery with a resolution that, at best, makes one meter objects visible. Hence, this limits the accuracy of the data collected.

There are several problems with analyzing satellite digital imagery for this project. First, the resolution and clarity of the digital image may not be adequate to identify smaller features. For example, the depth of gullies cannot be quantified. Second, some glacier surfaces are covered by debris that is difficult to distinguish. Snow facies and geomorphological landforms are indistinguishable in the images. In addition, the images are sometimes acquired when details

are obscured by shadows of adjacent slopes. Therefore, contour maps provide a means of comparing Google Earth interpretations.

Google allows the import of custom raster and vector datasets created using third party software, such as CALTOPO. This software allows for quick and simple design of maps for most regions in the US and Canada. The software also facilitates the creation of topographic maps, the generation of detailed elevation profiles and the export of Keyhole Markup language Zipped (KMZ) files directly into Google Earth. Google also allows users to export digital images into third party software, such as CALTOPO and Trimble, SketchUp. Trimble software facilitates the creation of three-dimensional geo-referenced models from their high resolution digital image.

2.3.2 Topographic Maps

Topographic maps depict ground relief (landforms and terrain) in detail. Large-scale mapping has been compiled in some countries and much less in others. Topographic maps with planimetric info, especially for remote regions, are for the most part not available. However, topographic maps with closely spaced contour lines are available for the selected regions in Canada, the United States, and other countries. Several sources for large scale topographic maps have been identified. These include, the United States Geological Survey, Natural Resources of Canada, the Province of British Columbia, the Government of Yukon and the ArcticDEM data hosted by the University of Minnesota. The ArcticDEM data is constructed from high-resolution (~0.5 meter) imagery acquired by the DigitalGlobe constellation of optical imaging satellites, but is limited to select regions. Additionally, contour lines were generated from a DigitalGlobe constellation using CALTOPO. However, the accuracy of the information is dependent on the resolution and clarity of the digital image. The image data for the 31 sites is summarized in Table 2.3.

Table 2.3: Image Data.

| <i>ID</i> | <i>Name</i> | <i>Location</i> | <i>High Resolution Image Pixels Size (m)</i> | <i>Contour Spacing (m)</i> | <i>Vector Point Spacing (Arcsecond)</i> |
|-----------|------------------------------|-----------------|--|--------------------------------|---|
| 050 | Tiedemann Glacier | Canada | 6 | 5 | 1/9 |
| 004 | Glacier Creek | Alaska | 9 | 5 | 1/9 |
| 006 | Fairweather Glacier | Alaska | 10 | 5 | 1/9 |
| 007 | Otter Glacier | Alaska | 10 | 5 | 1/9 |
| 009 | Matanuska Glacier | Alaska | 9 | 5 | 1/9 |
| 010 | Matanuska Glacier | Alaska | 9 | 5 | 1/9 |
| 011 | Matanuska Glacier | Alaska | 9 | 5 | 1/9 |
| 012 | <i>Tamdykul MTN</i> | Tajikistan | 7.5 | 10 | 1/3 |
| 021 | Ventisquero Grosse | Argentina | 6.5 | 10 | 1/3 |
| 022 | Exploradores Glacier | Argentina | 6.5 | 10 | 1/3 |
| 028 | Bell Glacier | Canada | 6 | 5 | 1/9 |
| 029 | Roovers Glacier | Canada | 6 | 5 | 1/9 |
| 030 | Geddes Glacier | Canada | 6 | 5 | 1/9 |
| 032 | Dorothy Glacier | Canada | 6 | 5 | 1/9 |
| 033 | Mt. Waddington A | Canada | 6 | 5 | 1.9 |
| 034 | <i>Mount Everest</i> | China | 8.5 | 10 | 1/3 |
| 036 | <i>Karakoram Range</i> | Asia | 8 | 10 | 1/3 |
| 040 | <i>Karakoram Range</i> | Asia | 8 | 10 | 1/3 |
| 041 | Virjerab Glacier | Afghanistan | 7.5 | 10 | 1/3 |
| 045 | Lupghar Yaz Glacier | Afghanistan | 7.5 | 10 | 1/3 |
| 046 | Shkuk Yoz Glacier | Afghanistan | 7.5 | 10 | 1/3 |
| 048 | <i>Nagong, China</i> | China | 8 | 10 | 1/3 |
| 051 | Donjek Glacier | Canada | 9 | 5 | 1/9 |
| 052 | Fee Glacier | Switzerland | 7 | 10 | 1/3 |
| 053 | Tsidjiore Nouve | Switzerland | 6.5 | 10 | 1/3 |
| 054 | Findelengletscher | Switzerland | 6.5 | 10 | 1/3 |
| 055 | Easton Glacier | USA | 6.5 | 5 | 1/9 |
| 056 | <i>Mount Everest_2</i> | China | 8.5 | 10 | 1/3 |
| 057 | Vadret da Tschierva, Grisons | Switzerland | 6.5 | 10 | 1/3 |
| 058 | Vadret Pers dams | Switzerland | 6.5 | 10 | 1/3 |
| 059 | Vadret da Tschierva | Switzerland | 6.5 | 10 | 1/3 |

A preliminary analysis of the 31 remaining sites was further evaluated using either Google Earth, CALTOPO or the Trimble SketchUp software. CALTOPO software provides analysis ready data which contain time-series stacks of overhead imagery that are prepared for a user to make use of without having to do their own pre-processing before analysis.

Using these evaluation tools, notable CALTOPO, slope profiles were generated for a number of locations on the moraine. Each site was divided into three sections: the up-glacier section ‘A’, the mid-glacier section ‘B’ and the down glacier section ‘C’. The up-glacier section is normally located up-glacier within the contemporary equilibrium line. The down glacier

section is located around the terminus, up-glacier from the terminal moraines. The mid-glacier position is located at an arbitrary location between the two foregoing locations. Due to the variation in glacier length and the extent of deglaciation, both the mid-glacier and up-glacier positions required adjustment to suit the profile of each study site. The appendix contains Mercator maps generated using the CALTOPO software, of each location. The transect locations are notated with red lines, the gully locations are numbered in blue and the fan locations are noted with an orange icon. Additionally, the appendix contains selected 2D graphics of the 3D models developed using Trimble software and selected images captured in Google Earth. A typical Mercator map is contained in Figure 2.1.

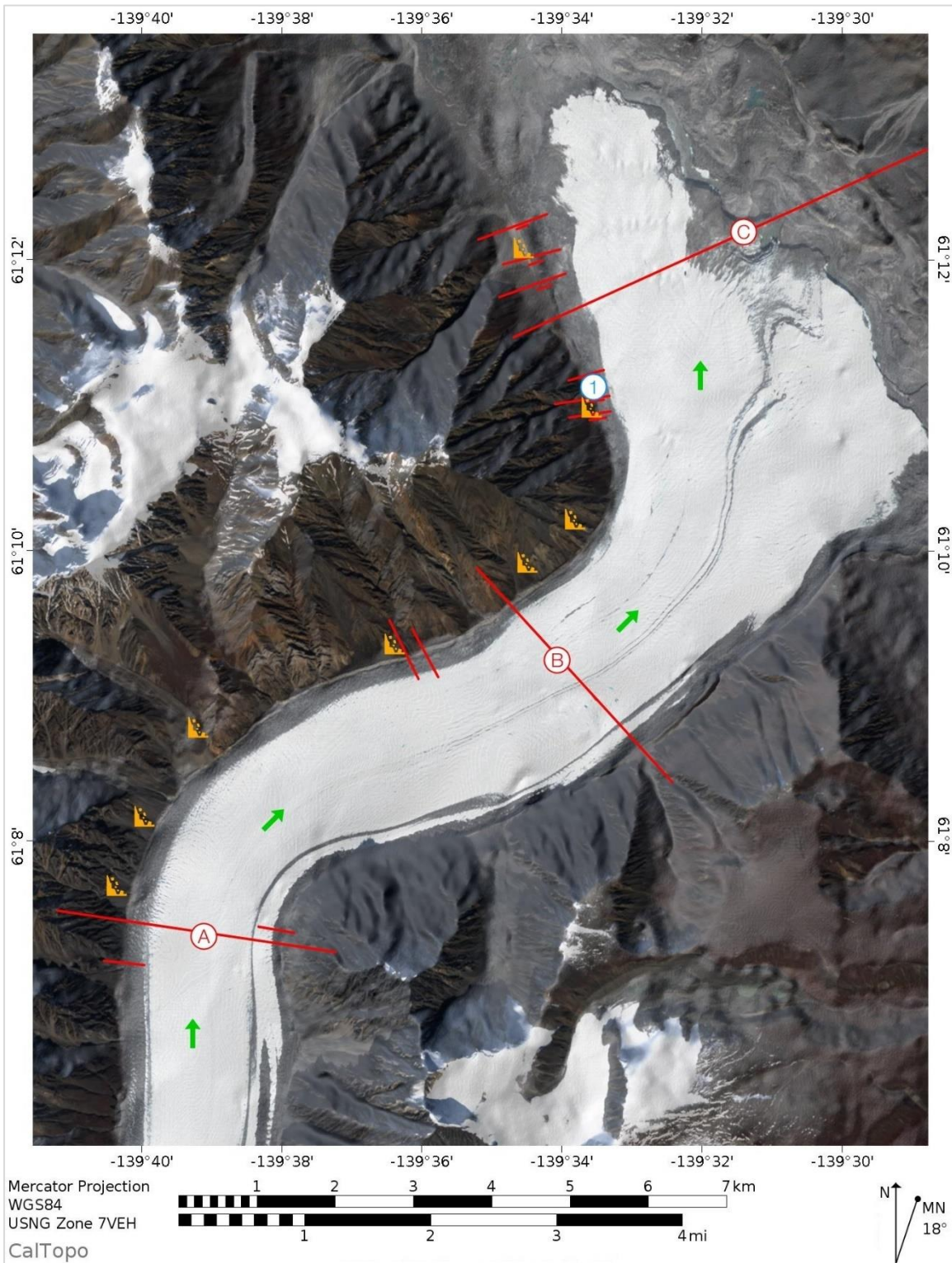


Figure 2.1: Mercator Map with Shaded Relief of Site ID 051 (Donjek Glacier) Created using CALTOPO Software.

Transect locations are notated with red lines, the gully locations are numbered in blue, fan locations are noted with an orange icon and the direction of glacier is indicated with green arrow.

A review of the data collected was completed, i.e. slope profiles developed using CALTOPO, the contour maps (also available in CALTOPO), the Google Earth image and the 3D model developed, using Trimbles software. Examples of the output data from third party GIS packages, i.e., Trimbles and CALTOPO software are illustrated in Figure 2.2 and Figure 2.3, respectively.

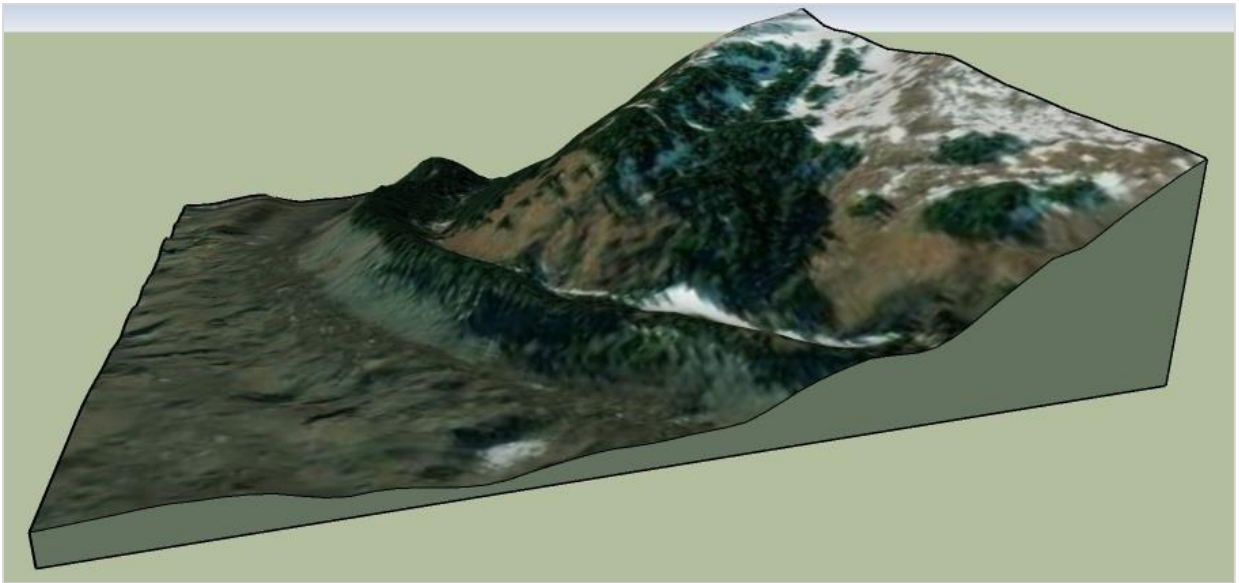
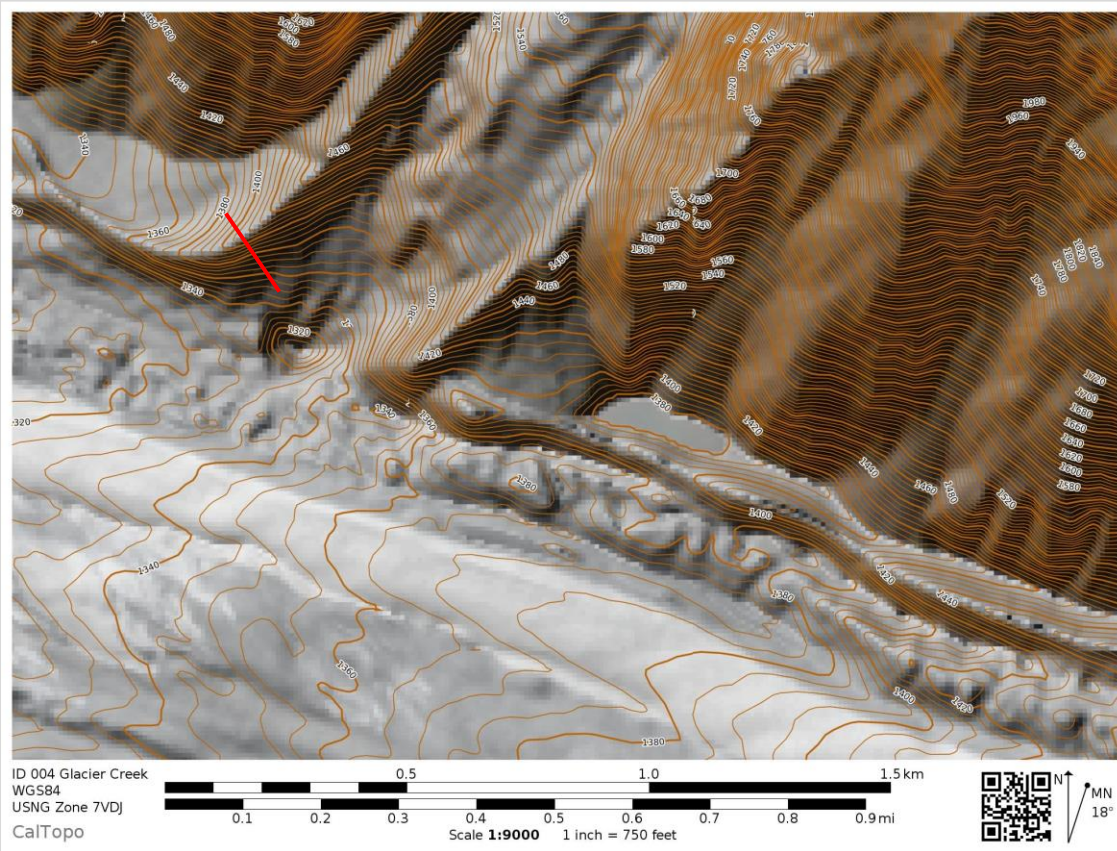


Figure 2.2: Example of the Trimbles SketchUp File for a Section of Study Site ID 007 (Otter Glacier).

a)



b)

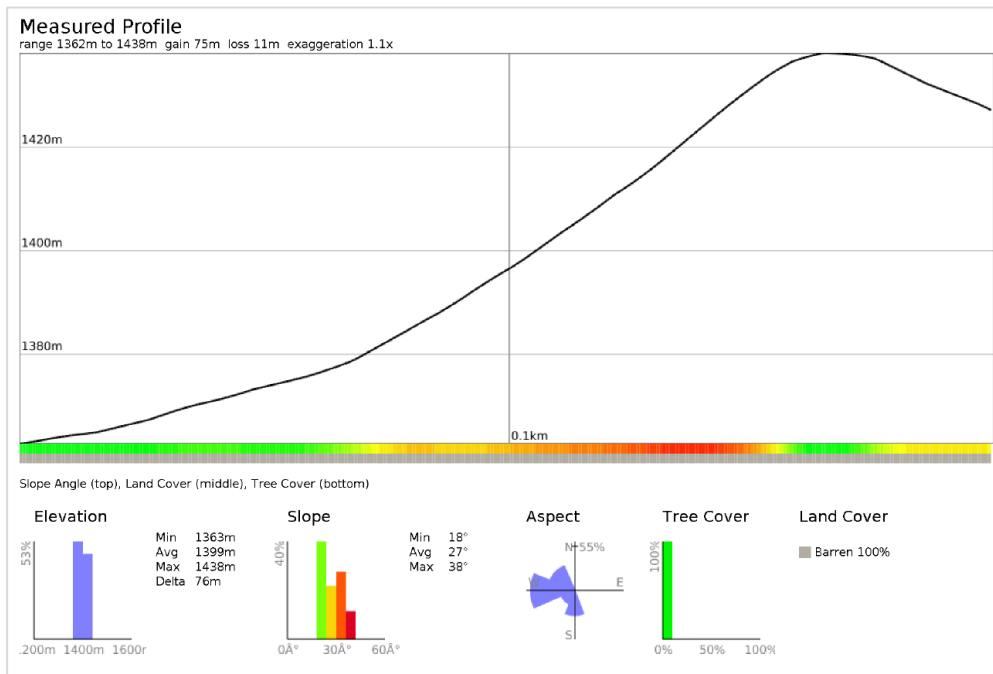


Figure 2.3: Examples of the Output Data from CALTOPO for Study Site ID 004 (Glacier Creek).
a) Mercator map with shaded relief and contour lines at 5 meter intervals and b) Elevation profile, for the red transect line on (a), with a heat line on the graph base representing slope angle.

2.3.3 Division of Study Sites by Geographic Region

This review elucidated that the sites could be divided based on location (geographically) because of geomorphologic similarity. The site that contained the most detailed geomorphological data of slope profiles was selected as the primary site. One or two sites from each location are used as the primary sites. The secondary sites are used for additional data. The list of primary sites and their secondary associated sites is summarized in Table 2.4. Sites 009, 010 and 011 are part of the same glacier trunk and tributary. However, there was limited data available as stand alone sites. Hence, these sites were combined for practical purposes.

Table 2.4: Study Sites.

| <i>Site ID</i> | <i>Name</i> | <i>Geographic Location</i> | <i>Primary Glacier</i> | <i>Secondary Glacier</i> |
|----------------|-------------------------|----------------------------|------------------------|--------------------------|
| 022 | Exploradores Glacier | Argentina | X | |
| 021 | Ventisquero Grosse | Argentina | | X |
| 007 | Otter Glacier | Alaska | X | |
| 009* | Matanuska Glacier | Alaska | X | |
| 010* | Matanuska Glacier | Alaska | X | |
| 011* | Matanuska Glacier | Alaska | X | |
| 004 | Glacier Creek | Alaska | | X |
| 006 | Fairweather Glacier | Alaska | | X |
| 055 | Easton Glacier | Continental USA | X | |
| 033 | Mt. Waddington A | Canada | X | |
| 050 | Tiedemann Glacier | Canada | X | |
| 051 | Donjek Glacier | Canada | X | |
| 028 | Bell Glacier | Canada | | X |
| 029 | Roovers Glacier | Canada | | X |
| 030 | Geddes Glacier | Canada | | X |
| 032 | Dorothy Glacier | Canada | | X |
| 048 | <i>Nagong</i> | China | X | |
| 034 | <i>Mount Everest</i> | China | X | |
| 056 | <i>Mount Everest -2</i> | China | | X |
| 012 | Tamdykul MTN | Tajikistan | X | |
| 041 | Virjerab Glacier | Afghanistan | X | |
| 046 | Shkuk Yoz Glacier | Afghanistan | X | |
| 036 | <i>Karakoram Range</i> | Asia | | X |
| 040 | <i>Karakoram Range</i> | Asia | | X |
| 045 | Lupghar Yaz Glacier | Afghanistan | | X |
| 054 | Findelengletscher | Switzerland | X | |
| 057 | Vadret da Tschierva | Switzerland | X | |
| 052 | Fee Glacier | Switzerland | | X |
| 053 | Tsidjiore Nouve | Switzerland | | X |
| 058 | Vadret Pers dams | Switzerland | | X |
| 059 | Vadret da Tschierva | Switzerland | | X |

Chapter 3

Paraglacial Reworking of Lateral Moraines

3.1 Introduction

Lateral moraine heights are typically less than 10-20 meters high in the extreme up-glacier section. However, larger lateral moraines are commonly perched along the margins of glaciers, with heights of more than 150 meters, near the terminus. Such moraines represent a major sediment sink and source. Over time, paraglacial reworking of the moraine slopes gives way to incised gullies of varying dimensions. Gullies are a land surface formed by the process of soil erosion. This erosion turns the sediment sink into a sediment source and modification of the lateral moraine slope angles.

3.2 Methods

Analysis ready data was utilized to document typical examples, analysis the typical setting and morphology and provide a quantitative comparative analysis of lateral moraines. This data contained pre-processed time-series stacks of overhead imagery. This analysis ready data was collected through various sources via a GIS of software packages. Three software packages were used for study site evaluation: 1) Google Earth, 2) CALTOPO and 3) Trimble SketchUp. These three programs were used extensively to either gather quantitative data or to make qualitative observations from a 2D or 3D perspective for each of the 31 sites listed in Table 2.4. Where possible, both quantitative data and qualitative observations for each of three study site sections (the up-glacier section, 'A', the mid-glacier section, 'B' and the down glacier section, 'C') were collected.

3.2.1 3D Analysis - Geographical Information Systems (GIS)

Google Earth and Trimble SketchUp are both simplified GIS software packages. Both were used to view the sites from a 3D perspective. They provided a means to gather quantitative data and make qualitative observations. The Google Earth 3D perspectives were limited to digital viewing, rendering accurate perspectives is not viable. This software provided a holistic view as well as particular elements of a study site. It also permitted the identification of study site elements to be modelled as digital elevation models in Trimble SketchUp software. Figure 2.2 is an example of the 3D model produced that permitted further quantitative and qualitative examination of the element.

3.2.2 Profile Generation - 2D Analysis Geographical Information Systems (GIS)

CALTOPO is a simplified GIS software package that was used extensively to view the sites from a 2D perspective. This software also provided a means to both gather quantitative data and make qualitative observations. Using this software, elevation profiles of the lateral moraines were generated to enable the two-dimensional analysis of the terrain. Profiles of the slopes were generated for a number of locations on the moraine. This software was also used to create a Mercator map for each of the study sites. A Mercator map of each the study sites is presented in the Appendix.

3.3 Results

3.3.1 Lateral Moraine Profiles

Three moraine cross-section profiles (up-glacier, mid-glacier, and down glacier) for each site were generated with Microsoft Excel using the data files from the CALTOPO software. The data is tabulated in Table 3.1. This data provided an overview of the moraine geometry

development over time. Specifically, the moraine height, the maximum angle of the proximal slope and the maximum angle of the distal slope for each of the three moraine profiles. This data also provided information on the changes in moraine geometry through paraglacial reworking. Additionally, comparison of moraine geometry between geographical settings could be analyzed.

Table 3.1: Moraine Profiles.

| Site ID | Name | Location | Down Glacier | | | Mid-glacier | | | Up-glacier | | |
|-------------|----------------------|-----------------|--------------------------------------|------------------------------------|------------|--------------------------------------|------------------------------------|------------|--------------------------------------|------------------------------------|------------|
| | | | Proximal Slope - Maximum Angle (Deg) | Distal Slope - Maximum Angle (Deg) | Height (m) | Proximal Slope - Maximum Angle (Deg) | Distal Slope - Maximum Angle (Deg) | Height (m) | Proximal Slope - Maximum Angle (Deg) | Distal Slope - Maximum Angle (Deg) | Height (m) |
| 022 | Exploradores Glacier | Argentina | 30 | 0 | 70 | 29 | 0 | 57 | 25 | 6 | 37 |
| 021 | Ventisquero Grosse | Argentina | 28 | 15 | 185 | 26 | 0 | 160 | 40 | 0 | 153 |
| 007 | Otter Glacier | Alaska | 41 | 22 | 75 | 45 | 16 | 62 | 51 | 22 | 84 |
| 009/010/011 | Matanuska Glacier | Alaska | 31 | 00 | 75 | 36 | 0 | 53 | 45 | 10 | 45 |
| 004 | Glacier Creek | Alaska | NA | 0 | 0 | 34 | 0 | 67 | 39 | 22 | 51 |
| 006 | Fairweather Glacier | Alaska | 45 | 26 | 100 | 44 | 35 | 80 | 45 | 30 | 73 |
| 055 | Easton Glacier | Continental USA | 42 | 40 | 73 | 45 | 25 | 85 | 40 | 35 | 23 |
| 033 | Mt. Waddington A | Canada | 28 | 22 | 73 | 27 | 20 | 89 | 25 | 0 | 95 |
| 050 | Tiedemann Glacier | Canada | 45 | 0 | 180 | 31 | 6 | 80 | 32 | 0 | 68 |
| 051 | Donjek Glacier | Canada | 34 | 00 | 40 | 40 | 0 | 40 | 10 | 0 | 10 |
| 028 | Bell Glacier | Canada | 46 | 0 | 100 | 34 | 0 | 100 | 33 | 0 | 60 |
| 029 | Roovers Glacier | Canada | 17 | 16 | 33 | 22 | 10 | 64 | 16 | 9 | 24 |
| 030 | Geddes Glacier | Canada | 24 | 0 | 72 | 24 | 0 | 60 | 26 | 16 | 105 |
| 032 | Dorothy Glacier | Canada | 20 | 0 | 72 | 36 | 0 | 150 | 36 | 0 | 160 |
| 048 | Nagong | China | 32 | 12 | 98 | 22 | 0 | 25 | 8 | 0 | 15 |
| 034 | Mount Everest | China | 24 | 0 | 110 | 27 | 0 | 95 | 16 | 0 | 30 |
| 056 | Mount Everest -2 | China | 24 | 0 | 30 | 12 | 7 | 35 | 13 | 12 | 40 |
| 012 | Tamdykul MTN | Tajikistan | 22 | 0 | 80 | 22 | 0 | 75 | 19 | 0 | 50 |
| 041 | Virjerab Glacier | Afghanistan | 6 | 0 | 25 | 18 | 0 | 6 | 14 | 0 | 10 |
| 046 | Shkuk Yoz Glacier | Afghanistan | 24 | 0 | 110 | 12 | 0 | 30 | 6 | 0 | 20 |
| 036 | Karakoram Range | Asia | 18 | 0 | 55 | 14 | 0 | 30 | 11 | 0 | 10 |
| 040 | Karakoram Range | Asia | 33 | 0 | 70 | 10 | 0 | 25 | 10 | 0 | 20 |
| 045 | Lupghar Yaz Glacier | Afghanistan | 30 | 00 | 100 | 18 | 0 | 30 | 10 | 0 | 30 |
| 054 | Findelengletscher | Switzerland | 42 | 24 | 82 | 40 | 36 | 87 | 50 | 42 | 106 |
| 057 | Vadret da Tschierva | Switzerland | 40 | 20 | 125 | 37 | 16 | 56 | 40 | 0 | 60 |
| 052 | Fee Glacier | Switzerland | 32 | 20 | 85 | 32 | 20 | 40 | 25 | 0 | 20 |
| 053 | Tsidjiore Nouve | Switzerland | 15 | 36 | 17 | 24 | 30 | 14 | 15 | 38 | 15 |
| 058 | Vadret Pers dams | Switzerland | 49 | 10 | 122 | 51 | 41 | 90 | 49 | 35 | 54 |
| 059 | Vadret da Tschierva | Switzerland | -- | -- | -- | 41 | 0 | 125 | 51 | 0 | 82 |

3.3.2 Lateral Moraine Setting

Additional general data related to the moraine setting was also collected and tabulated in Table 3.2. The moraine lateral slope and glacier lateral slope was determined based on the change in elevation over a selected glacier length between the up-glacier and down glacier positions. The moraine angle recorded is the maximum slope angle measured on the proximal slope. The moraine height recorded is the maximum height recorded above either the valley floor or glacier surface. A graphic illustration of these data records is presented in Figure 3.1. This data was used to evaluate the change in the moraine height in relation to glacier length.

Table 3.2: Moraine Site Particulars.

| <i>Site ID</i> | <i>Glacier lateral Slope (deg)</i> | <i>Length (m)</i> | <i>Elevation (m)</i> | <i>Moraine lateral Slope (deg)</i> | <i>Moraine Angle (deg)</i> | <i>Moraine Height (m)</i> |
|----------------|------------------------------------|-------------------|----------------------|------------------------------------|----------------------------|---------------------------|
| 050 | 3.5 | 5250 | 1300 | 3.7 | 45 | 150 |
| 004 | 2.2 | 13000 | 1500 | 3.2 | 38 | 50 |
| 006 | 4.3 | 12000 | 1000 | 2.5 | 49 | 80 |
| 007 | 3.1 | 11000 | 1000 | 2.74 | 50 | 80 |
| 009/010/011 | 2.8 | 8000 | 1200 | 2.2 | 43 | 50 |
| 012 | 7.8 | 2000 | 2800 | | 34 | 35 |
| 021 | 1.9 | 9000 | 600 | | 45 | 180 |
| 022 | 3.5 | 4000 | 450 | | | |
| 028 | 6.25 | 3200 | 1450 | 5.2 | 36 | 140 |
| 029 | 8 | 2350 | 1600 | 7.5 | 25 | 62 |
| 030 | 13 | 1000 | 2000 | 12.5 | 24 | 70 |
| 032 | 8.6 | 2500 | 1700 | 5.8 | 36 | 190 |
| 033 | 10 | 1500 | 1500 | 13 | 33 | 125 |
| 034 | 3.7 | 13000 | 5000 | 3 | 34 | 65 |
| 036 | 14 | 1000 | 5700 | | | |
| 040 | 7.7 | 1500 | 5600 | | | |
| 041 | 2.3 | 2500 | 4600 | | 55 | 165 |
| 045 | 4.6 | 5000 | 4200 | | 24 | 25 |
| 046 | 2.5 | 9750 | 4200 | | | |
| 048 | 7.7 | 3250 | 4200 | 5.8 | 42 | 45 |
| 051 | 2 | 10000 | 1500 | 1 | 24 | 25 |
| 052 | 11 | 2000 | 2150 | | | |
| 053 | 9.5 | 1750 | 2500 | | | |
| 054 | 9.5 | 2000 | 2800 | | 42 | 80 |
| 055 | 8.5 | 2000 | 1700 | | 53 | 100 |
| 056 | 3.8 | 3000 | 4500 | | | |
| 057 | 11 | 3500 | 2500 | | 40 | 40 |
| 058 | 9.5 | 3000 | 2500 | | 48 | 140 |
| 059 | 7.1 | 2000 | 2400 | | 35 | 75 |

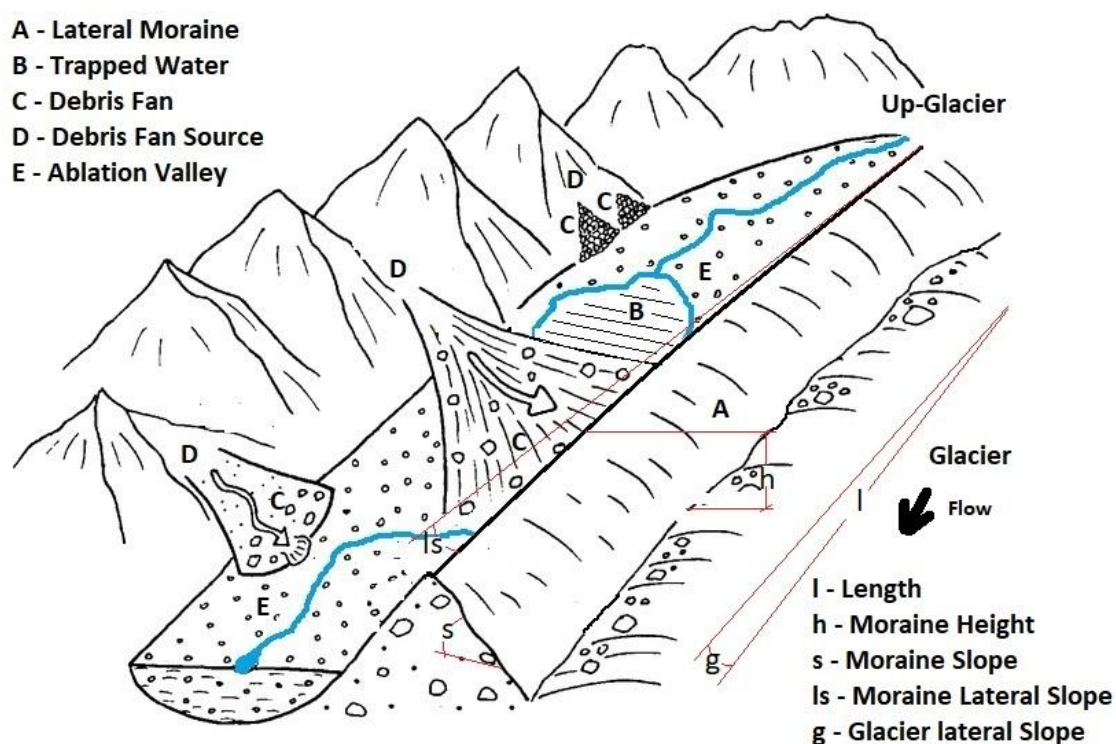


Figure 3.1: Moraine Setting Graphic Illustration.

The primary intent was to identify any relationship between moraine height and the moraine proximal slope angle up-glacier through the moraine length.

3.3.3 Morphological Descriptors of Gullies

Data was collected on a sample of 40 gully sections from various locations on the study sites, where obtainable. The data collected included the mean frequency of gullies, the moraine height and the gully length. The gully density per 100 meters sections was derived from 200 meter gully sections. The width of the gullies was determined based on the number of gullies per 100 meter section. The gully length is the vertical length of the gully measures from the lowest section to the top of the moraine. It was not possible to determine the depth of the gullies due to the image resolution. The results are tabulated in Table 3.3. Primarily, the intent was to look for

relationship between gully incision and lateral moraine height. Study sites that did not present gullies were omitted from the table.

Table 3.3: Morphological Details of Gullies.

| Site | Name | Location | Down Glacier | | | | | Mid-Glacier | | | | | Up-Glacier | | | | |
|------|------------------------------|-------------|--------------------|------------------|-----------------|-------------------|--------------------|--------------------|------------------|-----------------|-------------------|--------------------|--------------------|------------------|-----------------|-------------------|--------------------|
| | | | Density (# / 100m) | Gully Length (m) | Gully Width (m) | Gully Slope (deg) | Moraine Height (m) | Density (# / 100m) | Gully Length (m) | Gully Width (m) | Gully Slope (deg) | Moraine Height (m) | Density (# / 100m) | Gully Length (m) | Gully Width (m) | Gully Slope (deg) | Moraine Height (m) |
| 050 | Tiedemann Glacier | Canada | 4 | 62 | 25 | 45 | 150 | 7 | 57 | 14 | 35 | 74 | 7 | 28 | 14 | 22 | 38 |
| 006 | Fairweather Glacier | Alaska | 5 | 47 | 20 | 46 | 85 | NA | NA | NA | NA | NA | NA | NA | NA | NA | NA |
| 007 | Otter Glacier | Alaska | NA | NA | NA | NA | NA | NA | NA | NA | NA | NA | 10 | 13 | 10 | 39 | 53 |
| 009 | Matanuska Glacier | Alaska | 11 | 25 | 9 | 43 | 56 | 15 | 9 | 5 | 41 | 36 | 20 | 6 | 4 | 33 | 28 |
| 012 | Tamdykul MTN | Tajikistan | NA | NA | NA | NA | NA | 8 | 32 | 12.5 | 34 | 48 | 10 | 12 | 10 | 30 | 48 |
| 021 | Ventisquero Grosse | Argentina | 3 | 150 | 33 | 45 | 180 | NA | NA | NA | NA | NA | NA | NA | NA | NA | NA |
| 028 | Bell Glacier | Canada | NA | NA | NA | NA | NA | NA | NA | NA | NA | NA | 6 | 58 | 17 | 36 | 110 |
| 029 | Roovers Glacier | Canada | NA | NA | NA | NA | NA | 10 | 12 | 10 | 20 | 62 | 7 | 11 | 14 | 24 | 37 |
| 032 | Dorothy Glacier | Canada | NA | NA | NA | NA | NA | 5 | 76 | 20 | 36 | 150 | 8 | 71 | 12.5 | 31 | 84 |
| 033 | Mt. Waddington A | Canada | 7 | 39 | 14 | 30 | 67 | 5 | 30 | 20 | 28 | 72 | 2 | 65 | 50 | 33 | 125 |
| 034 | Mount Everest | China | 19 | 19 | 5 | 30 | 49 | 8 | 30 | 12.5 | 34 | 63 | 14 | 17 | 7 | 28 | 27 |
| 041 | Virjerab Glacier | Afghanistan | 6 | 125 | 16.5 | 55 | 165 | 15 | 6 | 6.5 | NA | 8 | 6 | 6 | 17 | NA | 8 |
| 045 | Lupghar Yaz Glacier | Afghanistan | NA | NA | NA | NA | NA | NA | NA | NA | NA | NA | 10 | 15 | 10 | 24 | 15 |
| 046 | Shkuk Yoz Glacier | Afghanistan | NA | NA | NA | NA | NA | NA | NA | NA | NA | NA | 19 | 4 | 5 | NA | 5 |
| 048 | Nagong, China | China | 7 | 30 | 14 | 42 | 44 | NA | NA | NA | NA | NA | NA | NA | NA | NA | NA |
| 051 | Donjek Glacier | Canada | 3 | 21 | 33 | 27 | 24 | NA | NA | NA | NA | NA | NA | NA | NA | NA | NA |
| 054 | Findelengletscher | Switzerland | 10 | 72 | 10 | NA | 78 | 10 | 70 | 10 | 42 | 80 | 18 | 43 | 5.5 | 28 | 50 |
| 055 | Easton Glacier | USA | 7 | 55 | 14 | 53 | 85 | NA | NA | NA | NA | NA | 20 | 34 | 5 | 48 | 55 |
| 057 | Vadret da Tschierva, Grisons | Switzerland | 8 | 50 | 12.5 | 40 | 50 | NA | NA | NA | NA | NA | 12 | 27 | 8.5 | NA | 50 |
| 058 | Vadret Pers dams | Switzerland | 7 | 71 | 14 | 48 | 138 | 12 | 34 | 8.5 | 35 | 74 | 20 | 11 | 5 | 20 | 15 |
| 059 | Vadret da Tschierva | Switzerland | NA | NA | NA | NA | NA | NA | NA | NA | NA | NA | 10 | 40 | 10 | 35 | 75 |

3.4 Analysis

3.4.1 Morphology of Distal and Proximal Slopes

Lateral moraines extend from the contemporary equilibrium line as non-continuous, ridges that increase down glacier in height. Their morphological features are illustrated in Figure 3.2. Lateral moraines are typically less than 20 meters high in the extreme up-valley section.

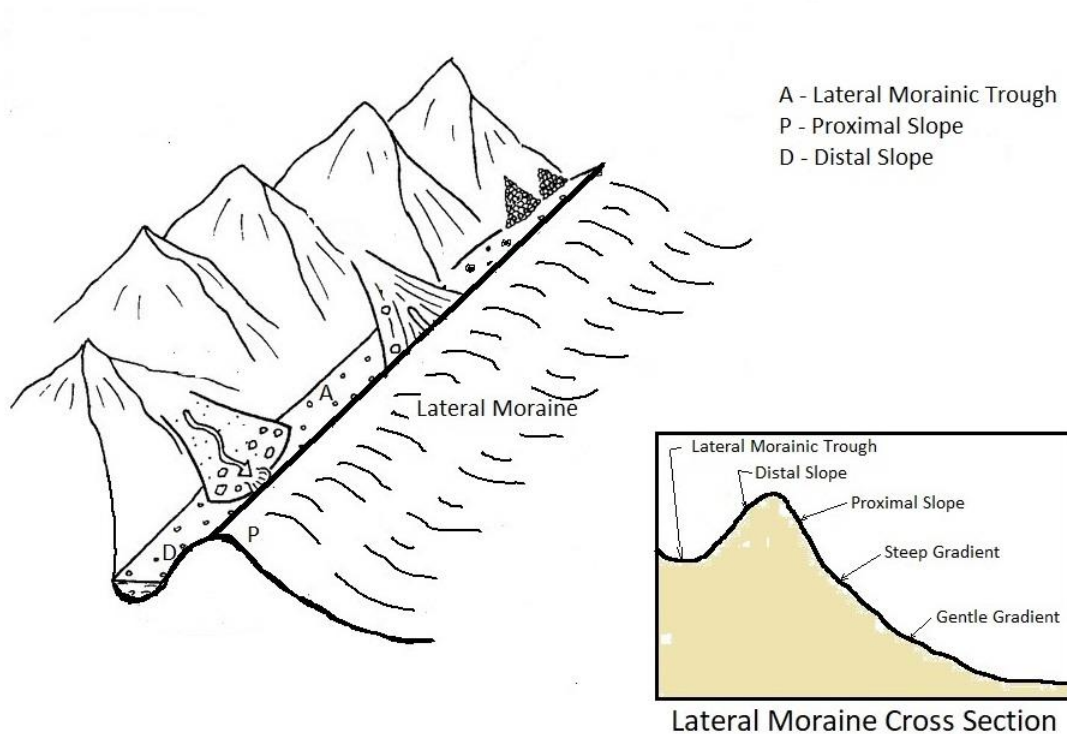


Figure 3.2 Moraine Morphological Features.

They may have little or no distal slope. Relationships between the glacier lateral slope vs the moraine lateral slope (defined in section 3.3.2) were investigated. A plot of the moraine lateral slope versus the glacier lateral slope data (Table 3.2) was generated using Microsoft Excel to

quantitatively analyze this tabulated data, as illustrated in Figure 3.3. The trendline indicates that their slopes are diverging. The lateral slope of the glacier has a slightly higher slope angle.

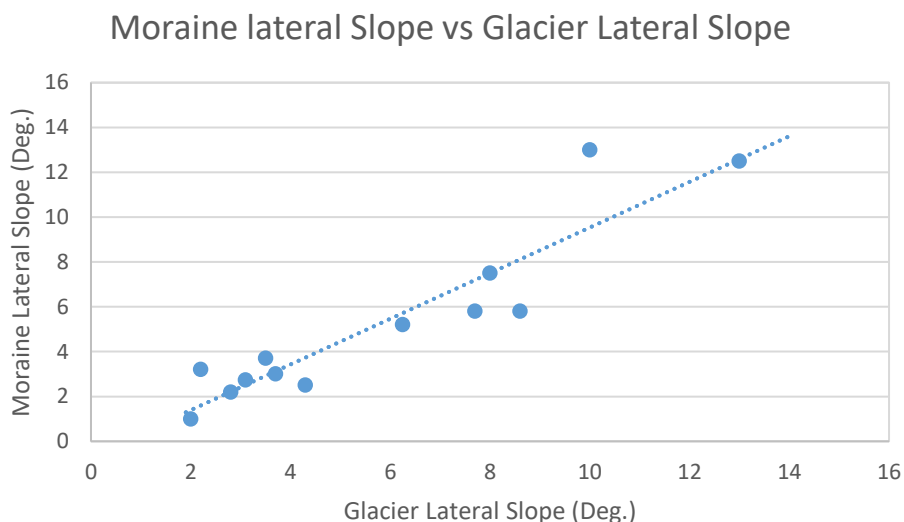


Figure 3.3: Moraine Lateral Slope vs. Glacier Lateral Slope.

Moving down valley, moraines become increasingly separated from the valley wall. Thus, forming lateral morainic troughs, separating the lateral moraine from valley side slopes, which act as gutters for glacial sediment and slope debris derived from the valley side. They are a feature of many sites investigated. This slope debris is transported by processes including rock fall, debris flow, snow avalanche and fluvial transport. The trough may contain ponds between larger obstructions in the lateral morainic trough, as illustrated in Figure 3.1. The infill by debris decreases the trough depth locally and, in some cases, completely infills the trough. In such cases the distal slope of the moraine is adjusted accordingly by the slope debris infill.

Following glacier thinning and retreat, lateral moraines are abandoned, and their proximal and distal slopes are subject to paraglacial reworking. Paraglacial reworking frequently gives rise to dissection of proximal moraine slopes and redistribution of sedimentary materials. Typical slope profiles, with the crest of the moraine centered at zero, of the up-glacier moraine, mid-glacier and down-glacier for the study sites are illustrated in Figure 3.4.

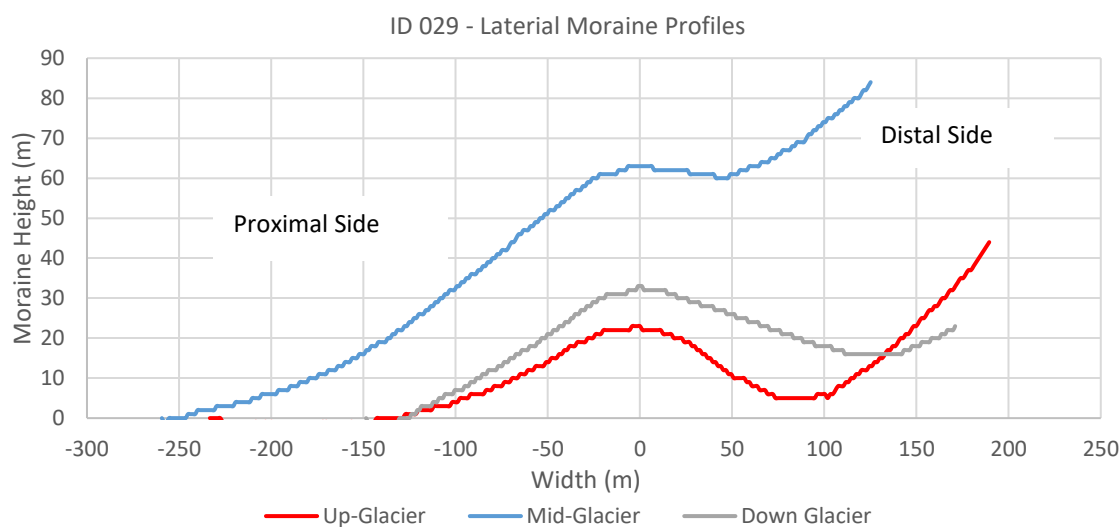


Figure 3.4: Lateral Moraine Profiles (Up-Glacier, Mid-Glacier and Down Glacier) for Study Site ID 029 – Roovers Glacier, BC.

Debris flow delivers material to the lateral moraine slope foot. Thus, progressively infilling slope units, reducing slope gradient, reducing proximal upslope sediment supply and potentially facilitates slope stability. It is visually obvious from the moraine profiles of study site 033 presented in Figure 3.5 that, moving down glacier, the lower section is being infilled. This redistribution is present in the slope profile for a number of the study sites. This dissection provides evidence of paraglacial reworking through the resultant redistribution and transfer of sediment from the upper section to the lower proximal slope sections of the moraine. This also illustrates the asymmetry of the lateral moraine throughout its length.

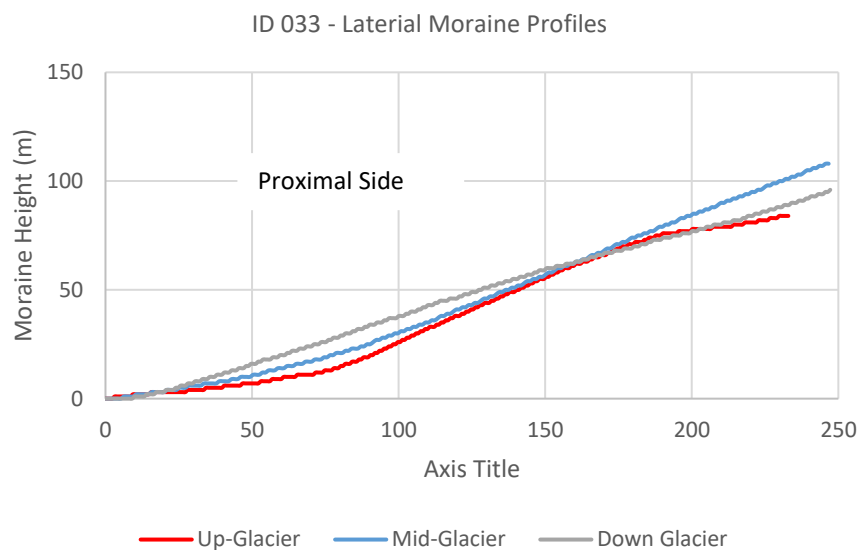


Figure 3.5: Lateral Moraine Profiles (Up-Glacier, Mid-Glacier and Down Glacier) for Study Site ID 029 – Roovers Glacier, BC. Proximal Side.

There is also a general impression of asymmetry across the opposing lateral moraines. Although, it should be noted that cross-sectional asymmetry is not a ubiquitous observation. Analysis of the cross-sectional distribution of the opposing lateral moraines were investigate on the down glacier section of study site ID 055 (Easton Glacier) (Figure 3.6). The area of the negative space, the area bound by the maximum height and the proximal profile for the opposing moraines, was calculated. The difference in square area of these two sections amounts to 13%. This may indicate that the amount of sediment deposited is somewhat equal, but that the distribution varies on opposing lateral moraines.

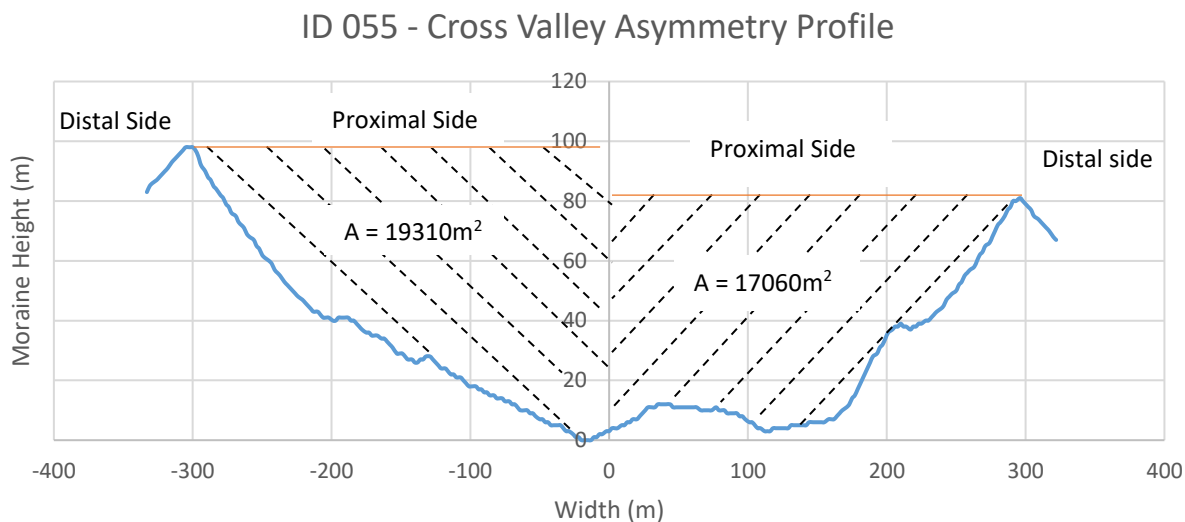


Figure 3.6: Cross Valley Asymmetry in the Down Glacier Section on Study Site ID 055 – Easton Glacier.

Various explanations may account for the varied height and asymmetry of opposing lateral moraines Benn (1989):

1. Greater delivery from debris slides to one side.
2. Pushing or thrusting of pre-existing materials.
3. Cross-valley differences in lithology or structure.
4. Differences in cross-valley glacier dynamics.

However, as was illustrated, ubiquitous asymmetry observation across the valley profiles may just be related to shape. The impression of asymmetry may be due the pattern of deposition.

3.4.2 Morphology of Gullies

A series of plots were generated using Microsoft Excel. The purpose was to analyze the tabulated data presented in Table 3.3. The following graphs were plotted for up-glacier, the mid-glacier and down glacier sections: Gully Length versus Moraine Height (Figure 3.7), Gully Slope versus Moraine Height (Figure 3.8), Gully Width versus Moraine Height (Figure 3.9) and a

graph of the combined trendlines for the each section (Figures 3.7.d, 3.8.d, & 3.9.d), in order to achieve this analysis. The trendline for gully length versus moraine height (Figure 3.7.d) indicates that the gully length increases with moraine height at a relatively constant rate. The trendlines for gully slope versus moraine height (Figure 3.8.d) indicates that the gully slope increases with moraine height both up-glacier and down glacier. There is relatively no change in the gully slope at mid-glacier relative to the moraine height. Gully width versus moraine height (Figure 3.9.d) indicate that width increases with height, but that there is no statistical correlation relative to the position of the gullying on the lateral moraine.

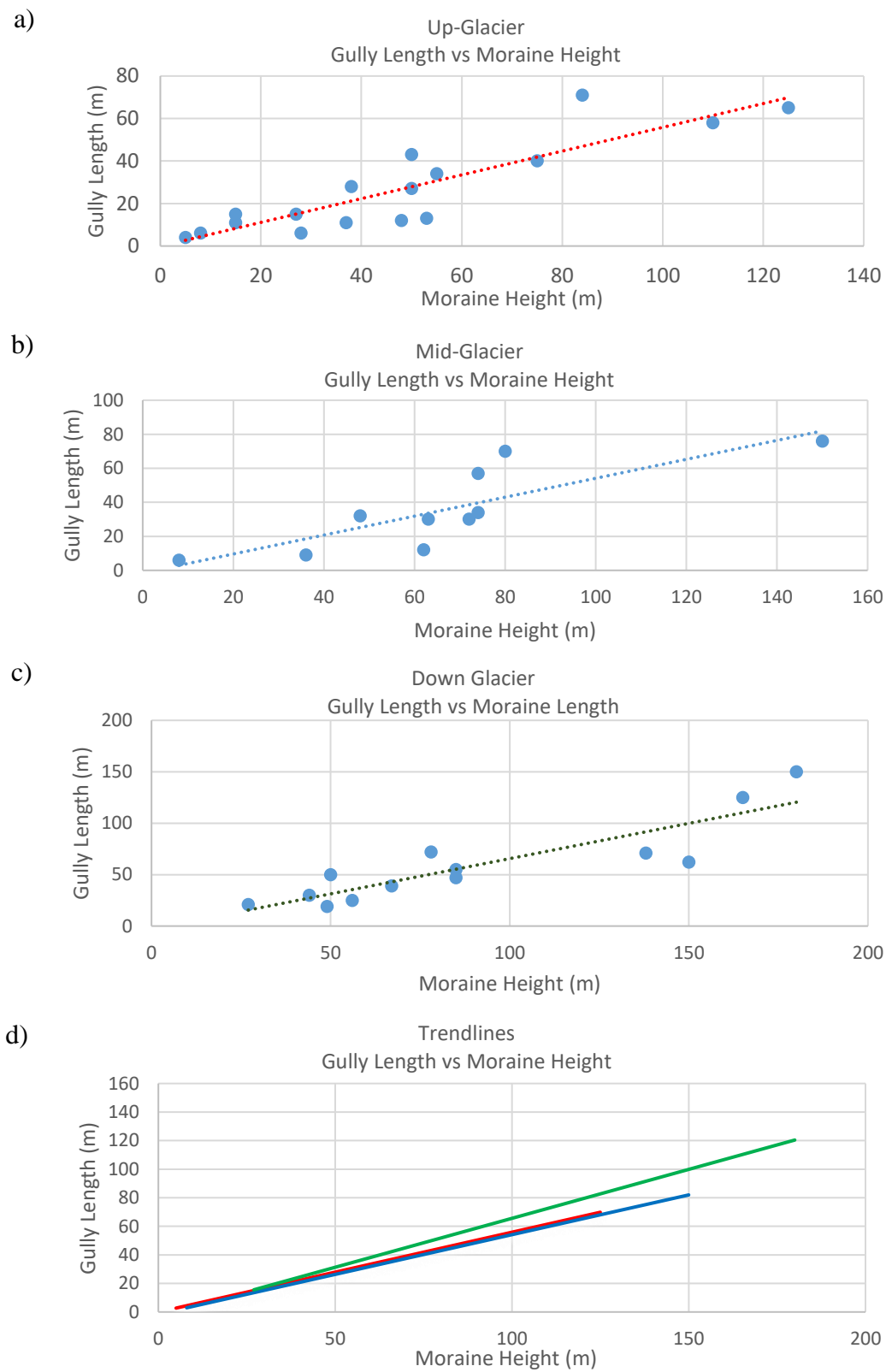


Figure 3.7: Gully Length vs. Moraine Height.
a) Up-Glacier, b) Mid-Glacier, c) Down Glacier and d) Trendlines (Up-Glacier - Red Line, Mid-Glacier- Blue Line and Down Glacier - Green Line).

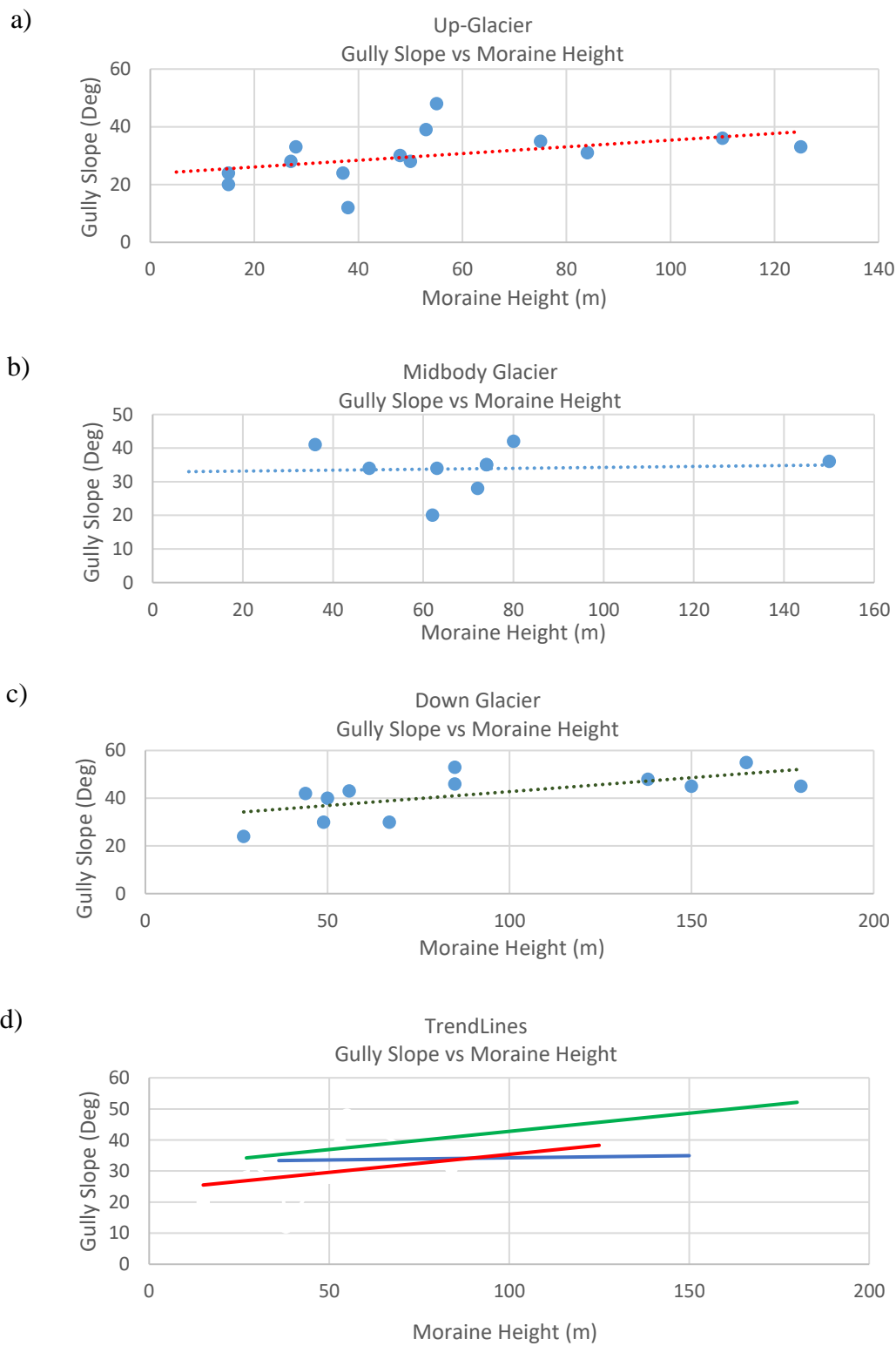


Figure 3.8: Gully Slope vs. Moraine Height. a) Up-Glacier, b) Mid-Glacier, c) Down Glacier and d) Trendlines (Up-Glacier - Red Line, Mid-Glacier- Blue Line and Down Glacier - Green Line).

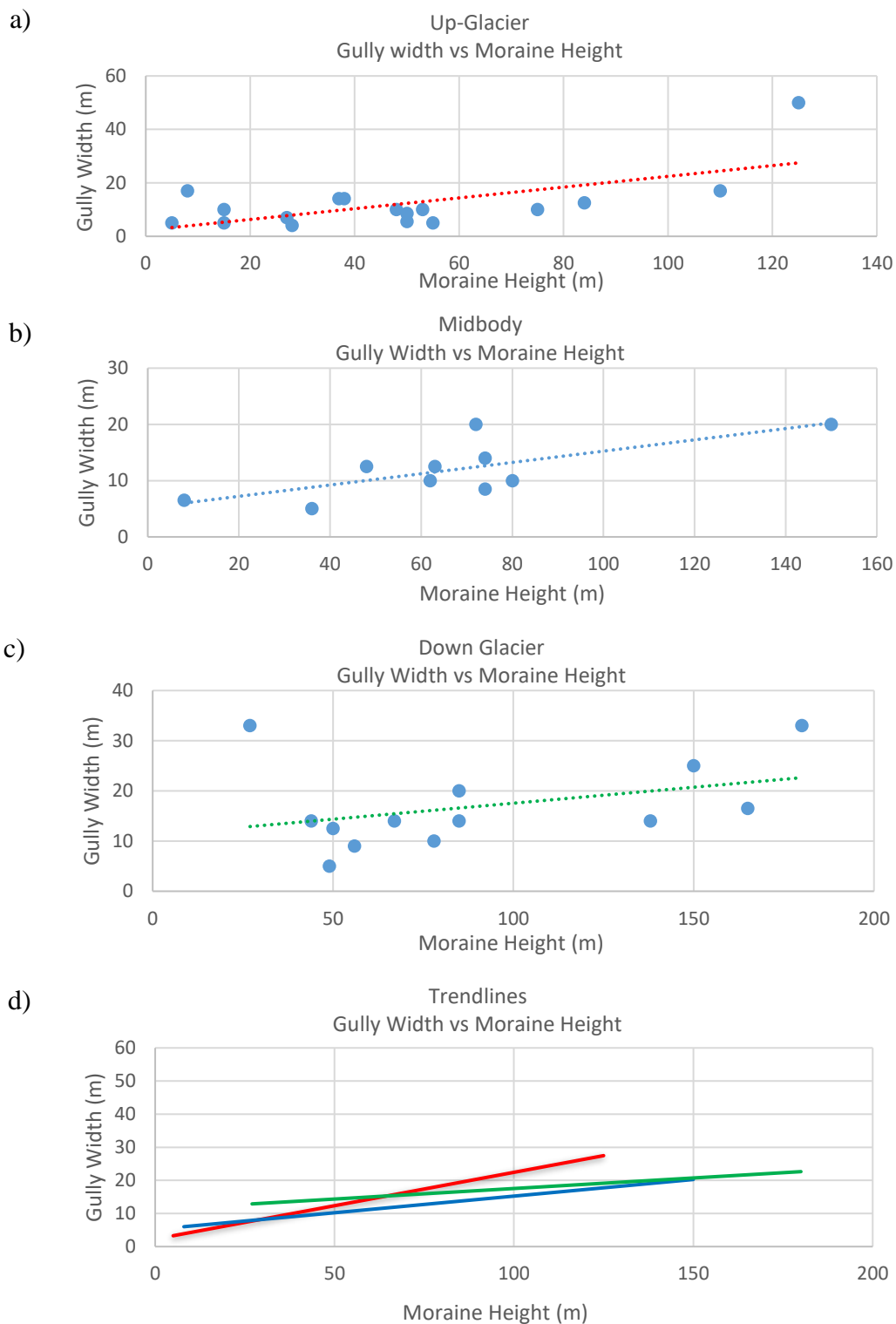


Figure 3.9: Gully Width vs. Moraine Height.
 a) Up-Glacier, b) Mid-Glacier, c) Down Glacier and d) Trendlines (Up-Glacier - Red Line, Mid-Glacier- Blue Line and Down Glacier - Green Line).

3.4.3 Paraglacial Reworking Through Gullies

Gully development is regarded as the result of surface erosion. The dissection of moraine slopes through paraglacial reworking is frequently exhibited in the formation of gullies by slope wash processes. This is exhibited through the reworking and redistribution of the upper sections of the lateral moraines primarily on the proximal slope by way of gulling. Gullies generally appear at a higher density rate in the up-glacier position as opposed to a lower density rate in the down glacier position where they are more frequently reworked by erosion over time. Typically, gully density decreases down glacier. In the down glacier position the gullies are generally larger. While the number of gullies per linear length of moraine decreases down glacier, they are still clustered together as illustrated in Figure 3.10.

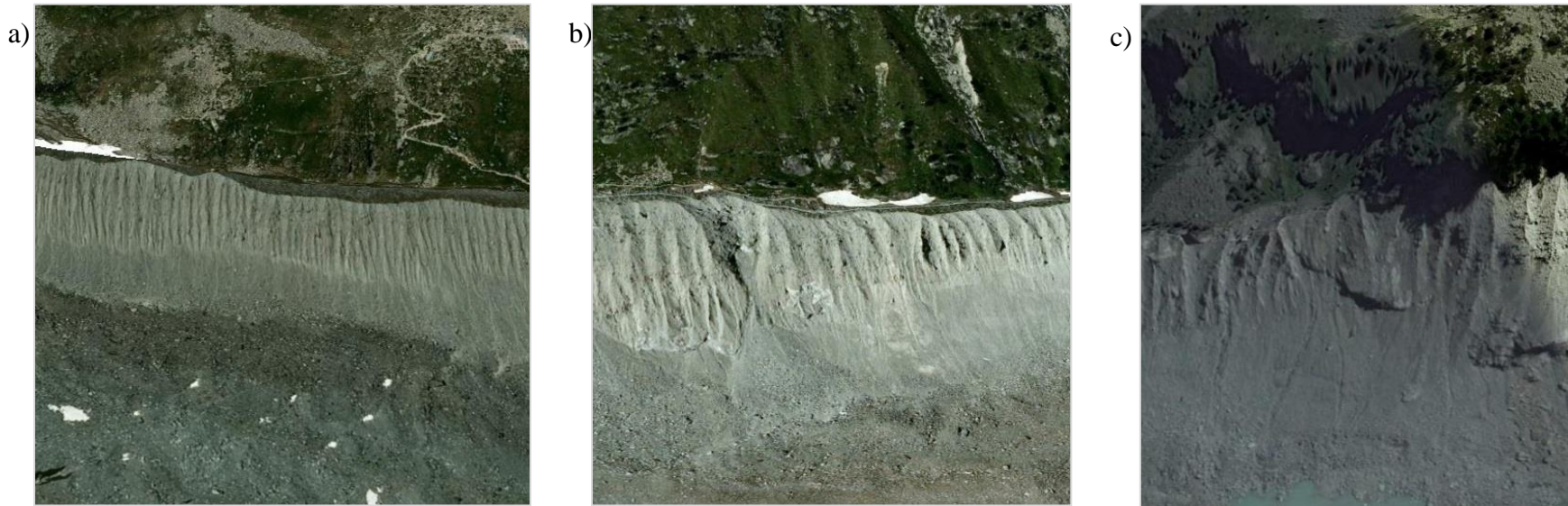


Figure 3.10: Photos Capture in Google Earth, of the Gullied Lateral Moraine of Site ID 057 (Vadret da Tschierva, Grisons).

a) is in the up-glacier section, where the gully density is 20 gillies per 100 meter (200/kilometer), b) is in the mid-glacier section where the gully density is 20 gillies per 100 meter (200/kilometer) and c) is in the down glacier position where the gully density is 7 gillies per 100 meter (70/kilometer).

Retrieved November 23, 2019 from <https://goo.gl/maps/2Pc7VbmHdp1wucgz7>.

The change in the geometry of the proximal slope through the redistribution of the upper slope sediment to the lower sections of the proximal slope is of particular note. Down glacier the proximal slope conforms to a more consistent gentler slope profile. Additionally there are localized sections of the lateral moraine that are more intensely gullied as a result of the infill of the lateral morainic trough and the resulting redistribution of water. The lateral morainic trough acts as a medium to convey adjacent valley wall slope water run-off down glacier laterally along the periphery of the glacier. The infill of the lateral morainic trough by debris or changes in the path creates a restriction whereby fluvial erosion of the proximal slope through the creation of gullies is intensified. An example of this is illustrated in Figure 3.11.

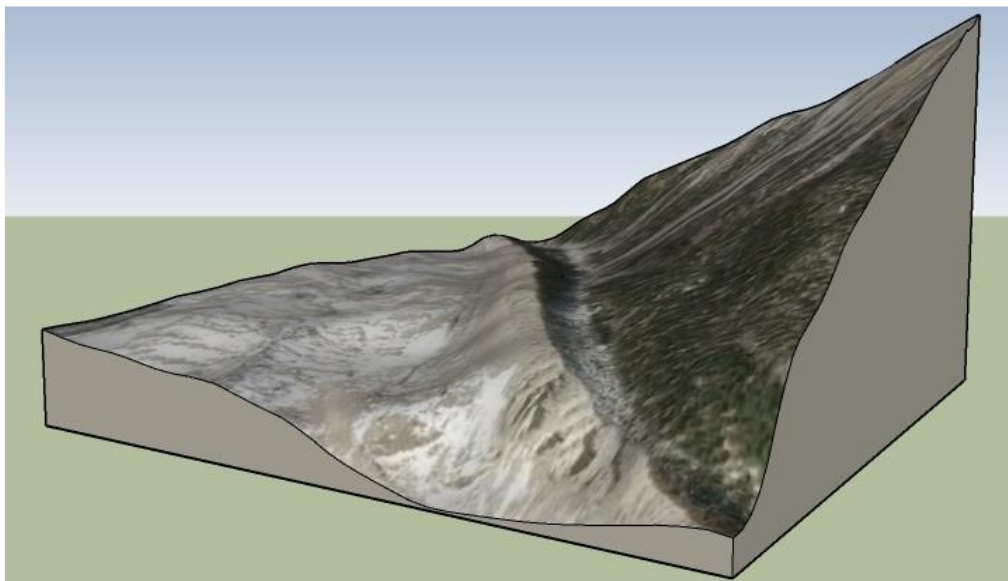


Figure 3.11: Increased Gully Activity at a Change in Lateral Morainic Trough Path from Study Site ID 048 (Nagong, China).

The gullying stage is characterized by debris flow processes. Upper proximal slopes can start to incise by slope wash processes during deglaciation. Later gullying, inter-gully walls (arêtes) develop (Curry et al., 2006). Debris flow deposits accumulate at slope foot positions with on-going glacier retreat. Gullies reach their maximum size and density within the first decades following glacier retreat (Curry et al., 2006), with highest sediment transport rates

shortly after deglaciation (Curry et al., 2009). Subsequently, incision decreases, and gullies widen. Lateral moraine slope gradients decrease most strongly in the gullying stage as a result of these processes (Curry et al., 2006). With decreasing sediment transport in the late gullying stage, the establishment threshold for ecosystem engineer species can be crossed. Once ecosystem engineer species manage to establish successfully and cover a certain area (35%, engineering threshold), the system moves into the biogeomorphic feedback window (Eichel et al., 2016). Ecosystem engineering induces a change from slope wash to solifluction processes (Eichel et al., 2016) and paraglacial adjustment transitions to a second stage. This is characterized by strongly decreasing sediment transport associated with solifluction processes. Which is consistent with findings by Curry et al. (2006) suggesting a duration of several decades to one century for the gullying stage. When gullying activity decreases due to decreasing slope gradient, a transition occurs, ecosystem engineering and unbound solifluction processes become dominant. These final stages are evident in the down glacier section on some sites. An example is illustrated in Figure 3.12.

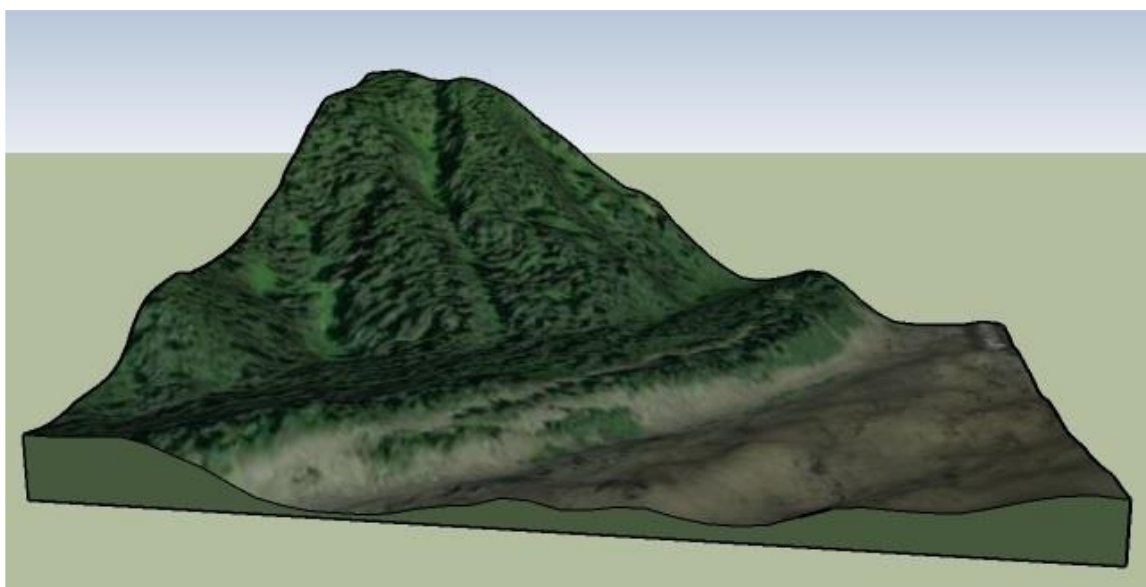


Figure 3.12: Ecosystem Engineering and Unbound Solifluction Processes Dominant from Study Site ID 007 (Otter Glacier).

Chapter 4

Alluvial Fans and Debris Flow Fans Buttressed by Lateral Moraines

4.1 Introduction

Alluvial and debris flow fans are fan-shaped landforms created over time by deposition of eroded sediment in an open valley. Specifically, in this study, they are buttressed by lateral moraines. Alluvial fans are gently sloping, fan-shaped landforms common at the base of deglaciating valley walls. Debris flow fans occur where sediment transport is triggered by the collapse of an accumulation of weathered rock, soil, or sediment in a steep source region. This creates a steep accumulation of sediment. The fans generally are composed with a fluvial component. These steep sloped debris flow fans migrate over time to larger gentler sloping alluvial fans with the continued deposition of eroded sediment. A typical study site example with alluvial and debris flow fans buttressed by a lateral moraine is captured in Figure 4.1.

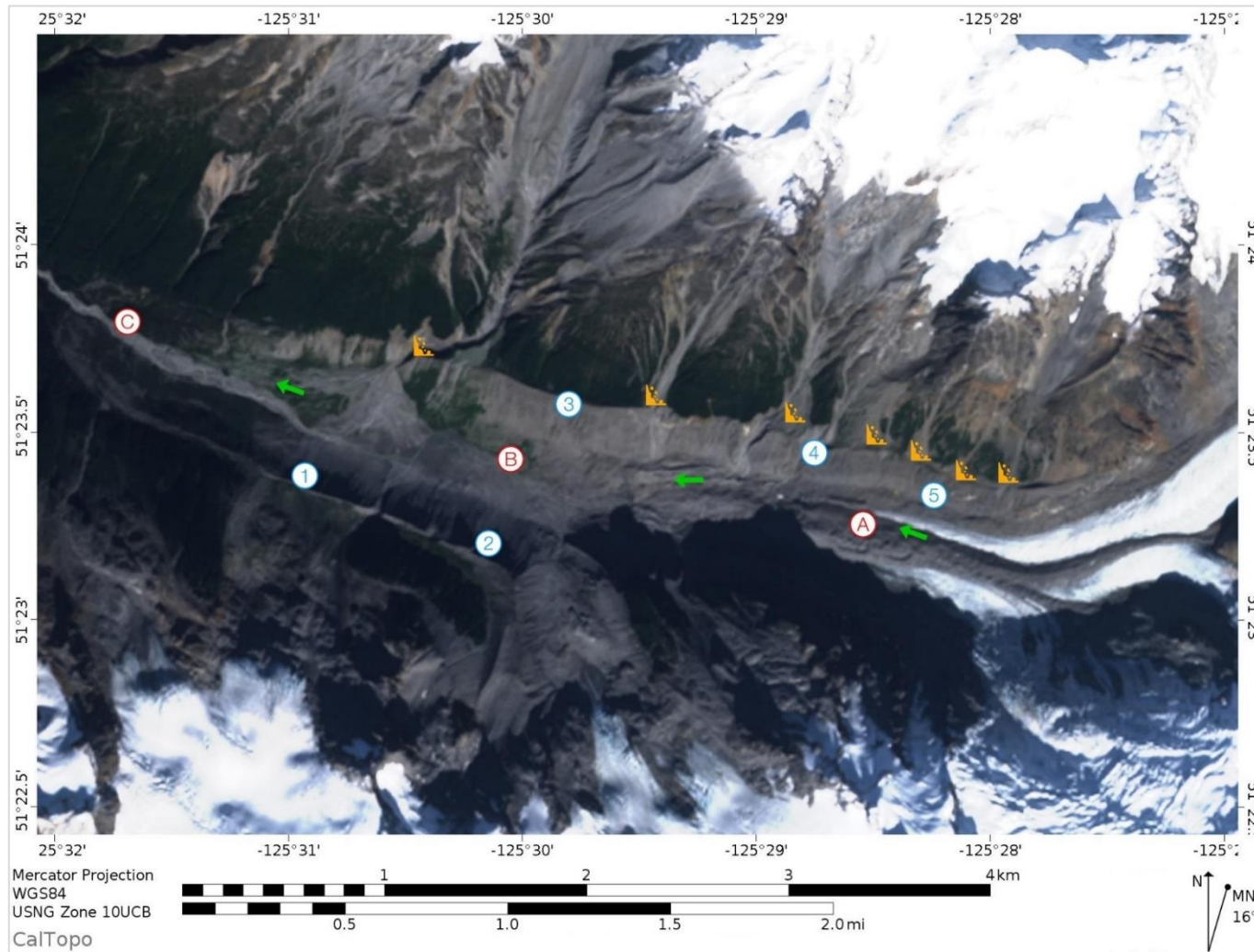


Figure 4.1: Example of a Glacial Valley with Alluvial Fans and Debris Flow Fans Buttressed by a Lateral Moraine Study Site ID 032 (Dorothy Glacier).

4.2 Methods

The software packages (Google Earth, CALATPO, and Trimble Sketchup) that were used for the analysis of lateral moraines were used in the same manner for the analysis of fans buttressed by lateral moraines. Elevation profiles, contour maps, 3D models and digital images of the fans were analyzed with respect to their topography, setting and interaction at the buttress. The analysis was more qualitative in nature than quantitative.

4.3 Results

The study sites contained numerous examples of fans buttressed by lateral moraines. Examples from several study sites are illustrated in Figure 4.2, Figure 4.3 and Figure 4.4.

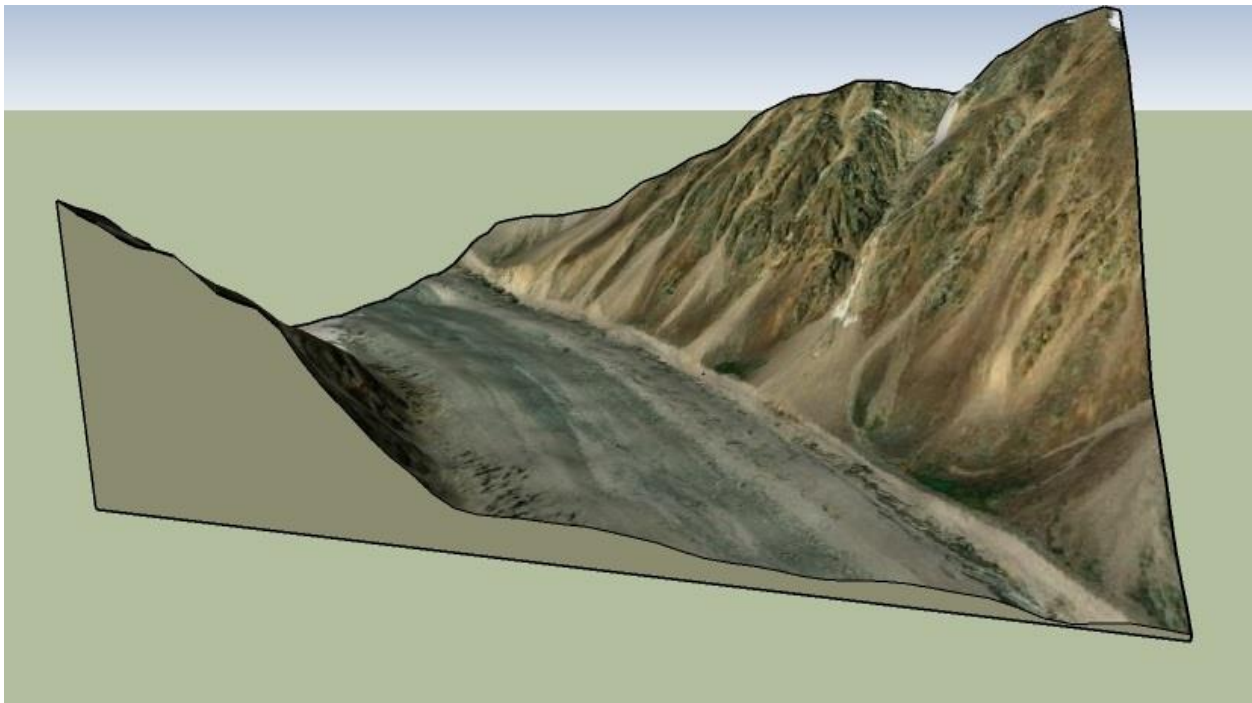


Figure 4.2: Example of Fans Buttressed by the Lateral Moraine from Study Site ID 041 (Afghanistan).

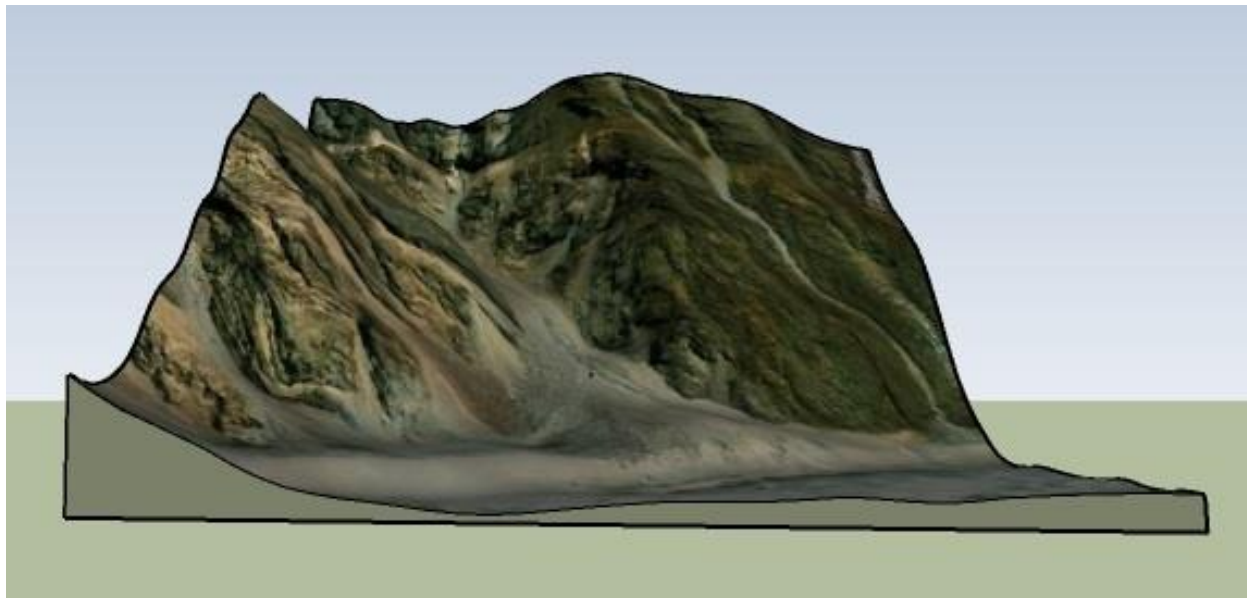


Figure 4.3: Example of a Fan Buttressed by the Lateral Moraine from Study Site ID 041 (Afghanistan).

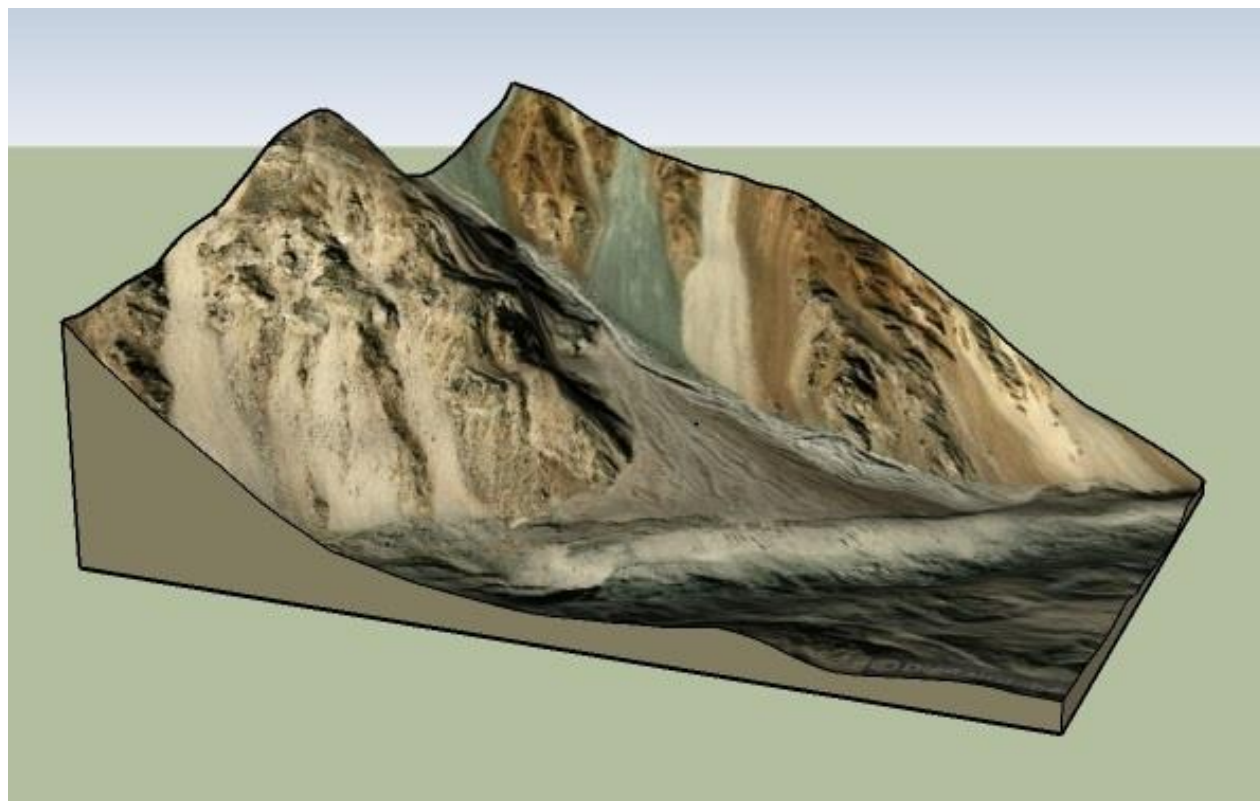


Figure 4.4: Example of a Fan Buttressed by the Lateral Moraine from Site ID 046 (Shkuk Yoz Glacier).

Fans could be found almost anywhere on the majority of study sites, but with an irregular spatial distribution. Fans were found at any altitude, but are more common on one of the two glacial valley slopes. Most fans have gradients of greater than 30° . Few are found under 12° . Their spatial distribution is not random. The more gentle sloping fans are generally more pronounced down glacier. The physical features of fans observed within study sites varied considerably. For example, fans down glacier on the Donjek Glacier (Figure 4.5) study site measured up to 1000 meters in width at the toe and 800 meters in length from the toe to the apex with an angle of repose measuring 12° . Vegetation engulfed part or all of the fan. Up-glacier, within five kilometers, the fans (Figure 4.5) are considerably smaller. They measured up to 100 meters in width at the toe. Up to 450 meters in length from the toe to the apex with an angle of repose measuring 38° . Vegetation was non-existent on these fans. A pattern of increased angle of repose, smaller displacement (width and length) and decreasing vegetation cover is exhibited moving up glacier.

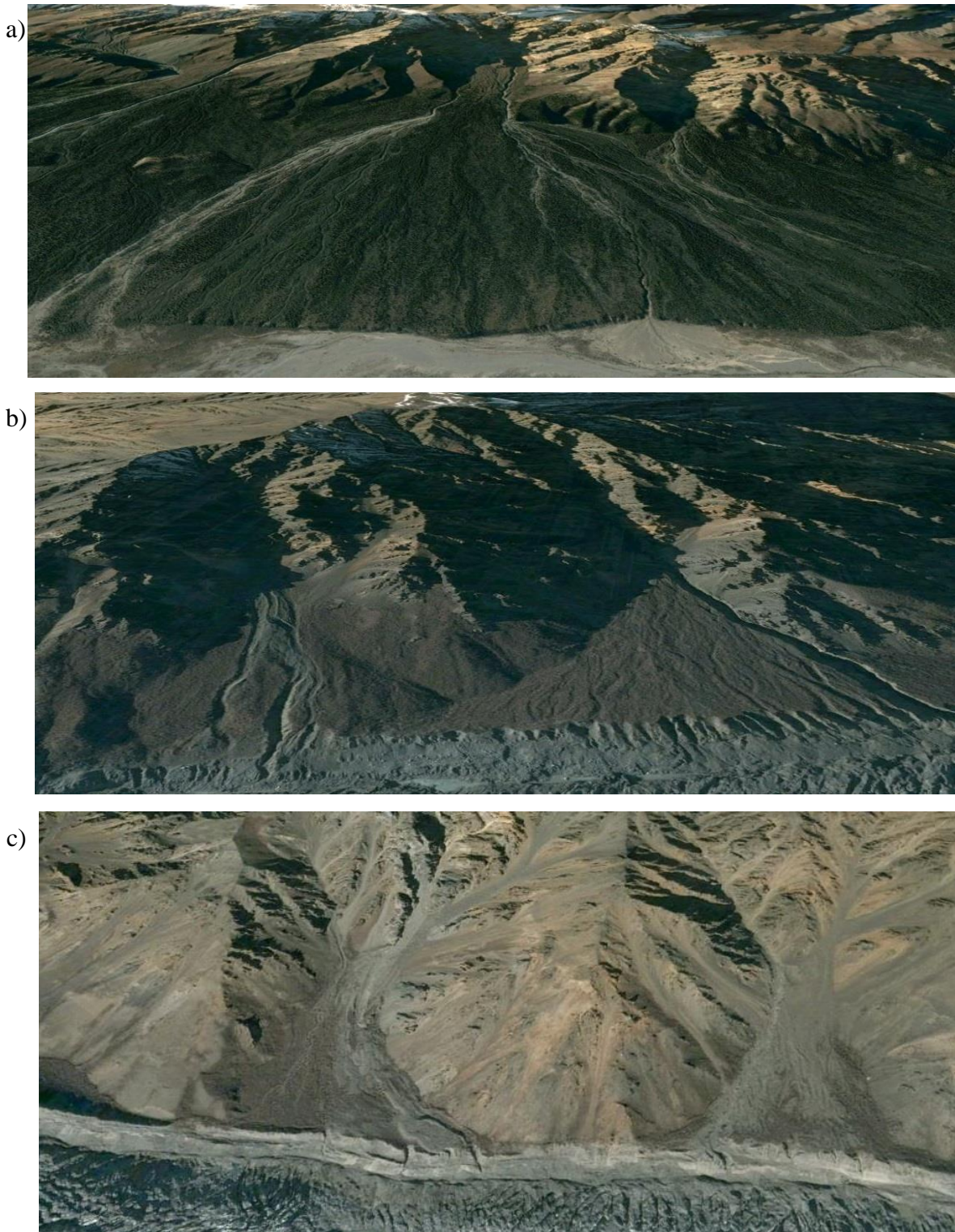


Figure 4.5: Photos of Study Site ID 051 (Donjek Glacier).

a) Photo of a large fan down glacier which is engulfed by vegetation, but with a large fluvial pathway b) photo of a large fan down glacier, devoid of vegetation, but with fluvial pathways and c) smaller fans further up-glacier, devoid of vegetation, but with fluvial pathways.

Retrieved November 23, 2019 from <https://goo.gl/maps/Q7vraEUanYLLEqbn6>
l/maps/Q7vraEUanYLLEqbn6.

4.4 Analysis

4.4.1 Debris Flow Fans

Debris flow fans are fan-shaped landforms created over time by deposition of eroded sediment. They are identifiable on most of the study sites, but with irregular spatial distribution. They appear at any altitude. however, they are more common up-glacier and are more common on one of the two glacial valley slopes. They have steep gradients which is a reflection of the steep valley side wall gradient. Their spatial distribution is not random. The more gentle sloping fans are generally more pronounced towards down glacier. This is a result of the continuous sediment supply through erosion of the valley side wall. The physical features of fans observed within study sites varied considerably. For example, as previously noted on the Donjek Glacier. Vegetation is non-existent on these fans. Further up-glacier, they are smaller in displacement. Their initial toe position relative to the crest of the lateral moraine is dependent on two factors: the amount of debris flow and the shape of the lateral morainic trough. Although, in some cases, the debris load is greater than the resistance capacity of the lateral moraine. In such cases the debris flow disconnects a section of the lateral moraine. This was the case with the debris deposit up-glacier on the Findelengletscher Glacier (Figure 4.6). Up-glacier valley wall slope increases and the lateral morainic trough narrows. In such cases, the deposit of sediment may be more than the moraine resistance capacity, as illustrated in Figure 4.6. The debris flow may also be sufficient to engulf the lateral moraine. The later was the case with the debris deposit up-glacier on the Tiedemann Glacier as illustrated in Figure 4.7.

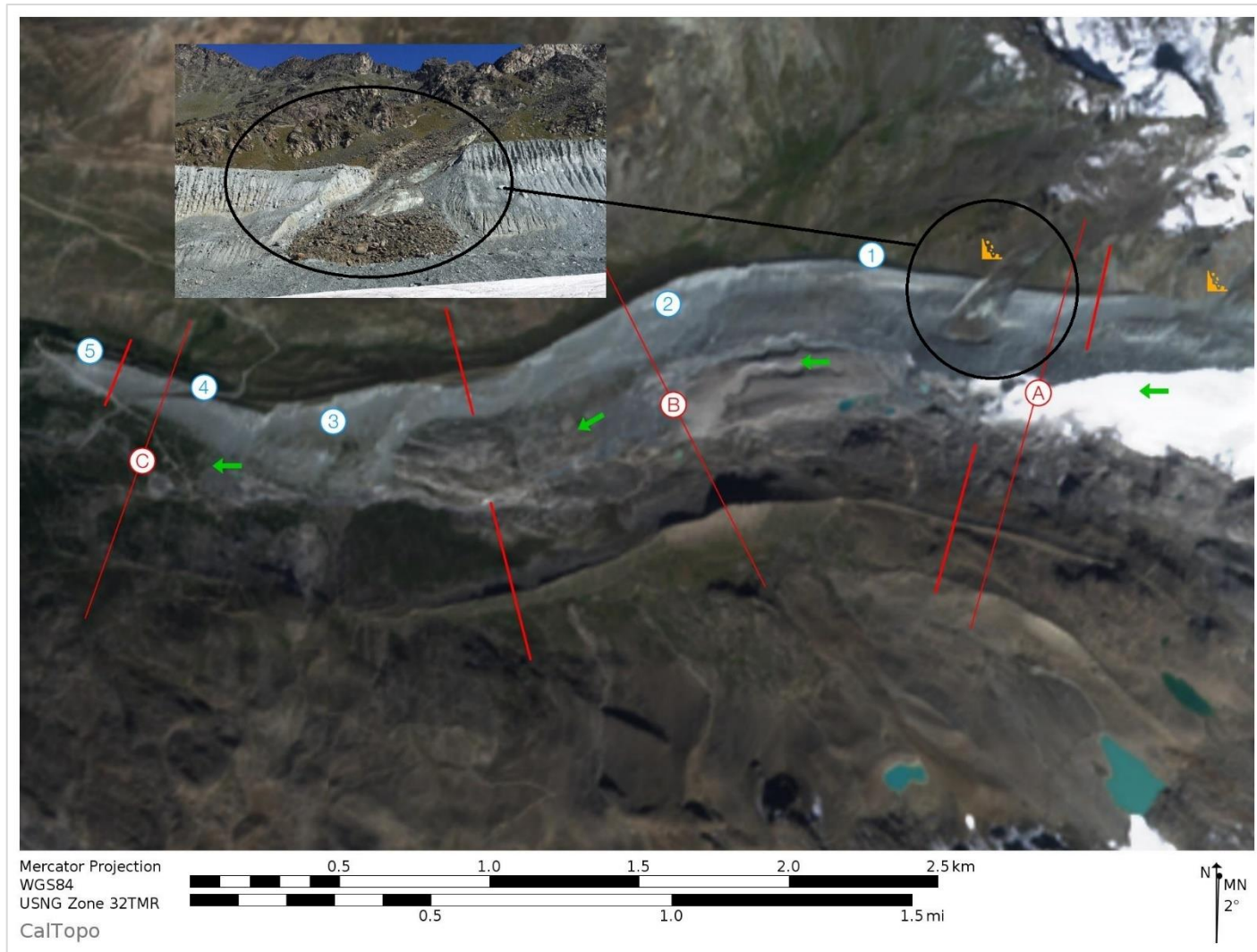


Figure 4.6: Example of a Disconnected Section of the Lateral Moraine in way of a Debris Flow from Study Site ID 054 (Findelengletscher Glacier).

Photo retrieved from

https://www.google.com/search?q=Findelengletscher+debris+slide+pinterest&tbm=isch&ved=2ahUKEwi6jzbzNmOPoAhUPI-AKHSFvAYUQ2cCegQIABAA&oq=Findelengletscher+debris+slide+pinterest&gs_lcp=CgNpbWcQDDoECCMQJ1D11QJY348.

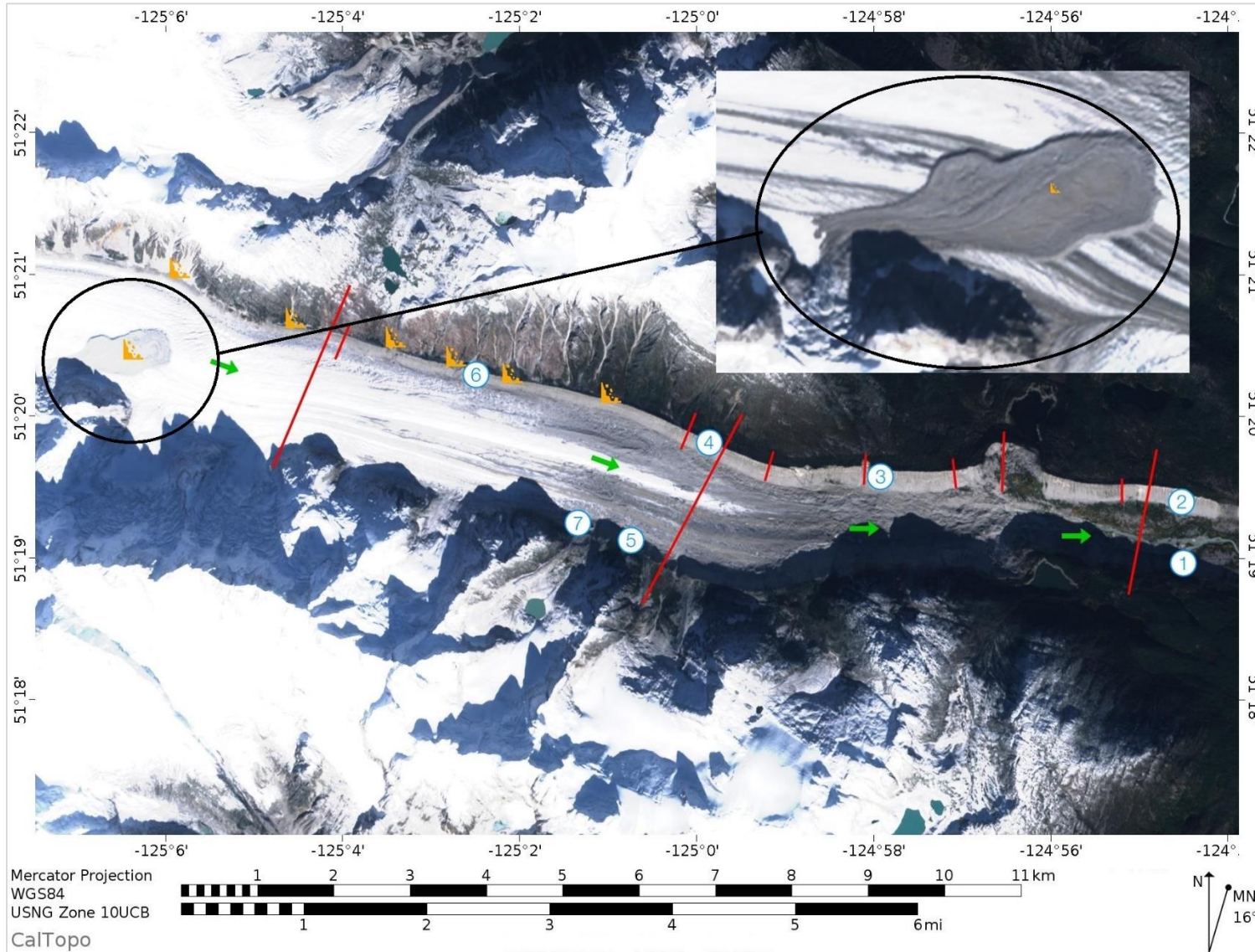


Figure 4.7: Example of an Engulfed Section of the Lateral Moraine in way of a Debris Flow from Study Site 050 (Tiedemann Glacier).

Moving down glacier the lateral morainic trough widens. When the initial flow is insufficient to infill the trough, over time, more debris flow from the sediment source, through erosion, is added to the initial deposition. Eventually, if sufficient debris is available from the sediment source, the fan cone will continue to grow. The sediment deposit will increase both laterally and upward at the toe of the cone on the distal slope of the lateral moraine and upward on the cone itself. Eventually the toe of the fan conforms to the slope profile of the proximal slope as illustrated in Figure 4.8.

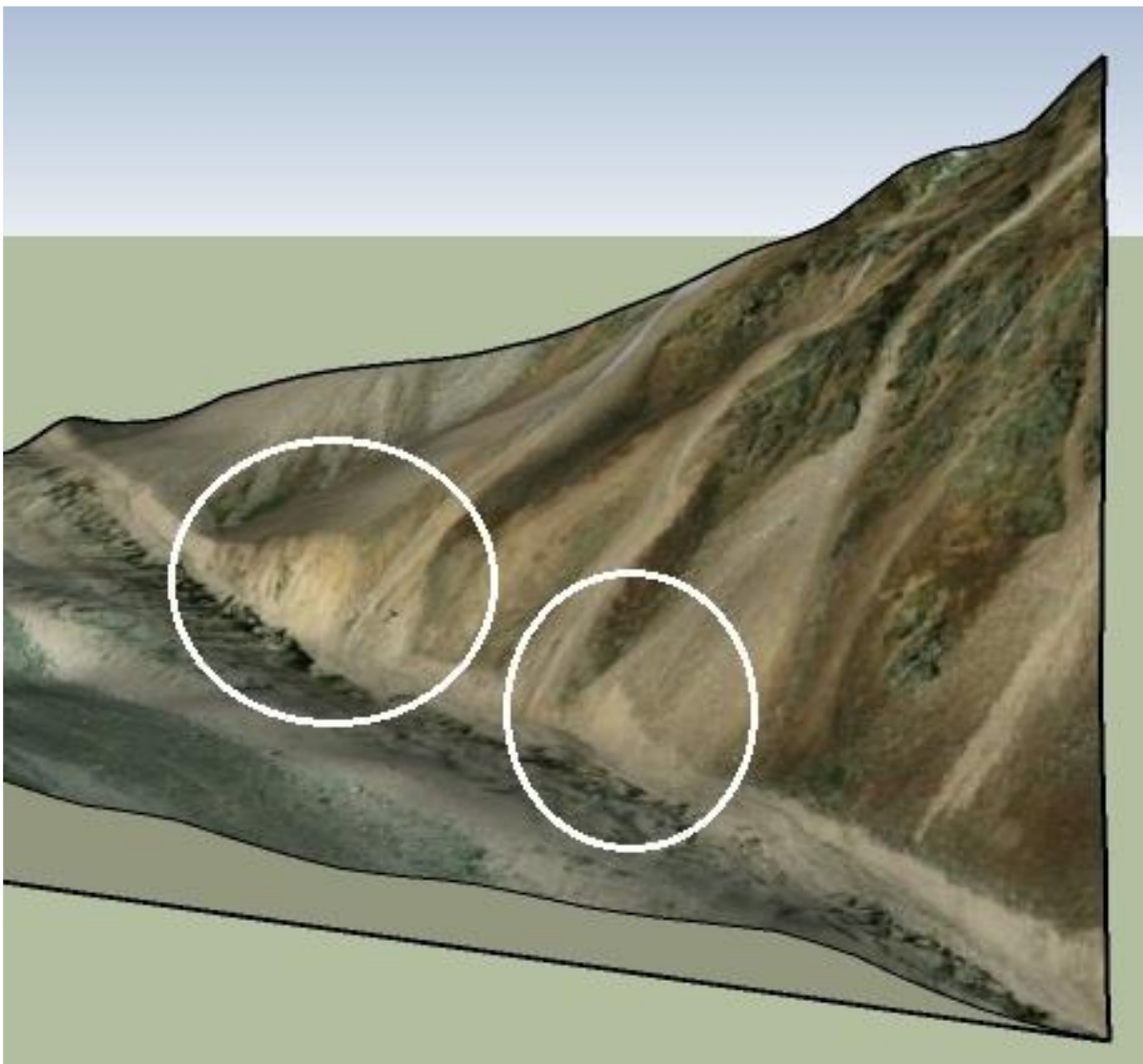


Figure 4.8: Example of a Fans buttressed by the Lateral from Study Site ID 041 (Afghanistan). The toe of the fan conforms to the slope profile of the lateral moraine proximal slope.

Whether the lateral morainic trough is partially or completely infilled, the lateral moraine becomes increasingly gullied and debris advances over the lateral moraine as illustrated in Figure 4.9. In this case, vegetation has colonized in the lateral morainic trough and on the distal slope. The lateral moraine is incised by gullies where the trough has been completely infilled by the fan deposit.

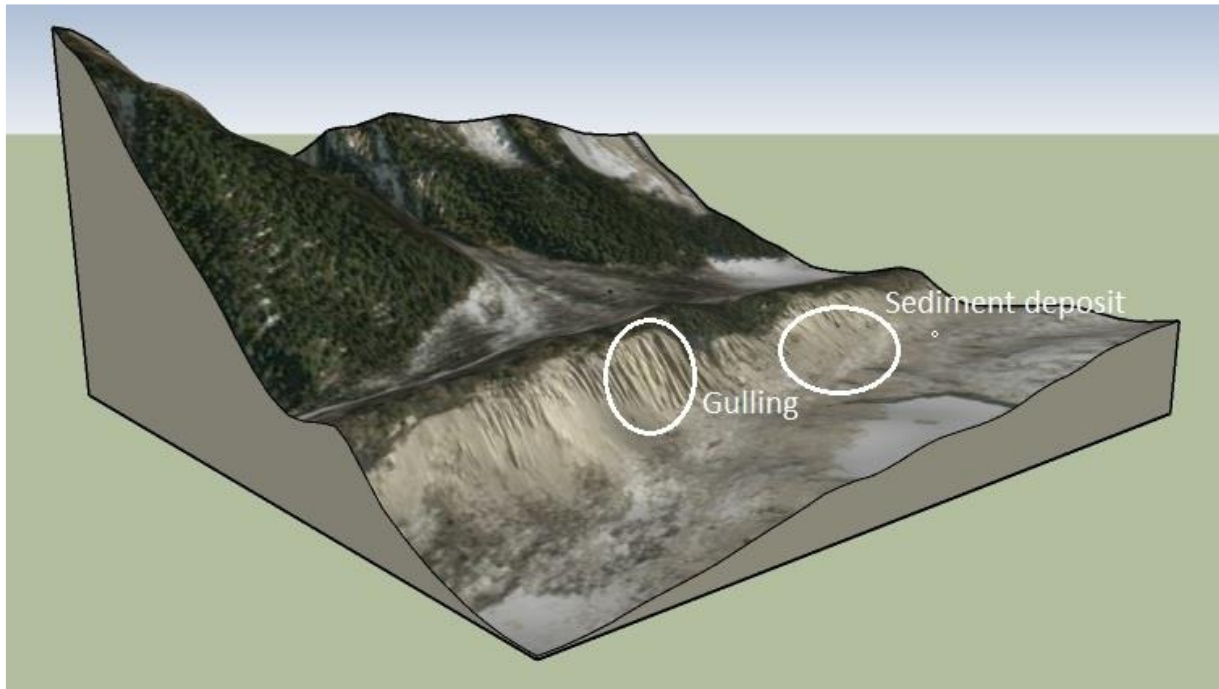


Figure 4.9: Example of a Fan Buttressed by the Lateral Moraine with Incised Gullying from Study Site ID 048 (Nagong, China).

A typical example of the earlier stages, prior to vegetation colonization, is exhibited in Figure 4.10. There is no gullying of the lateral moraine on the left, up-glacier. Directly adjacent to the debris cone and down glacier (to the right) of the fan deposit there is intense gullying. The gullying in both positions extends over the crest and into the distal slope. The sediment from the gullying has been deposited on the lower slopes of the lateral moraine. Typically, the upper part of the lateral moraine is intensely gullied, that indicates erosion takes place at these locations.

Curry et al. (2006) found similar features, with debris flows being the most important transport phenomena.

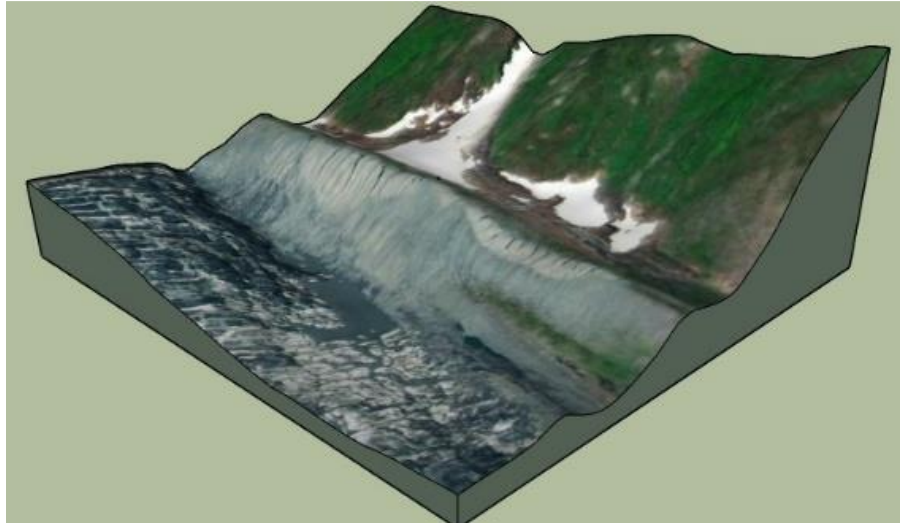


Figure 4.10: Example of the Earlier Stages of Gullying Prior to Vegetation Colonization from Study Site ID 046 (Shkuk Yoz Glacier).

There is frequently a fluvial component to debris flows. The fluvial flow is typically in a radial pattern down slope of the cone, but is generally more pronounced on the down valley side

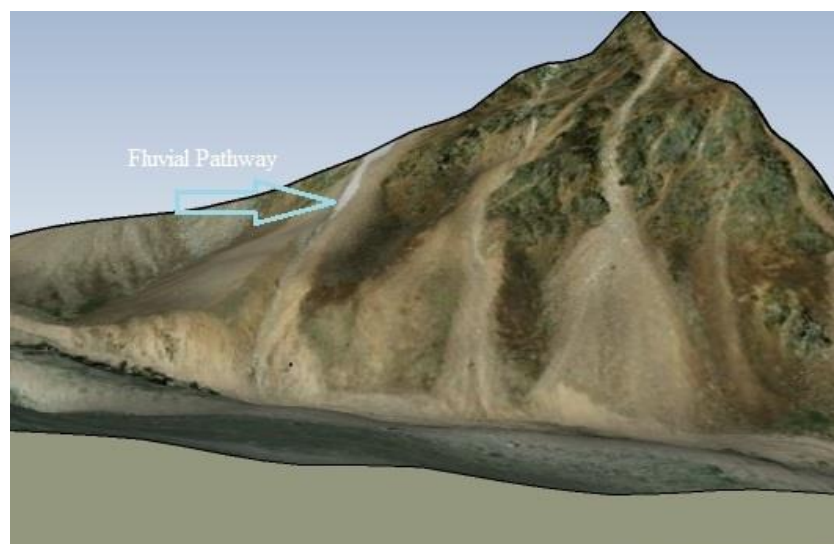


Figure 4.11: Example of the Fluvial Component of a Debris Flow from Study Site ID 041 (Afghanistan).

of the cone as illustrated in Figure 4.11 This is a natural hydraulic reaction of water to flow towards the lower side.

Additionally, the lateral morainic trough acts a medium to convey the fluvial component further downward along the perimeter of the moraine. Upon a restriction, such as another debris cone or sudden change in the direction of the lateral morainic trough, the fluvial component will either stagnant in a pool at the base of the obstructing cone (Figure 4.12) and/or breach the crest of lateral moraine (Figure 4.13). This increased supply of glaciogenic melt water along the perimeter of the cone increases the erosion of the lateral moraine, as illustrated in (Figure 4.13).



Figure 4.12: Example of a Stagnant Pool at the Base of a Fan Cone from Study Site ID 041 (Afghanistan).

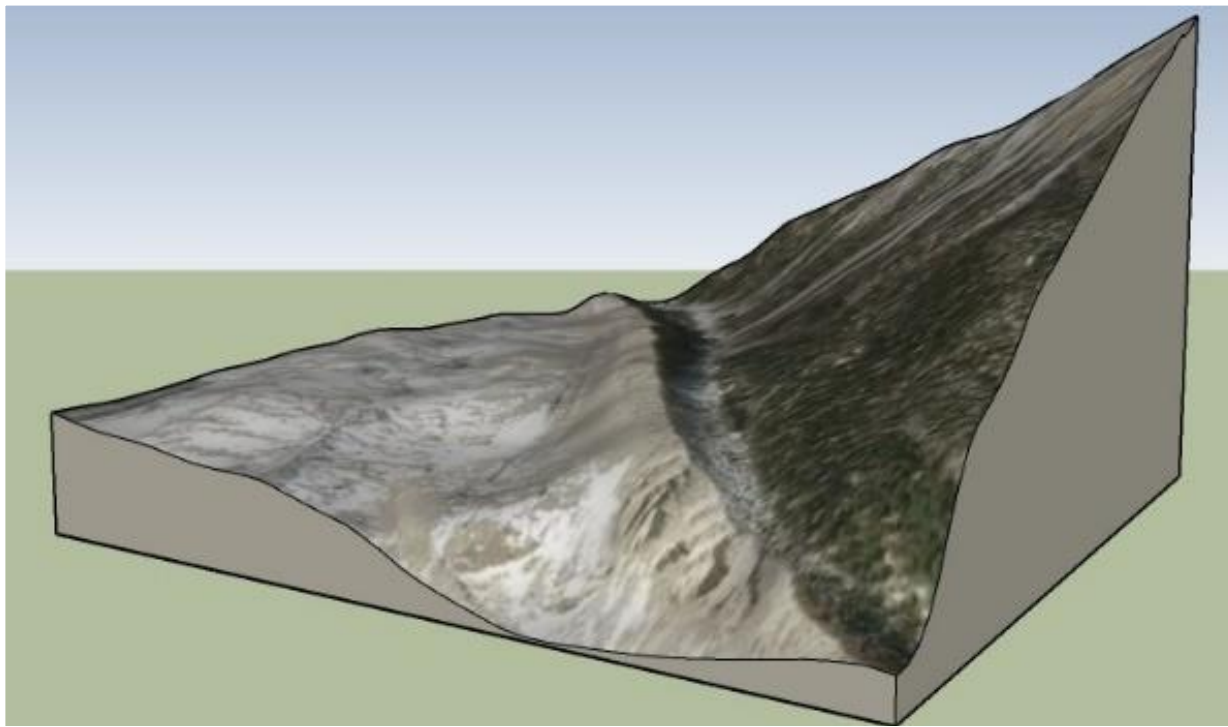


Figure 4.13: Example of Incised Gullying at a Restriction in the Lateral Morainic Trough from Study Site ID 048 (Nagong, China).

4.4.2 Alluvial Fans

Debris flow fans with a fluvial component could also be considered alluvial fans. However, in addition to the more notable fluvial component, alluvial fans are in contrast to the characteristics of debris flow fans. The distinction between fluvial fans and debris fans is displacement (width and length), and a gentler angle of repose and time. For example, alluvial fans down glacier on the Donjek Glacier (Figure 4.5) study site measured up to 1000 meters in length at the toe and 800 meters from the toe to the apex with an angle of repose measuring 12° . Vegetation may be non-existent or may have engulfed part or all of the fan. Alluvial fans are fan-shaped landforms, just like debris flow fans, created over time by deposition of eroded sediment. They are located on some study sites, with an irregular spatial distribution. Alluvial fans are more common on one glacial valley slope and appear at any altitude, but are more common down glacier. They have gentle gradients that is a result of the continuous supply of

sediment from the source through erosion deposition. Their spatial distribution is not random. The more gentle sloping fans are generally more pronounced further down glacier. This is a result of the continuous sediment supply over time. The physical features of fluvial fans observed at study sites varied considerably. Vegetation is more prevalent further down glacier. Some fans are completely covered by vegetation while other fans have one lateral side that is still actively being eroded through fluvial action. Areas of the fan where vegetation is abundant have in-active radial channel incisions that approximately measure 10's of meters in width by several meters in depth. The active lateral sides of the fans have radial channel incision that could not be measured. In both cases, at the toe of these fans, there still exist a lateral moraine that is incised with gullies, in some cases. In other cases, the sediment deposits from the fluvial channels are creating new debris fans at the toe of the alluvial fan cone. Here the lateral moraine has been completely engulfed by the new debris fan.

The change in vegetation growth is visible in the imagery for the majority of study sites. The more humid coastal sites of Canada, Alaska and Argentina tend to have an increased area of vegetation without the transitional shift to an unvegetated terrain. In comparison, the higher elevations of more arid areas of Asia, Tajikistan and Afghanistan are devoid of vegetation. However, the resolution of the images may account for these discrepancies.

According to Christenson and Purcell (1985), if a part of a fan surface has not been disturbed by flooding or erosion for 15,000 years, its surface will have become weathered and covered by a soil profile and vegetation. This would suggest that sections of the down valley alluvial fans have been not actively disturbed by flooding or erosion for 15,000 years. This implies that the extreme down valley debris fans are considerably older than the up-valley fans.

Chapter 5

Conclusion

5.1 Introduction

The general characteristics of the moraines investigated are typical for a paraglacial environment. The proximal slope at many locations have a steeper angle of repose compared to the distal slope. Many have multiple moraine ridges below each other. This indicates different stages of glacial retreat and growth (Lukas et al., 2012). The general form of the moraine, with decreasing slopes towards the bottom and a difference between an intense gullied upper section of the moraine, and a sediment deposit at the bottom conforms to the description by Curry et al. (2005). It is also recognized that there are many feedbacks between vegetation and geomorphic activity on a moraine, that influence the processes and decrease erosion (Eichel et al., 2016).

5.2 Lateral Moraine Paraglacial Transformation

The lateral moraines are typically less than 20 meters in height in the extreme up-glacier position. Although, this is more prevalent as the length of the glacier increases. Up-glacier, they have little or no distal slope and are devoid of vegetation on both the proximal and distal slopes. Moving towards the down glacier position, near the glacier terminus, these lateral moraines can reach heights of tens to hundreds of meters with shallow or no distal slope. They are either devoid of vegetation colonization or vegetation colonies are well established. The vegetation is found on the distal slope or both the proximal and distal slopes. In the down glacier section, lateral moraines are often separated from the adjacent walls. In the lateral morainic trough, the space between the moraine and the wall, debris can be captured. One source of the debris is from the steep walls of the glacier catchment, lodged in the lateral morainic through by debris flows. The debris is transported gravitationally.

A relationship between moraine and the glacier lateral slope becomes apparent by comparing their slope angles. Relationships between the glacier slope versus the lateral slope of the moraine were investigated (Figure 3.3). The trend indicates that their slopes are diverging. For every degree of change in the glaciers lateral slope, there is a 0.86° change in the moraines lateral slope. The trend indicates that, on average their slopes are diverging down glacier. This would imply that the height of the lateral moraine should be increasing down glacier in relation to the glacier.

Paraglacial lateral moraine adjustment at the sites investigated is evident through the development of gullying. They incised into the upper sections of the proximal slope with the sediment being redeposited on the lower slope periphery.

The average gully density was calculated, based on 200 meter sections along the lateral moraines. The down glacier, mid-glacier and up-glacier average gully densities were found to be 65 per kilometer, 95 per kilometer and 130 per kilometer respectively. Gullies appear to have reached their maximum dimensions in the down glacier position. There were sections throughout the length of the lateral moraines where no gullying was identifiable. There may be several reasons for this, one of which is the resolution of the images. There were also sections of the lateral moraine where increased gully erosion from local impacts, such as debris flow, were identified. These were omitted from the calculated average per kilometer.

Relationships between the gully length, slope angle, width and moraine height were investigated (Figures 3.7, 3.8 & 3.9). This revealed that there is a trend for the gully slope to increase with moraine height both up-glacier and down glacier. At mid-glacier there is relatively no change in the gully slope relative to the moraine height. The gully length versus moraine height trend revealed that the gully length increases with moraine height throughout the length of

the lateral moraine at a relatively constant rate. The gully width versus moraine height did not revealed a statistical correlation relative to the position of the gully on the lateral moraine.

A significant difference of the proximal and distal slopes of the lateral moraines becomes apparent by comparing slope angles, as shown in Table 3.1. The average slope angle on the proximal side and distal side is 34° and 22° respectively. The maximum proximal slope angle obtained was 51° . The opposing, distal slopes offer values between 0° to 42° . With one exception, site ID 053 (Tsidjiore Nouve, Switzerland), where the proximal slope angle is larger than distal slope angle.

The difference of about 12° in slope angle, combined with the presence of vegetation on some distal slopes, clearly shows that the distal slopes are much more stable. This difference between slopes is characteristic of the study sites and indicates the erosional active on the proximal slopes as well as the more or less in activity on the distal slopes.

In most cases, the lateral moraines gave an impression of asymmetry. This arose because deposition on one side is seemingly more pronounced. However, this asymmetry across the valley profile may just be related to shape as opposed to moraine volume. This is demonstrated in the case of study site ID 055 where the area difference in the negative space above the moraine profile of opposing moraines is within 13%.

5.3 Sharp-crested Lateral Paraglacial Morphology

Sharp-crested lateral moraines were identified in only six study sites, they included:

1. ID 007 Otter Glacier, Alaska.
2. ID 006 Fairweather Glacier, Alaska.

3. ID 055 Easton Glacier, USA
4. ID 050 Tiedemann Glacier, Canada.
5. ID 054 Findelengletscher, Switzerland.
6. ID 058 Vadret Oers dams, Switzerland

Sharp-crested lateral moraines were identified in all three sections (down glacier, mid-glacier and up-glacier), but 70% were located in either the down glacier section or the mid-glacier section. The remaining 30% were located in the up-glacier section. The maximum moraine height and corresponding proximal slope angle recorded was 180 meters and 45° respectively. The maximum proximal slope angle and corresponding moraine height recorded was 51° and 84 meters respectively. However, the data collected did not replicate proximal slope angles higher than 51° as reported in other literature that studied some of the same sites. These other studies were complimented with on-site surveys. Resolution of the images in this study may account for this discrepancy.

5.4 Alluvial and Debris Flow Fans Buttressed by Lateral Moraine Paraglacial Transformation

Extensive paraglacial modification of lateral moraines by debris flows is limited to sections of the glacial valley where valley wall slopes gradients are steep. Debris fans are more common up-glacier and are more common on one of the two glacial valley slopes. Their initial toe position relative to the crest of the lateral moraine is dependent on two factors: the amount of debris flow and the shape of the lateral morainic trough.

The lateral moraine becomes increasingly gullied as the infill of the lateral morainic trough increases. Where the lateral morainic trough has been completely infilled by the fan deposit, the lateral moraine is incised with gullies. Eventually the toe of the fan conforms to the

slope profile of the of the lateral moraine proximal slope. Although, in some cases the debris flow load is greater than the resistance capacity of the lateral moraine. In such cases the debris flow disconnects a section of the lateral moraine.

The fluvial component to the debris flow is typically in a radial pattern down slope of the cone, but is generally more pronounced on the down valley side of the cone. Directly in way of the debris cone and down glacier of the fan deposit the gullying is more intense than up-glacier of the fan deposit. Typically, the upper proximal slope of the lateral moraine is often intensely gullied. As a result, the lateral moraine profile is reshaped as the sediment from the gullying is redeposited on the lower slopes of the lateral moraine.

Larger fluvial fans are more common down glacier and are more common on one of the two glacial valley slopes. At the toe of these fans, there still exist a lateral moraine that is being actively incised with gullies, in some cases. The gully density in way of these fans is on average 30 per kilometer. In other cases, the sediment deposit from the fluvial deposit is creating a new debris fan at the toe of the alluvial fan cone. In this scenario the lateral moraine has been completely engulfed by the debris fan.

5.5 Summary

The majority of glaciers are currently retreating globally. Retreat will continue to be the dominant terminus response. Perhaps, the most visually obvious manifestation of glacial sediment storage, release, and redistribution within deglaciating alpine environments are the large lateral moraines that flank deglaciating landscape throughout alpine regions. It is known that erosion on paraglacial slopes diminishes after time (Ballantyne, 2002). The moraine deformation described in this study provides examples of the paraglacial response to deglaciation over time.

List of References

- Arndt, D.S., and Blunden, J. (2019). State of the Climate in 2018. *Bulletin American Meteorological Society*, 100(9).
- Ballantyne, C.K. (1995). Paraglacial debris-cone formation on recently deglaciated terrain, western Norway. *Holocene*, 5, 25–33.
- Ballantyne, C. (2001). A general model of paraglacial landscape response. *The Holocene*, 12(3), 371-376.
- Ballantyne, C. (2002). Paraglacial geomorphology. *Quaternary Science Reviews*, 21(18-19), 1935-2017.
- Ballantyne, C.K., and Benn, D.I. (1994). Paraglacial slope adjustment and resedimentation following recent glacier retreat, Fåbergstølsdalen, Norway. *Arctic and Alpine Research*, 26(3), 255–269.
- Barr, I.D., and Lovell, H. (2014). A review of topographic controls on moraine distribution. *Geomorphology*, 226, 44–64.
- Beakawi, H.M., and Al-Amoudi, O.S., (2018). A Review on the Angle of Repose of Granular Materials. *Powder Technology*, 330, 397-417.
- Benn, D.I., (1989). Debris transport by Loch Lomond Readvance glaciers in Northern Scotland: basin form and the within-valley asymmetry of lateral moraines. *Journal of Quaternary Science*. 4, 243–254.
- Burrows C.J. (1973). Studies on Some Glacial Moraines in New Zealand. *New Zealand Journal of Geology and Geophysics*, 16(4), 831-856.
- Christenson, G. E., and Purcell, C. (1985). Correlation and age of Quaternary alluvial fan sequences, Basin and Range province, southwestern United States. *The Geological Society of America*, 203, 115–122.
- Church, M., and Ryder, J.M. (1972). Paraglacial sedimentation: consideration of fluvial processes conditioned by glaciation. *Geological Society of America*, 83, 3059-3072.

- Church, M., and Slaymaker, O. (1989). Disequilibrium of Holocene Sediment Yield in Glaciated British Columbia. *Nature*, 337, 452-454.
- Curry, A.M. (1999). Paraglacial modification of slope form. *Earth Surface Process and Landforms*, 24, 1213–1228.
- Curry, A.M. (2000). Observations on the distribution of paraglacial reworking of glacial drift in western Norway. *Norsk Geografisk Tidsskrift*, 54(4), 139–147.
- Curry, A.M., Cleasby, V., and Zukowskyj, P. (2006), Paraglacial response of steep, sediment-mantled slopes to post-‘Little Ice Age’ glacier recession in the central Swiss Alps. *Journal of Quaternary Science*, 21(3), 211-225.
- Curry, A.M., Sands, T.B., and Porter, P.R. (2009). Geotechnical controls on a steep lateral moraine undergoing paraglacial slope adjustment. *Geological Society, London, Special Publications*, 320, 181-197.
- Google (2019). <https://support.google.com/earth/answer/>.
- Hambrey, M.J., Quincey D.J., Glasser, N.F., Reynolds, J.M., Richardson, S.J., and Clemmens, S. (2009) Sedimentological, Geomorphological and Dynamic Context of Debris-mantled Glaciers, Mount Everest (Sagarmatha) Region, Nepal. *Quaternary Science Reviews*, 1084.
- Lukas, S., Graf, A., Coray, S., and Schlüchter, C. (2012). Genesis, stability and preservation potential of large lateral moraines of alpine valley glaciers – towards a unifying theory based on Findelengletscher, Switzerland. *Quaternary Science Reviews*, 38, 27-48.
- Oestreich, K. (1906). Die Täler des nordwestlichen Himalaya. Ergänzung-sheft, zu *Petermanns Geographische Mitteilungen*, 106.
- Pelto, M. S. (2018). How unusual was 2015 in the 1984–2015 period of the North Cascade glacier annual mass balance?. *Water*, 10(543).
- National Research Council. (1996). Alluvial Fan Flooding. Washington, DC: Author.

Small, R. (1983). Lateral moraines of glacier de Tsidjiore Nouve: form, development, and implications. *Journal of Glaciology*, 29, 250–259.

State of the Climate in 2018, the American Meteorological Society: Author.

Tonkin, T.N., Midgley, N.G., Graham, D.J., and Labadz, J.C. (2017). Internal structure and significance of ice-marginal moraine in the Kebnekaise Mountains, northern Sweden. *Boreas*, 46, 199–211.

Über SwissEduc. (n.d.). *Glaciers online*. Retrieved from <https://www.swisseduc.ch/glaciers/glossary/lateral-moraine-tschierva-en.html>. Accessed on Sept 19, 2019.

Über SwissEduc. (n.d.). *Glaciers online*. Retrieved from <https://www.swisseduc.ch/glaciers/morteratsch/2011-2012/index-en.html?id=4>. Accessed on Sept 19, 2019.

Über SwissEduc. (n.d.). *Glaciers online*. Retrieved from <https://www.swisseduc.ch/glaciers/glossary/fluted-lateral-moraine-en.html>. Accessed on Sept 19, 2019.

Whalley, W. (1975). Abnormally steep slopes on moraines constructed by valley glaciers. *The Engineering Behaviour of Glacial Materials*, 60–66.

Zemp, M., Frey, H., Gärtner-Roer, I., Nussbaumer, S.U., Hoelzle, M., Paul, F., Haeberli, W., Denzinger, F., Ahlstrom, A.P., Anderson, B., Bajrachary, S., Barobi, C., Braun, L.N., Caceres, B.E., Casassa, G., Cobos, G., Davila, L. R., Delgadogranados, H., Demuth, M.N., Espizua, L., Fischer, A., Fujita, K., Gadek, B., Ghazanfar, A., Hagen, J.O., Holmlund, P., Karimi, N., Li, Z., Pelto, M., Pitte, P., Popovnin, V.V., Portocarrero, C.A., Prinz, R., Sangewar, C.V., Severskiy, G., Sigurdsson, O., Soruco, A., Usabaliev, R., and Vincent, C. (2015). Historically unprecedented global glacier decline in the early 21st century. *Journal of Glaciology*, 61, 745–762.

Zemp, M., Nussbaumer, S.U., Gärtner-Roer, I., Huber, J., Machguth, H., Paul, F., and Hoelzle, M. (2017). Global Glacier Change Bulletin No. 2. *World Glacier Monitoring Service*.

Zemp, M., Nussbaumer, S.U., and Gärtner-Roer, I. (2020). Global Glacier Change Bulletin No. 3. *World Glacier Monitoring Service*.

Appendix
Images of Study Sites

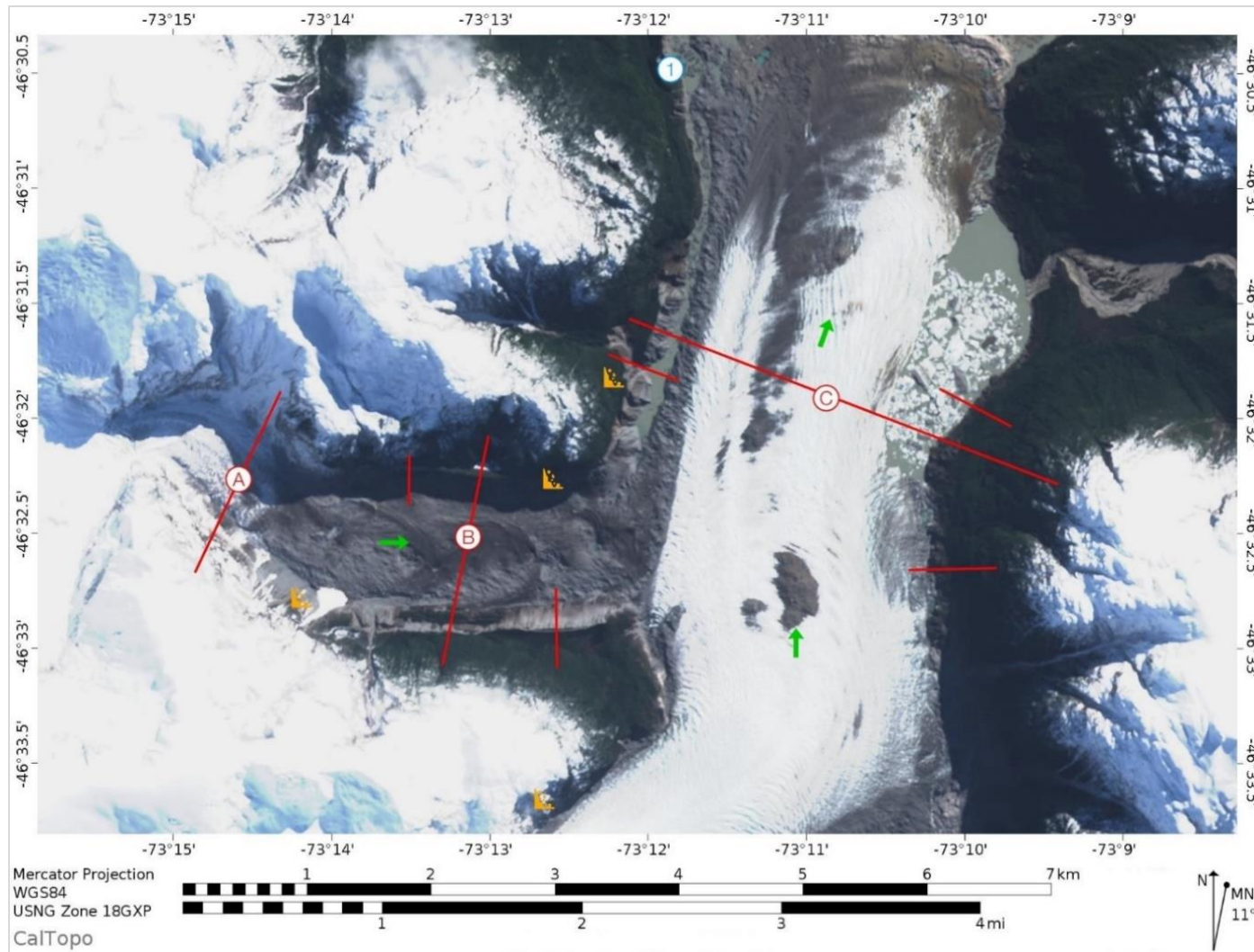


Figure A.1a: Study Site ID 022 (Exploradores Glacier) Mercator Map.

The green arrow indicates the direction of the glacier flow path. The blue numbers identify the location of gullies. The orange icon identifies the location of debris fans. The red lines identify the locations where transit sections were taken; up-valley is identified by red letter A, mid-glacier is defined by the red letter B and down glacier is defined by the red letter C.

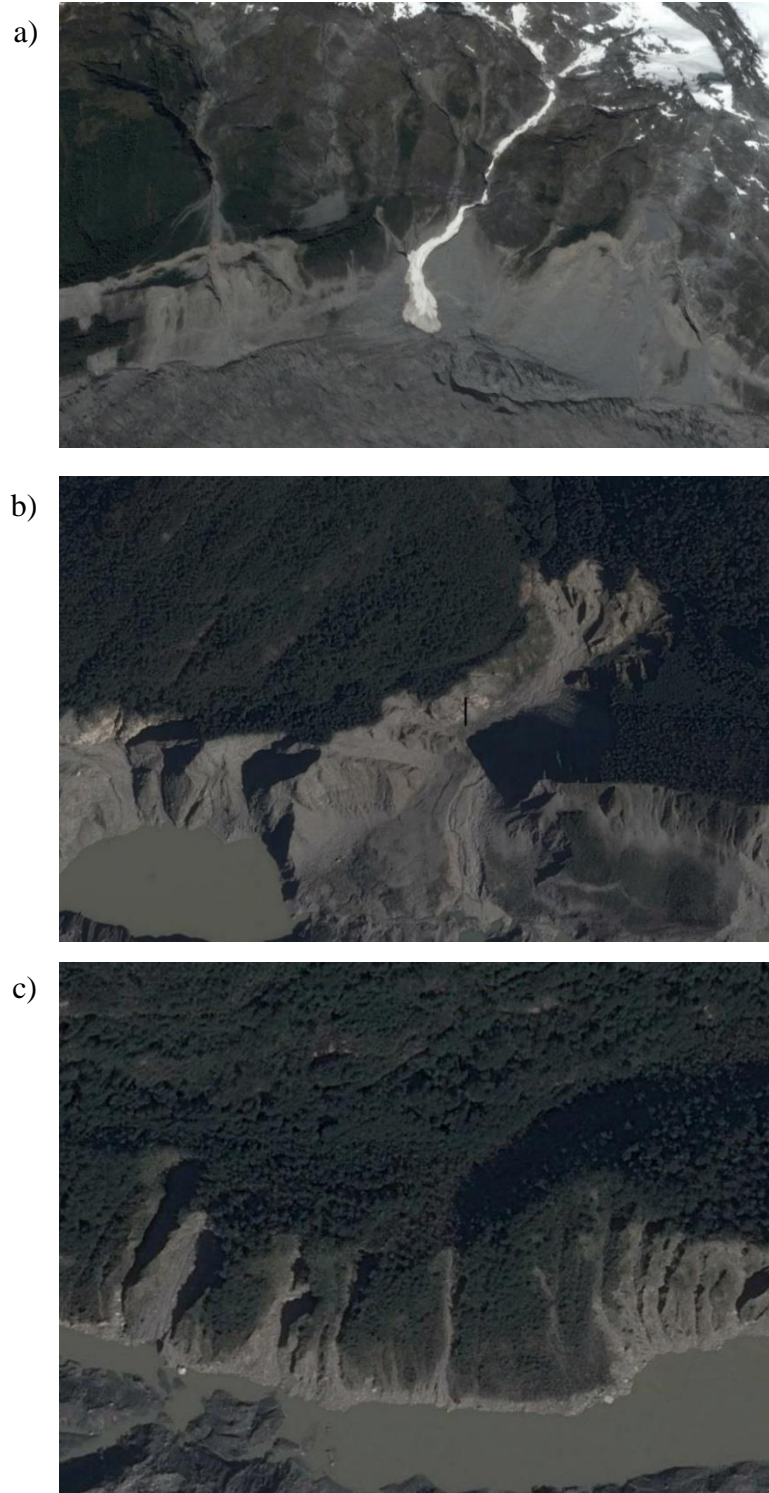


Figure A.1b: Study Site ID 022 (Exploradores Glacier) Photos. a), b) and c) are photos retrieved from Google Earth, (a) and (b) capture the debris fans in the up-glacier section and c) capturing the gullying of the lateral moraine in the down glacier section. Retrieved November 23, 2019 from <https://goo.gl/maps/73Xs5coxB9Q1Mrfn7>.

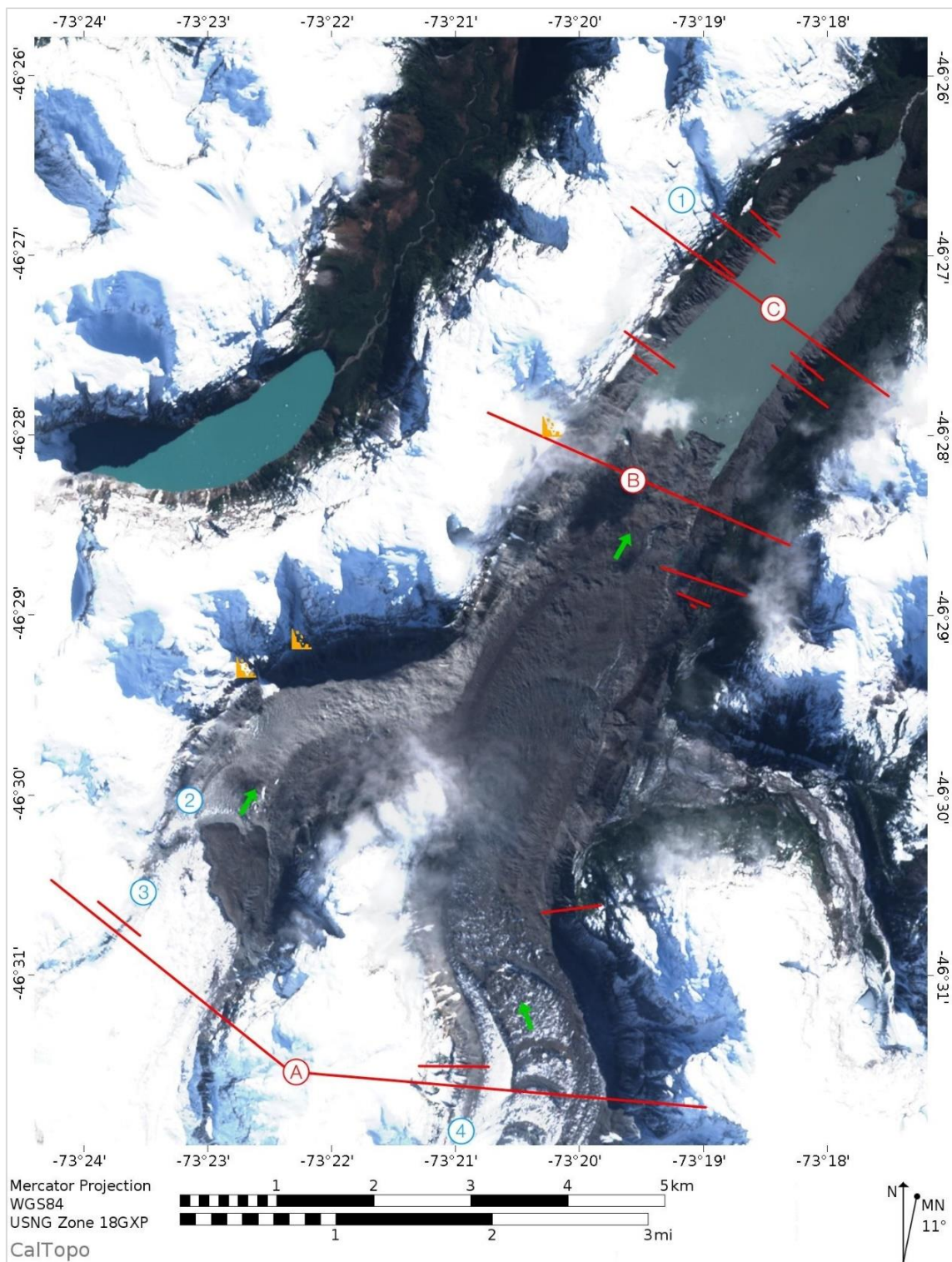


Figure A.2a: Study Site ID 021 (Ventisquero Grosse) Mercator Map.

The green arrow indicates the direction of the glacier flow path. The blue numbers identify the location of gullies. The orange icon identifies the location of debris fans. The red lines identify the locations where transit sections were taken; up-valley is identified by the red letter A, mid-glacier is defined by the red letter B and down glacier is defined by the red letter C.

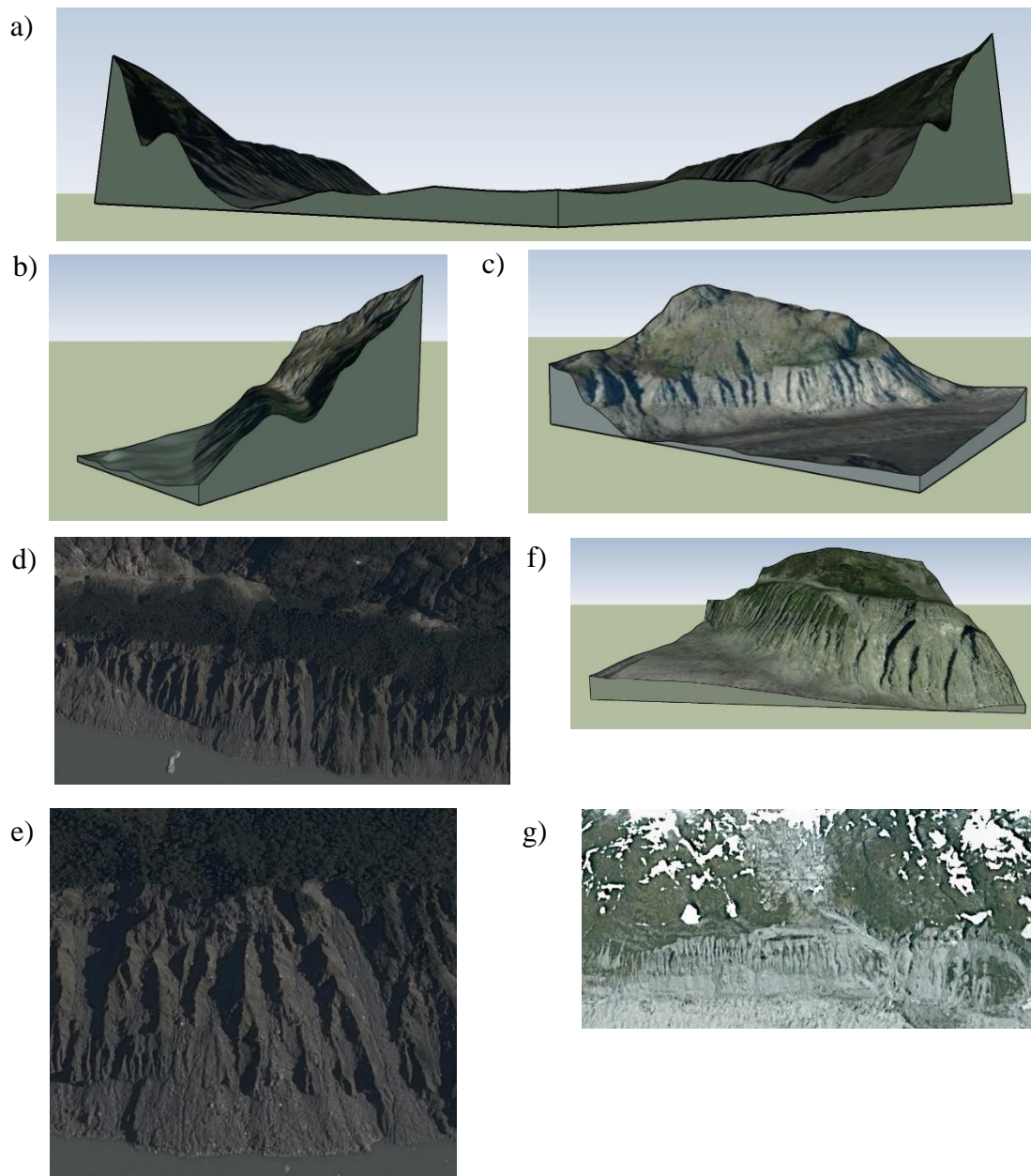


Figure A.2b: Study Site ID 021 (Ventisquero Grosse) Terrain Models and Photos.

a) 2D graphic of the 3D terrain model, of the valley the down glacier b) and c) are 2D graphics of 3D terrain models of the north and south perimeter respectively, d) and e) are photos retrieved from Google Earth, capturing the gullying of the north lateral moraine captured in (b), f) is a 3D terrain model of the north ,up glacier, and g) is a photo, retrieved from Google Earth, capturing the gullying of the north lateral moraine captured in (f).

Photos Retrieved November 23, 2019 from <https://goo.gl/maps/73Xs5coxB9Q1Mrfn7>.

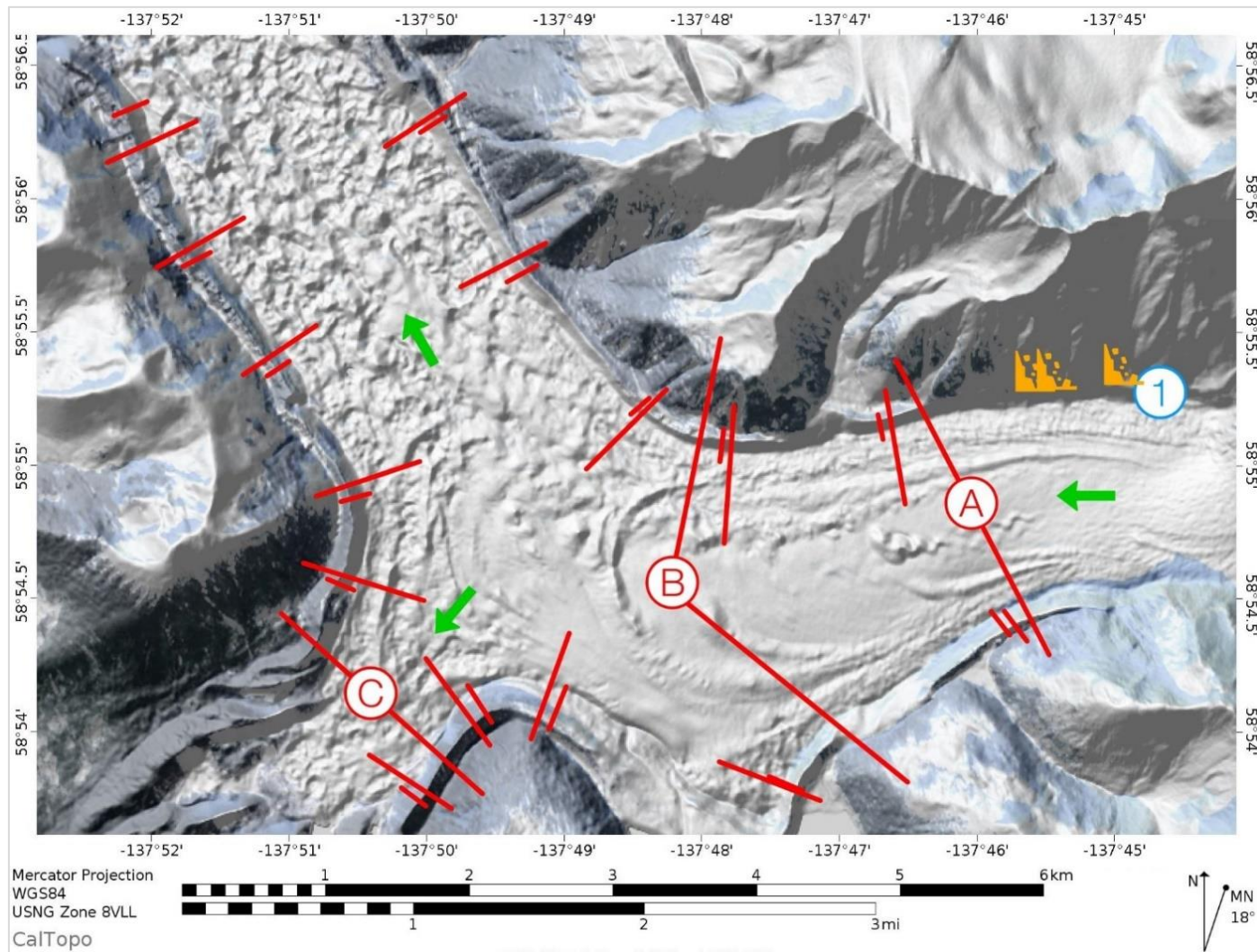


Figure A.3a: Study Site ID 007 (Otter Glacier) Mercator Map.

The green arrow indicates the direction of the glacier flow path. The blue numbers identify the location of gullies. The orange icon identifies the location of debris fans. The red lines identify the locations where transit sections were taken; up-valley is identified by red letter A, mid-glacier is defined by the red letter B and down glacier is defined by the red letter C.

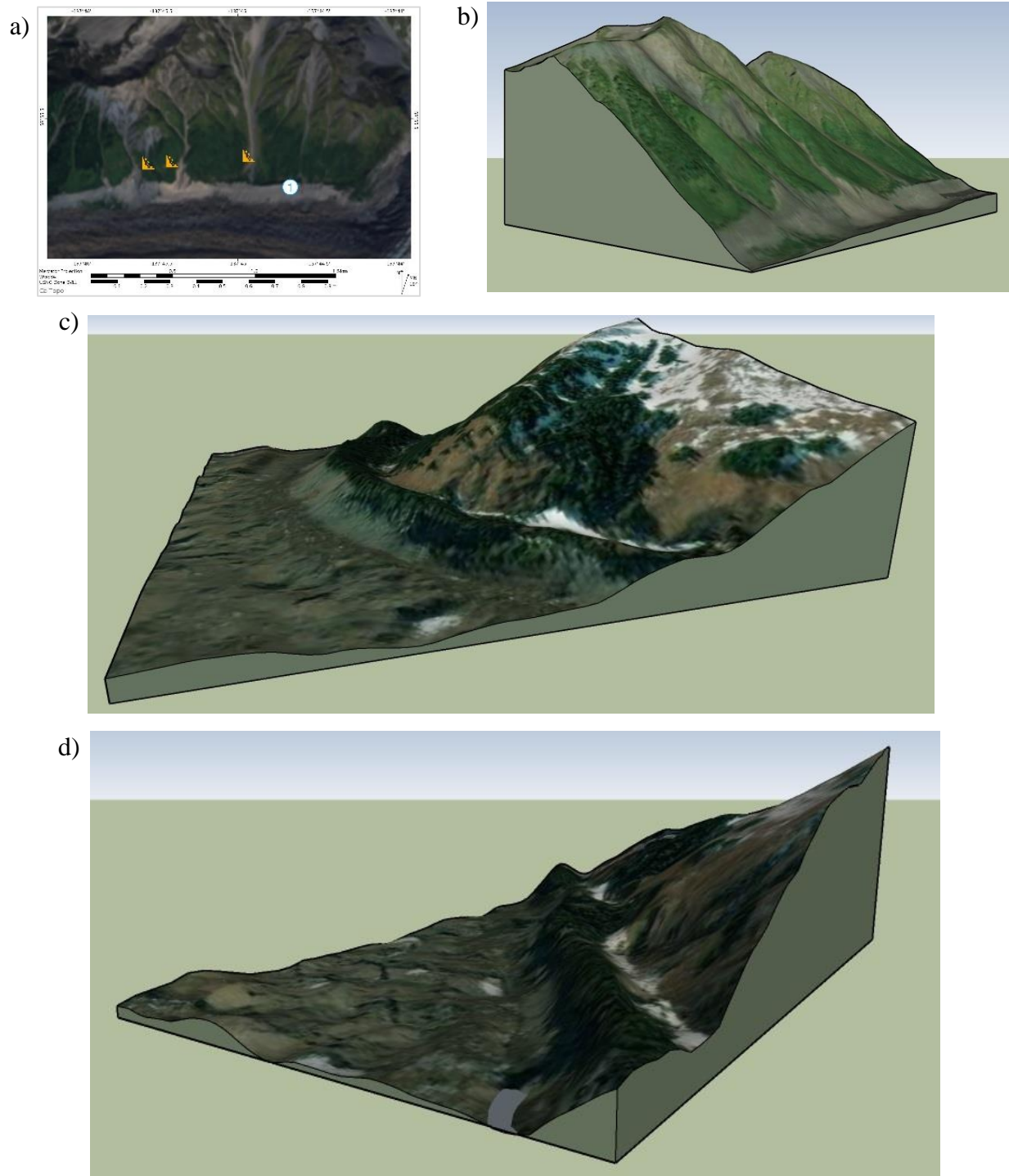


Figure A.3b: Study Site ID 007 (Otter Glacier) Mercator Map and Terrain Models.

a). Study Site ID 007 (Otter Glacier) Mercator Map of the up-glacier position in way of the debris fans, b) is a 2D graphic of the 3D terrain model of the debris fan area mapped in (a), c) and d) are 2D graphics of 3D terrain models of sections of the lateral moraines in the down glacier and mid-glacier positions respectively.

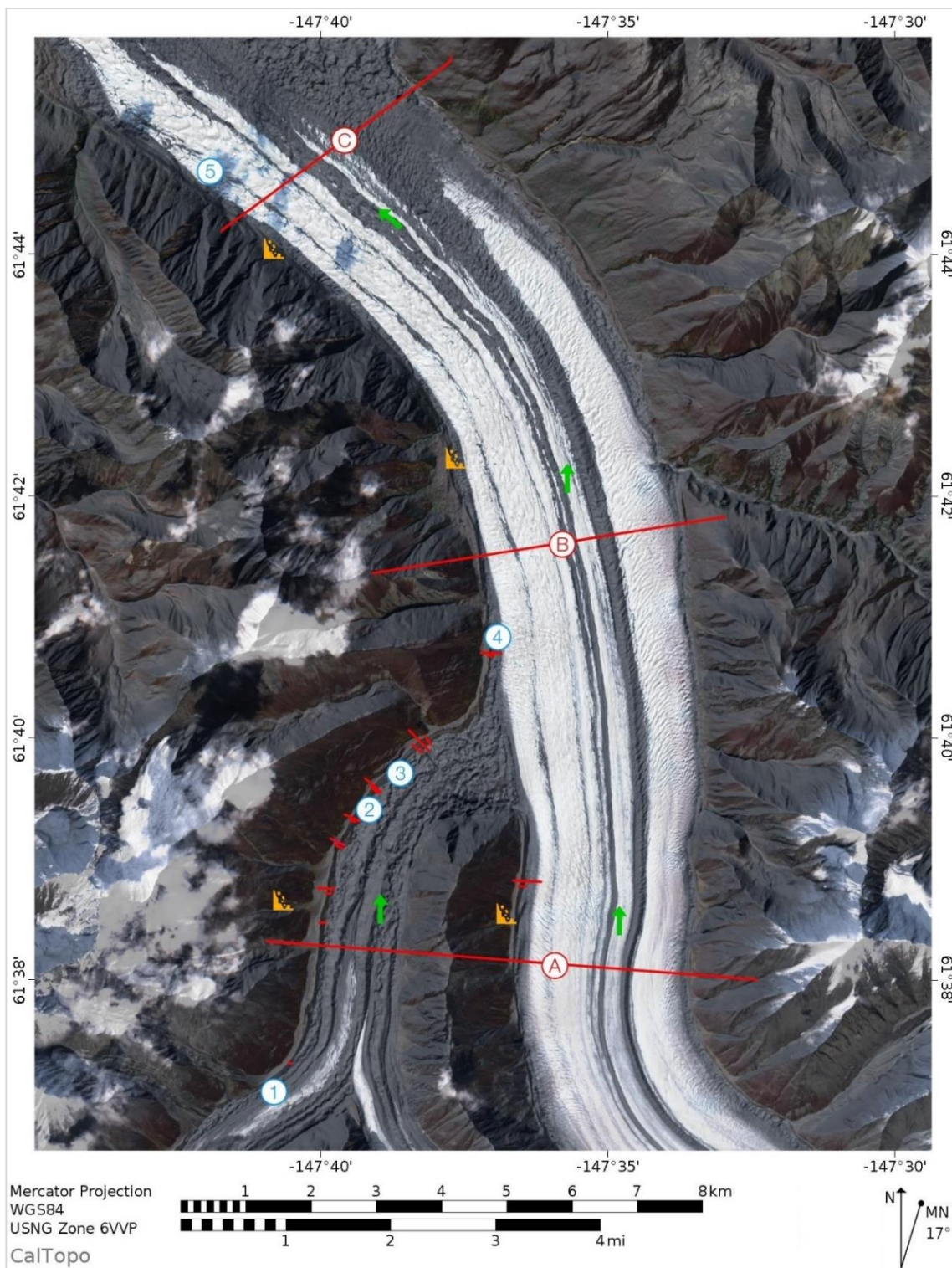


Figure A.4a: Study Site ID 009, 010, and 011 (Mantanuska) Mercator Map.

The green arrow indicates the direction of the glacier flow path. The blue numbers identify the location of gullies. The orange icon identifies the location of debris fans. The red lines identify the locations where transit sections were taken; up-valley is identified by the red letter A, mid-glacier is defined by the red letter B and down glacier is defined by the red letter C.

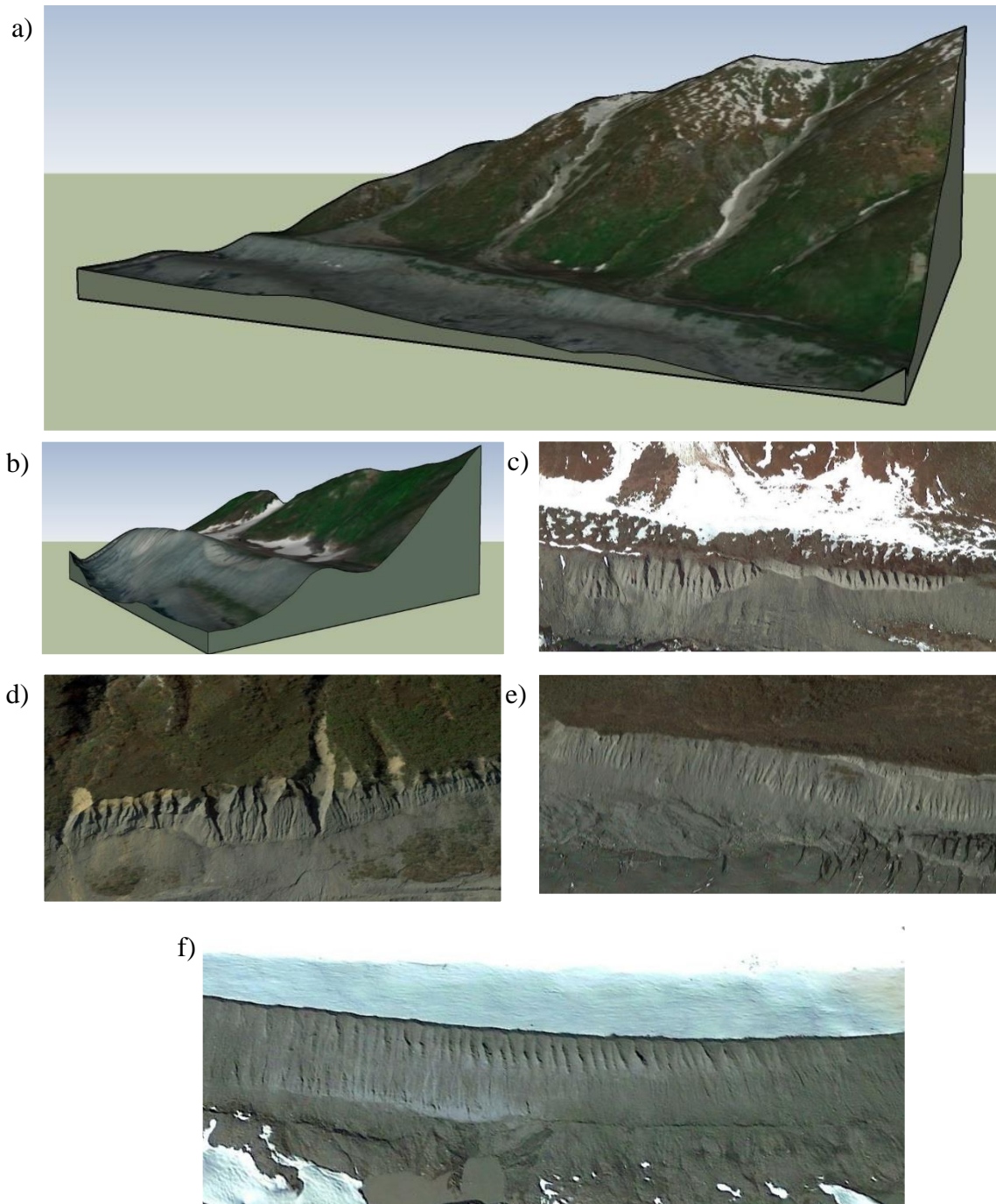


Figure A.4b: Study Site ID 009, 010, and 011 (Mantanuska) Terrain Models and Photos. a) and b) are 2D graphics of 3D terrain models of the lateral moraines and debris fans in the up-glacier section, c) photo retrieved from Google Earth, capturing the gullying of the lateral moraine in way of the debris fans buttressed by the lateral moraine captured in (b). c), d), e) and f) are photos, retrieved from Google Earth, capturing the gullying of the lateral moraine in the down glacier, mid-glacier and up-glacier positions respectively. Photos Retrieved November 23, 2019 from <https://goo.gl/maps/M3Jpk5YsmKuaDpmTA>.

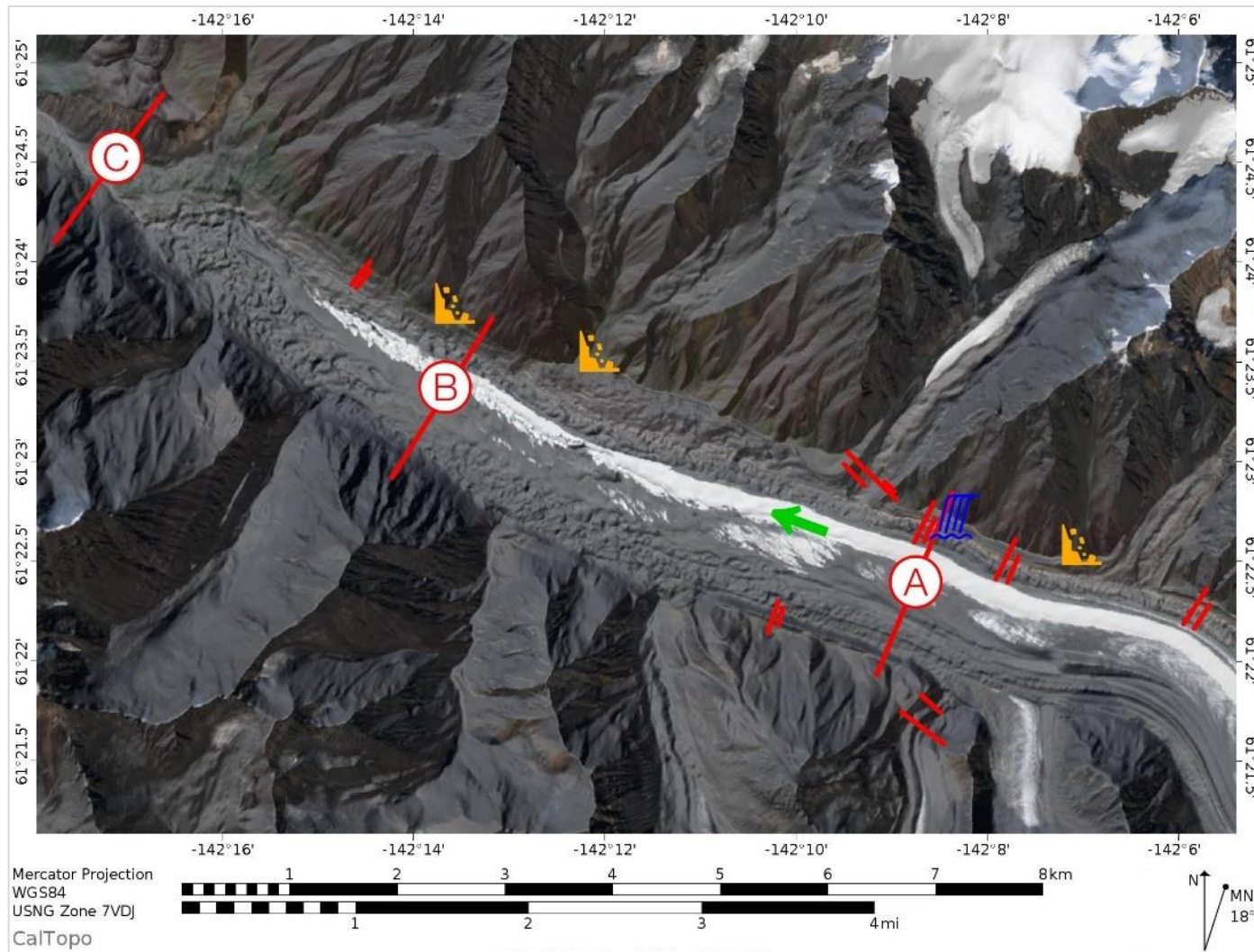


Figure A.5a: Study Site ID 004 (Glacier Creek) Mercator Map.

The green arrow indicates the direction of the glacier flow path. The blue numbers identify the location of gullies. The orange icon identifies the location of debris fans. The royal blue icon identifies an area where a pool of water has collected. The red lines identify the locations where transit sections were taken; up-valley is identified by red letter A, mid-glacier is defined by the red letter B and down glacier is defined by the red letter C.

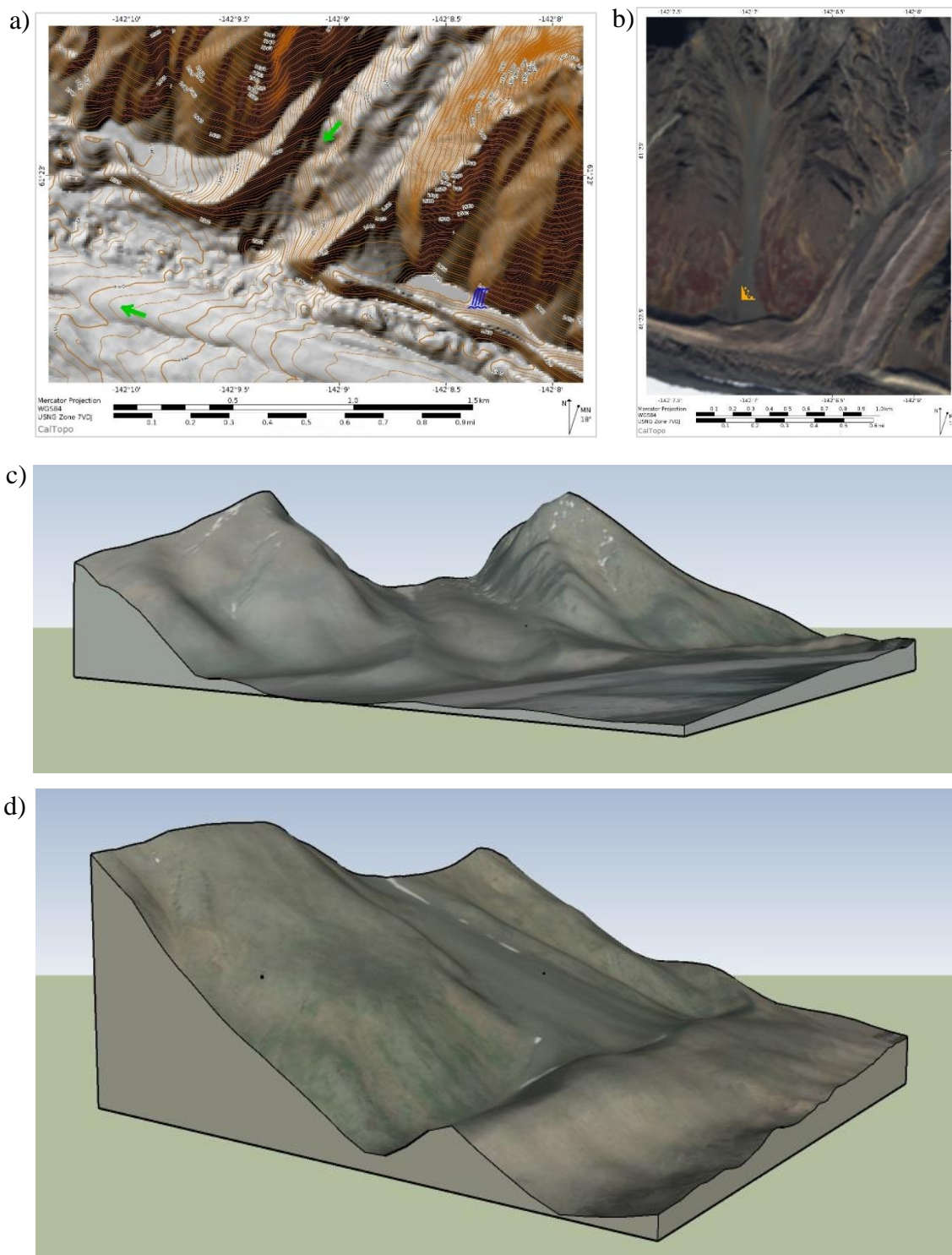


Figure A.5b: Study Site ID 004 (Glacier Creek) Mercator Map and Terrain Models.
 a) Mercator Map with shaded relief and 5m contour lines of a lateral moraine located at the junction of a tributary glacier and the trunk glacier in the up-glacier position, b) a Mercator Map of a debris fan buttressed by a lateral moraine in the up-glacier position, c) is a 2D graphic of the 3D terrain model at the junction of the tributary glacier and the trunk glacier shown in (a) and d) Is a 2D graphic of the 3D terrain model of the lateral moraine and debris fans shown in (b).

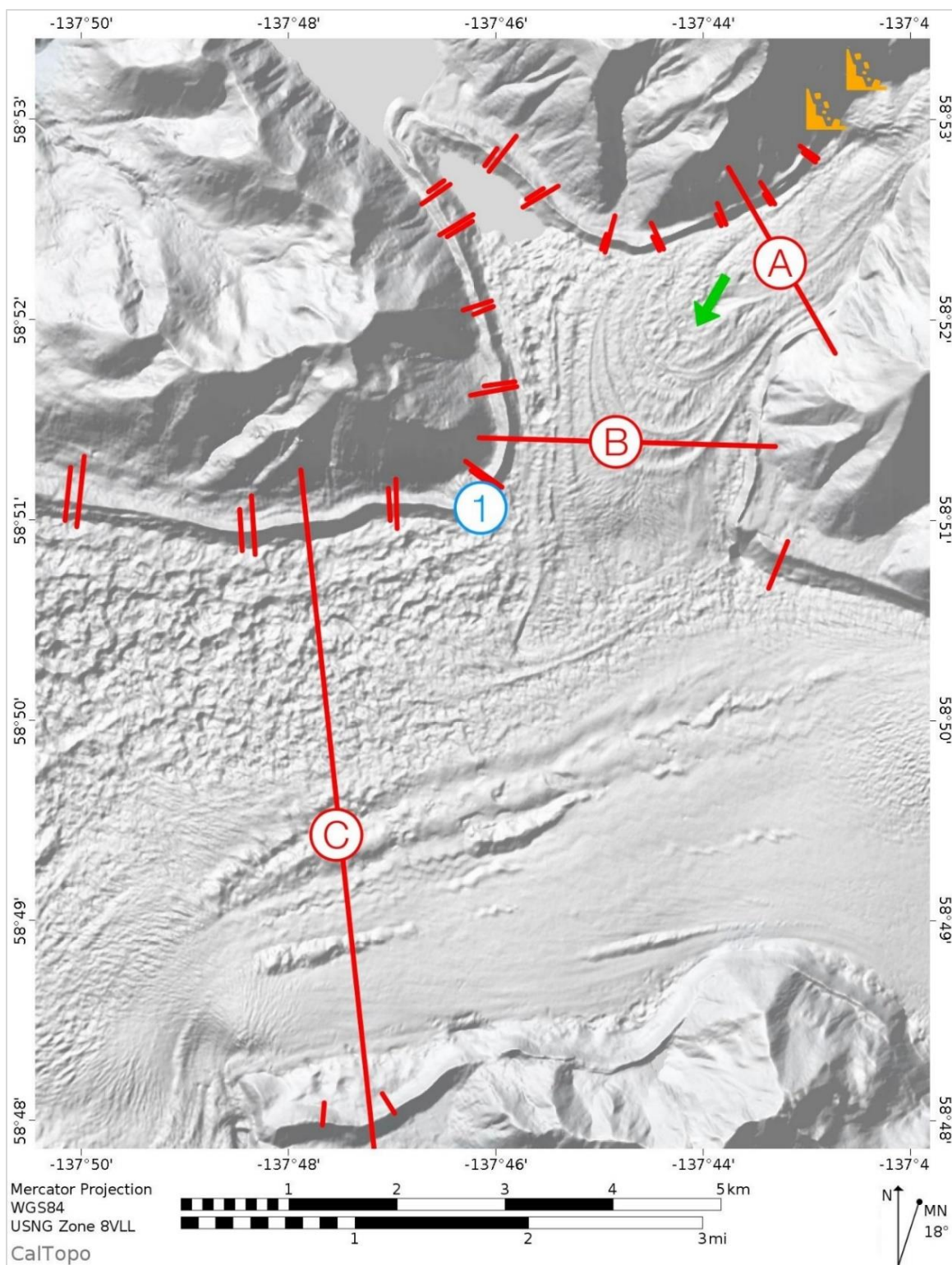


Figure A.6a: Study Site ID 006 (Fairweather Glacier) Mercator Map.

The green arrow indicates the direction of the glacier flow path. The blue numbers identify the location of gullies. The orange icon identifies the location of debris fans. The red lines identify the locations where transit sections were taken; up-valley is identified by the red letter A, mid-glacier is defined by the red letter B and down-glacier is defined by the red letter C.

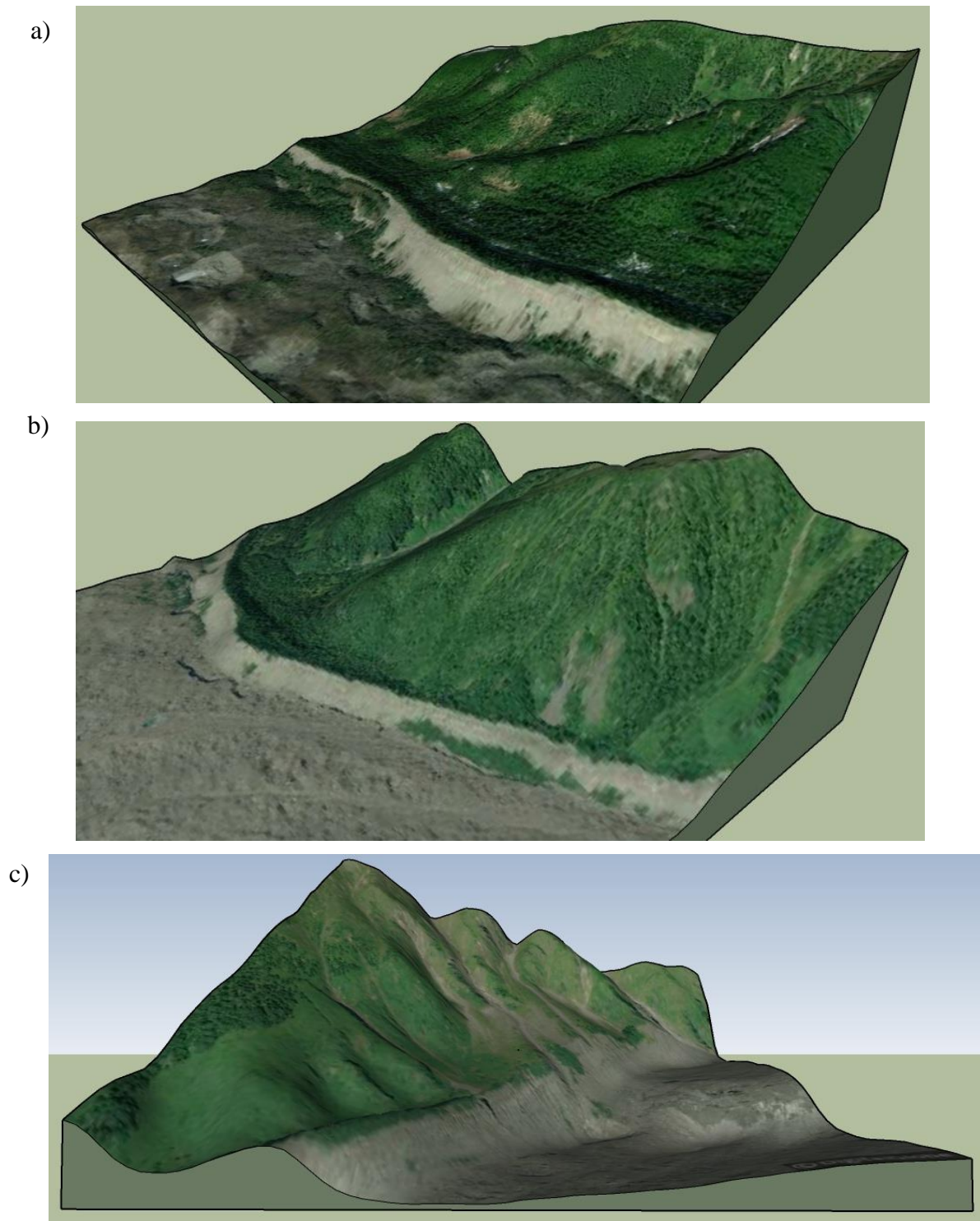


Figure A.6b: Study Site ID 006 (Fairweather Glacier) Terrain Models.

a), b) and c) are 2D Graphics of 3D Terrain Models. a) is a portion of the moraine in the down glacier section, b) is a portion of the moraine in the mid-glacier section and c) is a portion of the moraine in the up-glacier section.

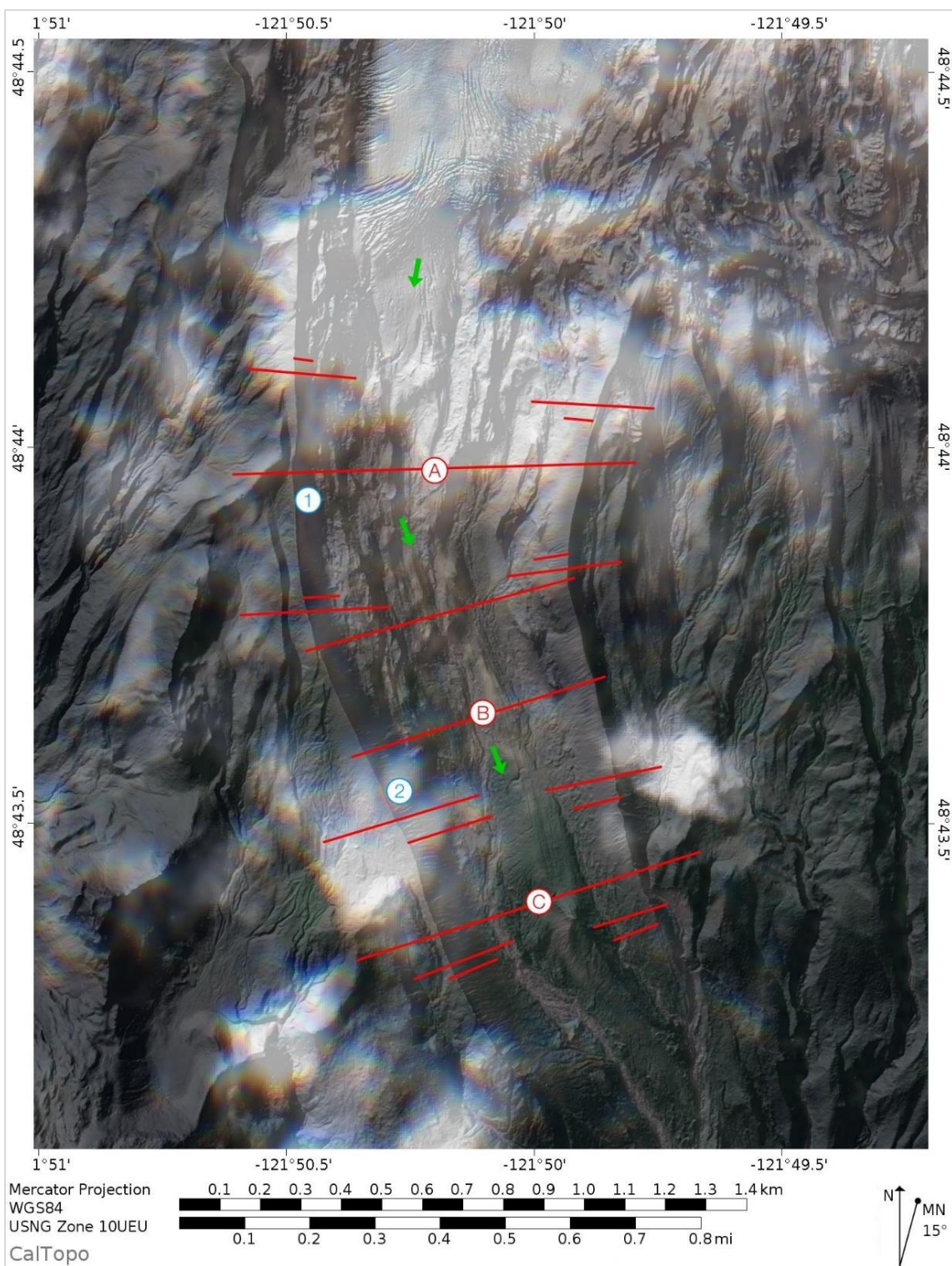


Figure A.7a: Study Site ID 055 (Easton Glacier) Mercator Map.

The green arrow indicates the direction of the glacier flow path. The blue numbers identify the location of gullies. The orange icon identifies the location of debris fans. The red lines identify the locations where transit sections were taken; up-valley is identified by red letter A, mid-glacier is defined by the red letter B and down glacier is defined by the red letter C.

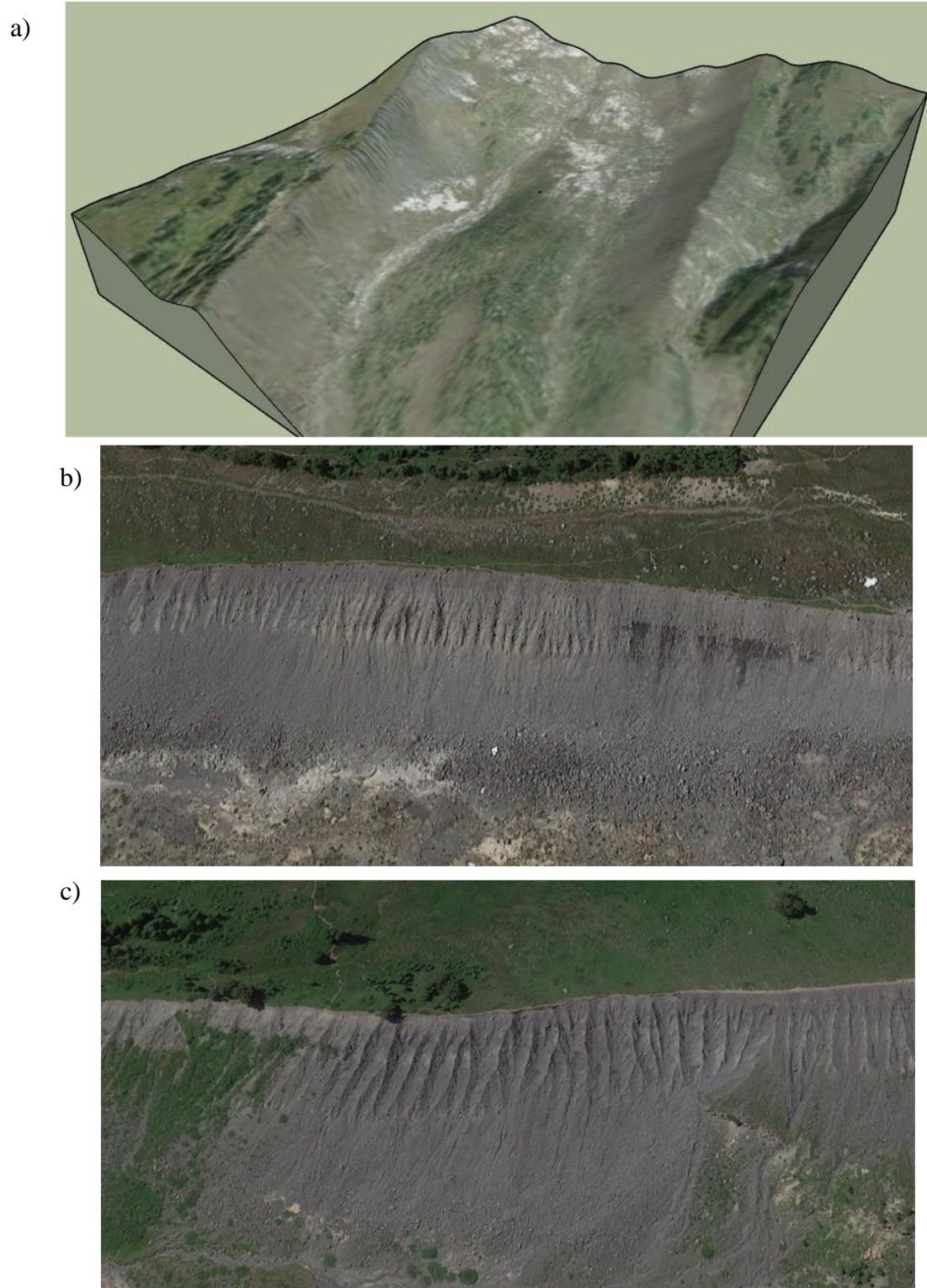


Figure A.7b: Study Site ID 055 (Easton Glacier) Terrain Model and Photos.

a) is a 2D graphic of the 3D terrain model in the down glacier position, b) and c) are photos, retrieved from Google Earth, capturing the gullying of the lateral moraine in the mid-glacier and down glacier sections respectively.

Photos Retrieved November 23, 2019 from <https://goo.gl/maps/5SWmYQNx6YtVS>.

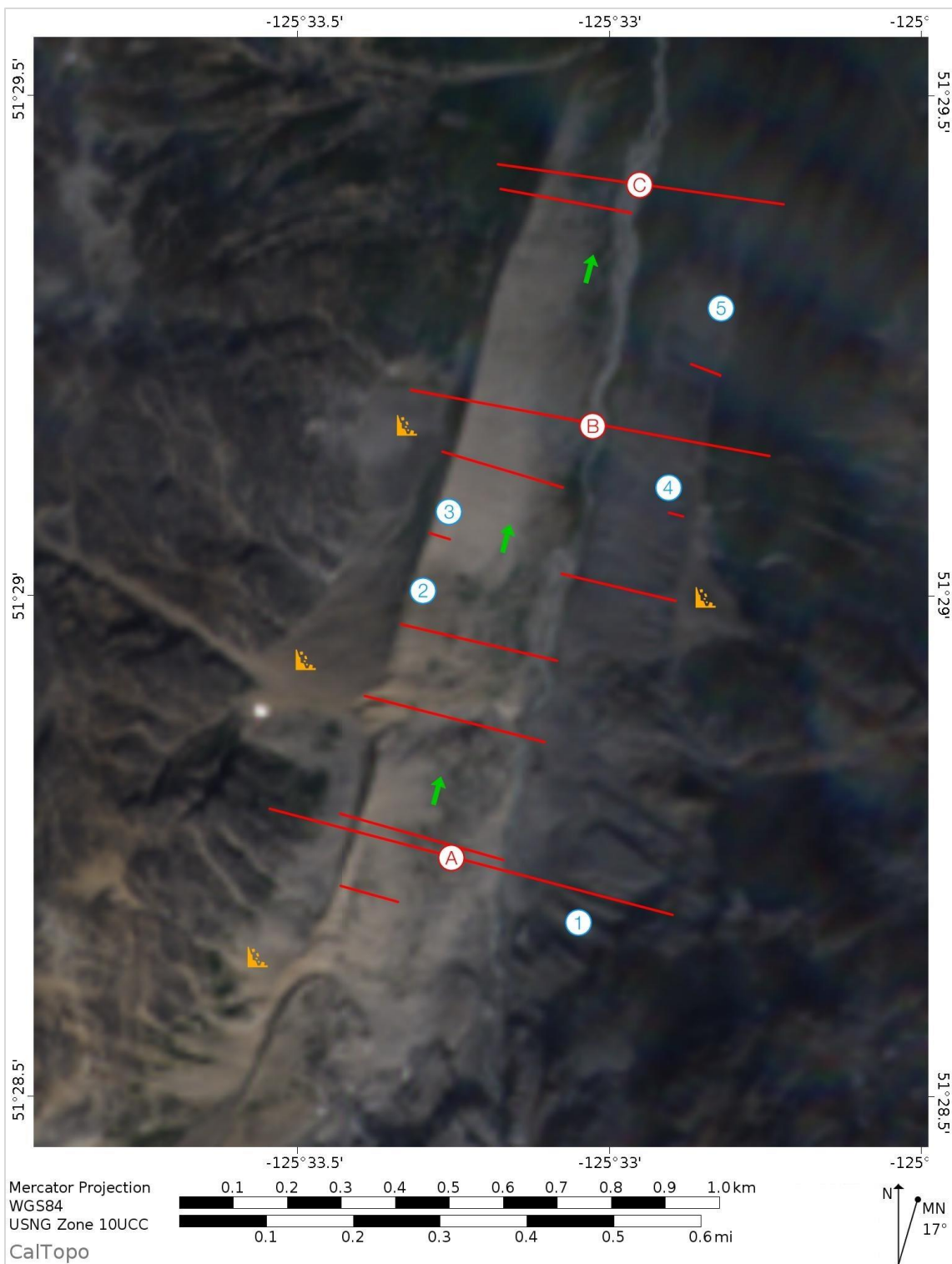


Figure A.8a: Study Site ID 033 (Mount Waddington A) Mercator Map.

The green arrow indicates the direction of the glacier flow path. The blue numbers identify the location of gullies. The orange icon identifies the location of debris fans. The red lines identify the locations where transit sections were taken; up-valley is identified by red letter A, mid-glacier is defined by the red letter B and down glacier is defined by the red letter C.

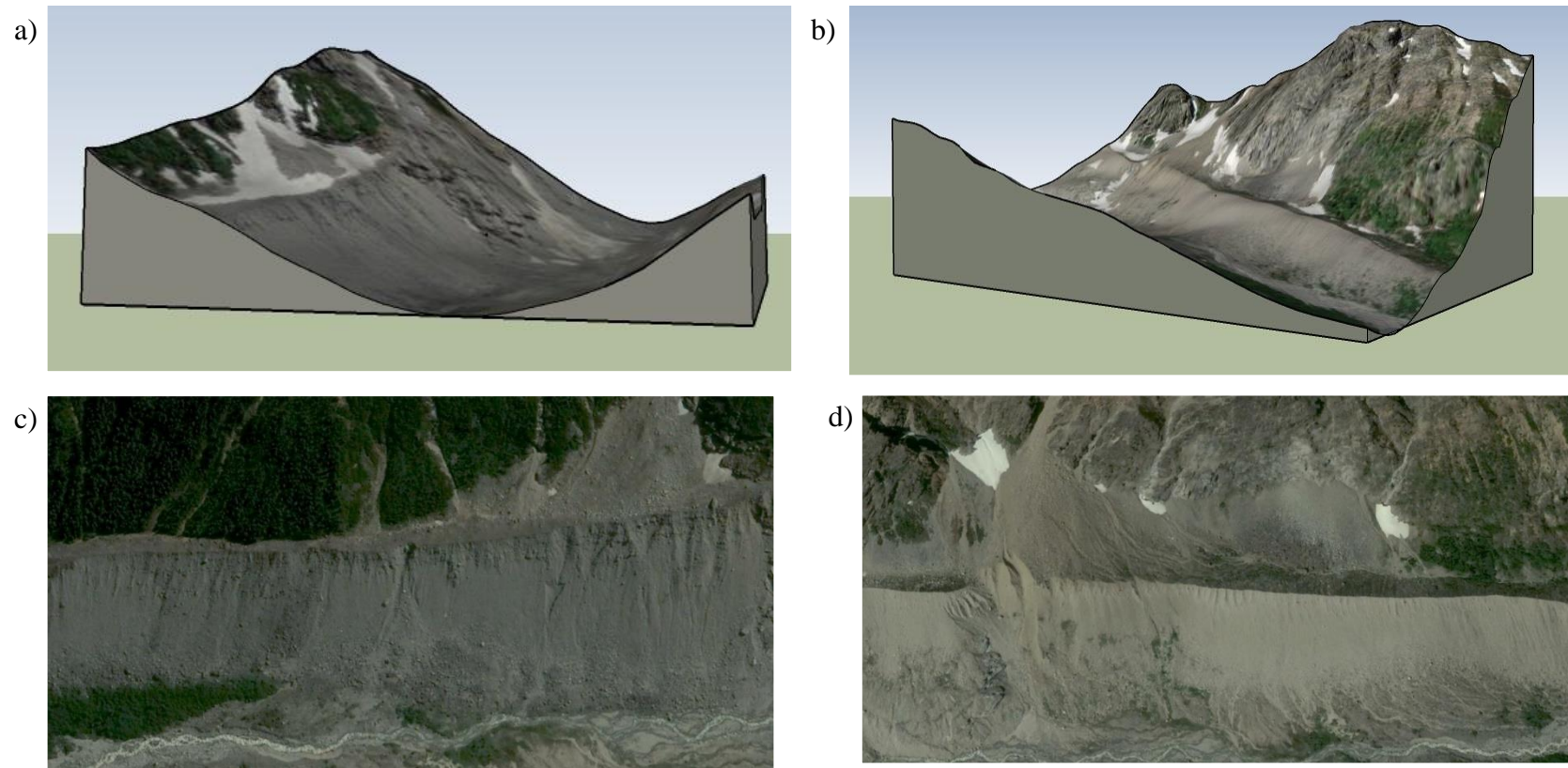


Figure A.8b: Study Site ID 033 (Mount Waddington A) Terrain Models and Photos.

a) and b) are 2D graphics of 3D terrain models of the east and west lateral moraines respectively with gullies (location 2, 3 and 4) and debris fans buttressed by the moraines, c) and d) are photos retrieved from Google Earth, capturing the same elements along the east and west lateral moraine respectively.

Photos Retrieved November 23, 2019 from <https://goo.gl/maps/5rK8AQJnNM9apzci6>.

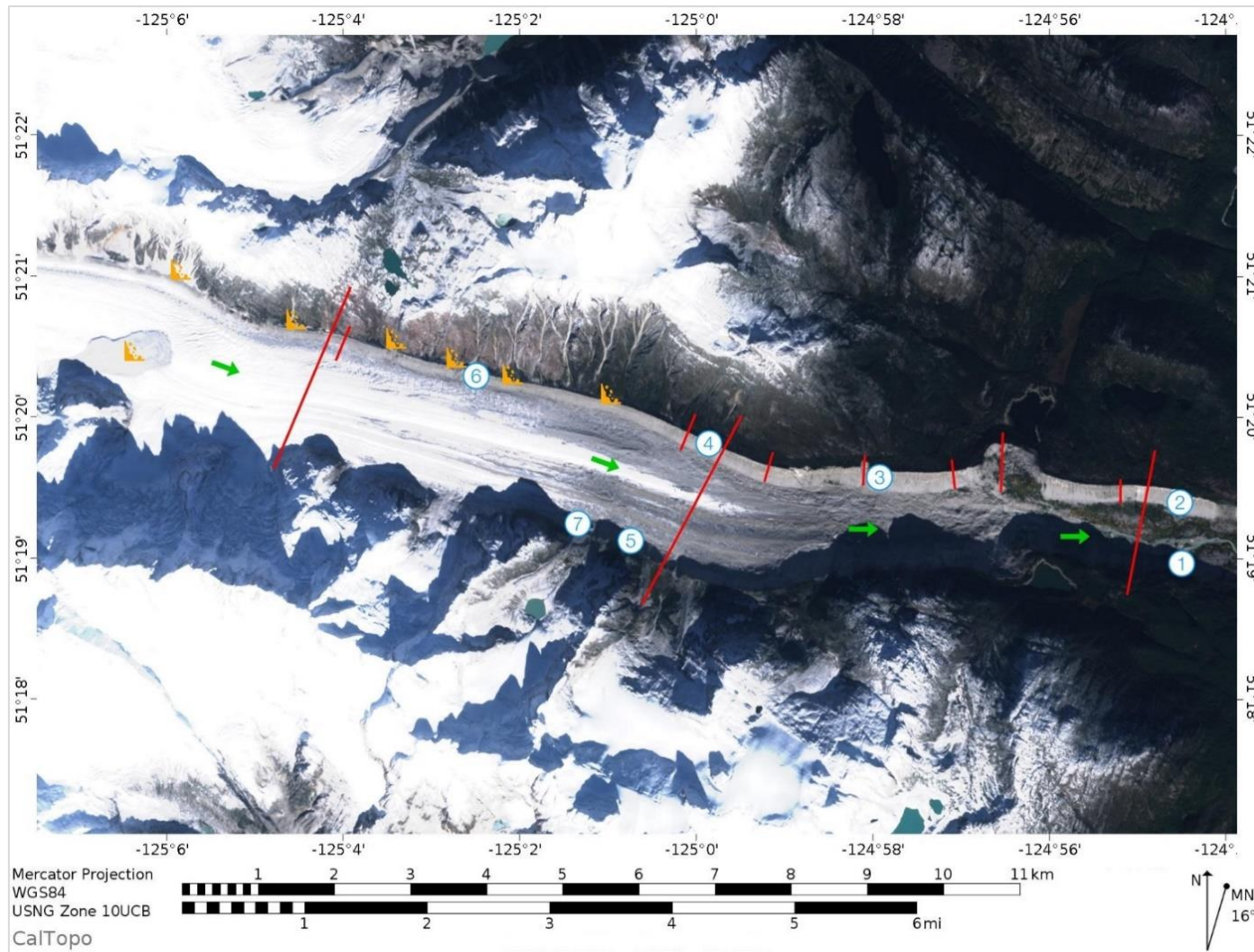


Figure A.9a: Study Site ID 050 (Tiedemann Glacier) Mercator Map.

The green arrow indicates the direction of the glacier flow path. The blue numbers identify the location of gullies. The orange icon identifies the location of debris fans. The red lines identify the locations where transit sections were taken; up-valley is identified by red letter A, mid-glacier is defined by the red letter B and down glacier is defined by the red letter C.

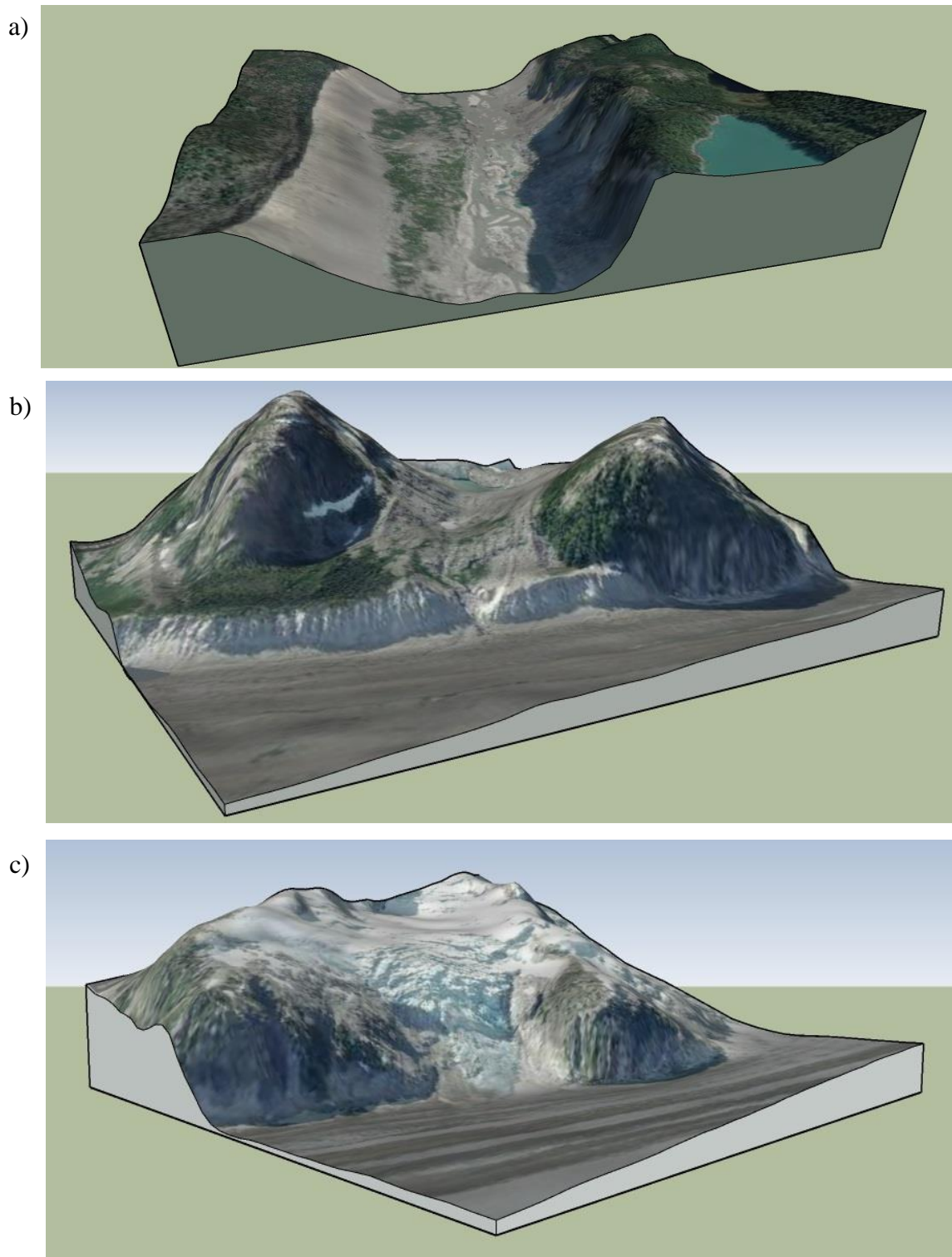


Figure A.9b: Study Site ID 050 (Tiedemann Glacier) Terrain Models.

a), b) and c) are 2D graphics of 3D terrain models, (a) is a view up-glacier from the down glacier position (b) is a view down glacier of the east lateral moraine at mid-glacier and (c) is a view, up-glacier, of the east lateral moraine.

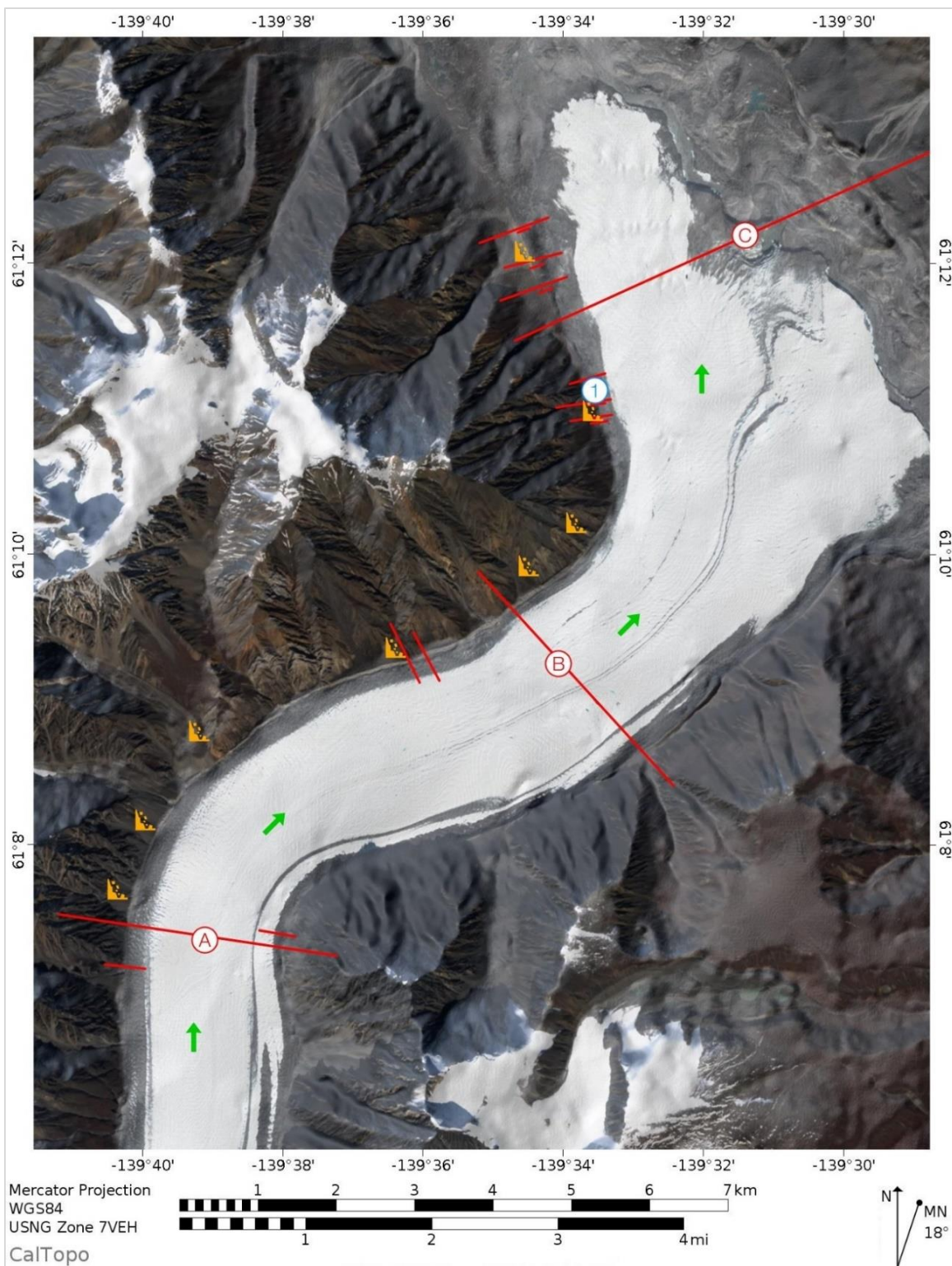


Figure A.10a: Study Site ID 051 (Donjek Glacier) Mercator Map.

The green arrow indicates the direction of the glacier flow path. The blue numbers identify the location of gullies. The orange icon identifies the location of debris fans. The red lines identify the locations where transit sections were taken; up-valley is identified by red letter A, mid-glacier is defined by the red letter B and down-glacier is defined by the red letter C.

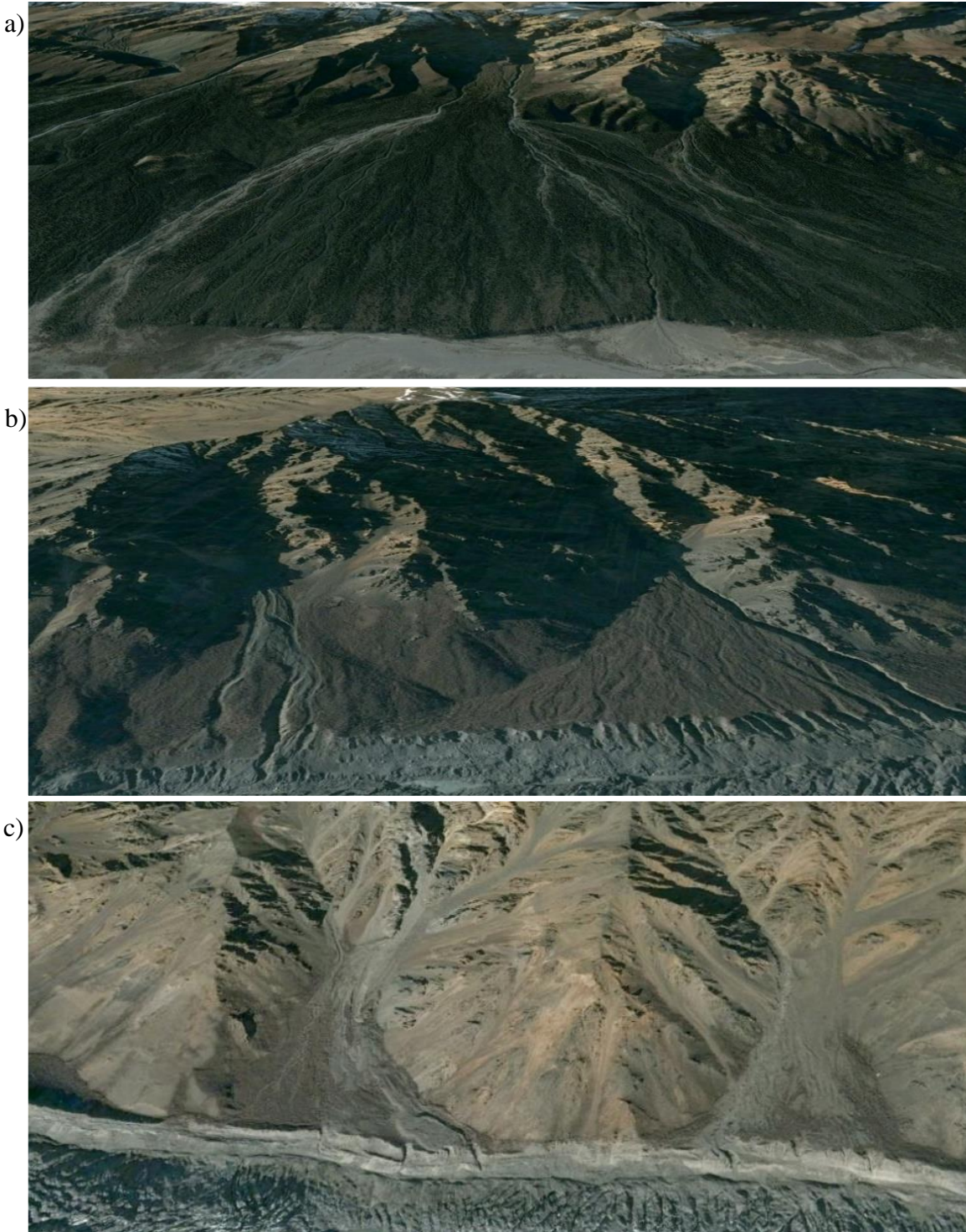


Figure A.10b: Study Site ID 051 (Donjek Glacier) Photos.

a), b) and c) are photos retrieved from Google Earth, a) is a photo of a large fan down glacier which is engulfed by vegetation, but with a large fluvial pathway b) is a photo of a large fan down glacier, devoid of vegetation, but with fluvial pathways and c) is a smaller fans further up-glacier, devoid of vegetation, but with fluvial pathways.

Photos Retrieved November 23, 2019 from <https://goo.gl/maps/Q7vraEUanYLLEqb>.

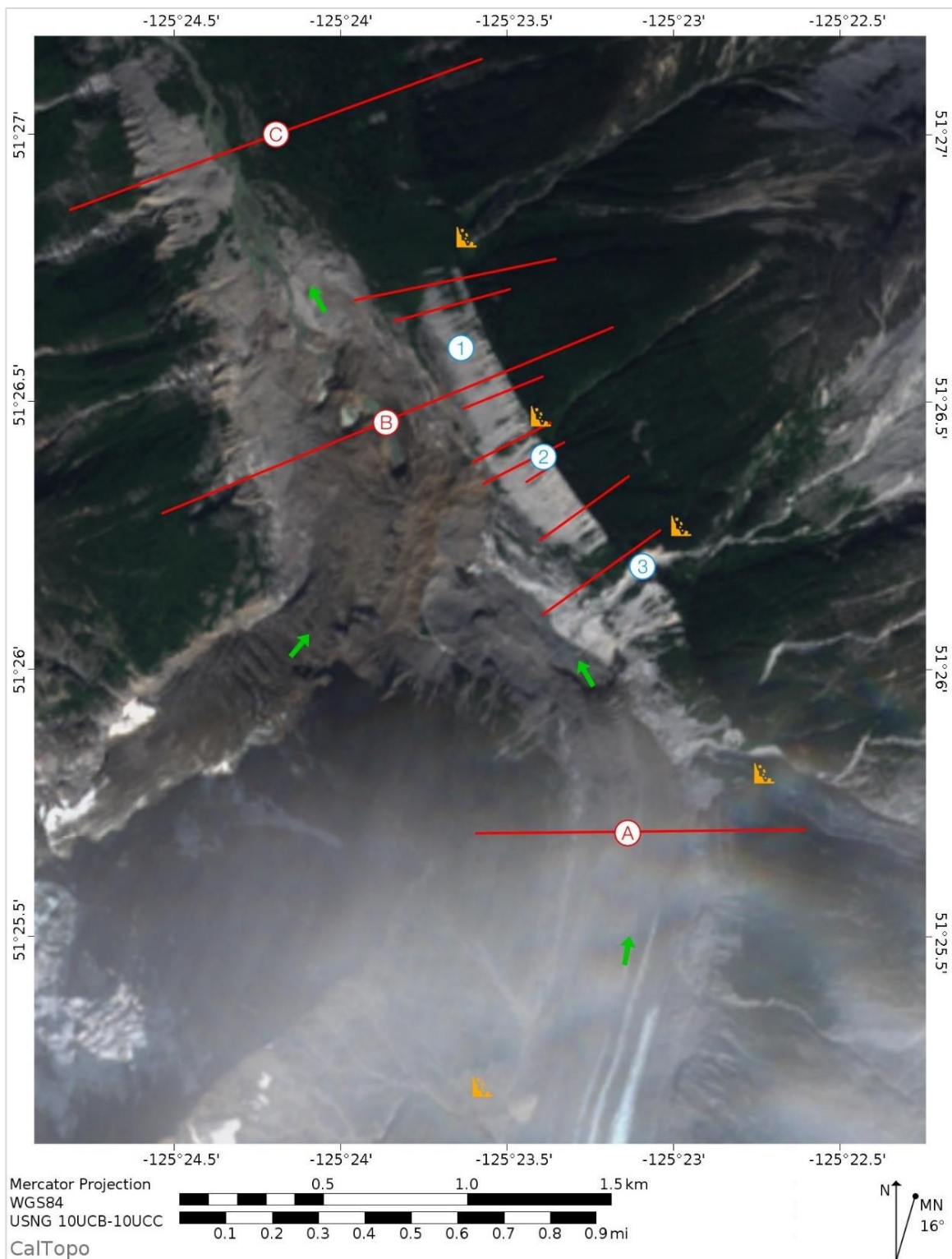


Figure A.11a: Study Site ID 028 (Bell Glacier) Mercator Map.

The green arrow indicates the direction of the glacier flow path. The blue numbers identify the location of gullies. The orange icon identifies the location of debris fans. The red lines identify the locations where transit sections were taken; up-valley is identified by red letter A, mid-glacier is defined by the red letter B and down-glacier is defined by the red letter C.

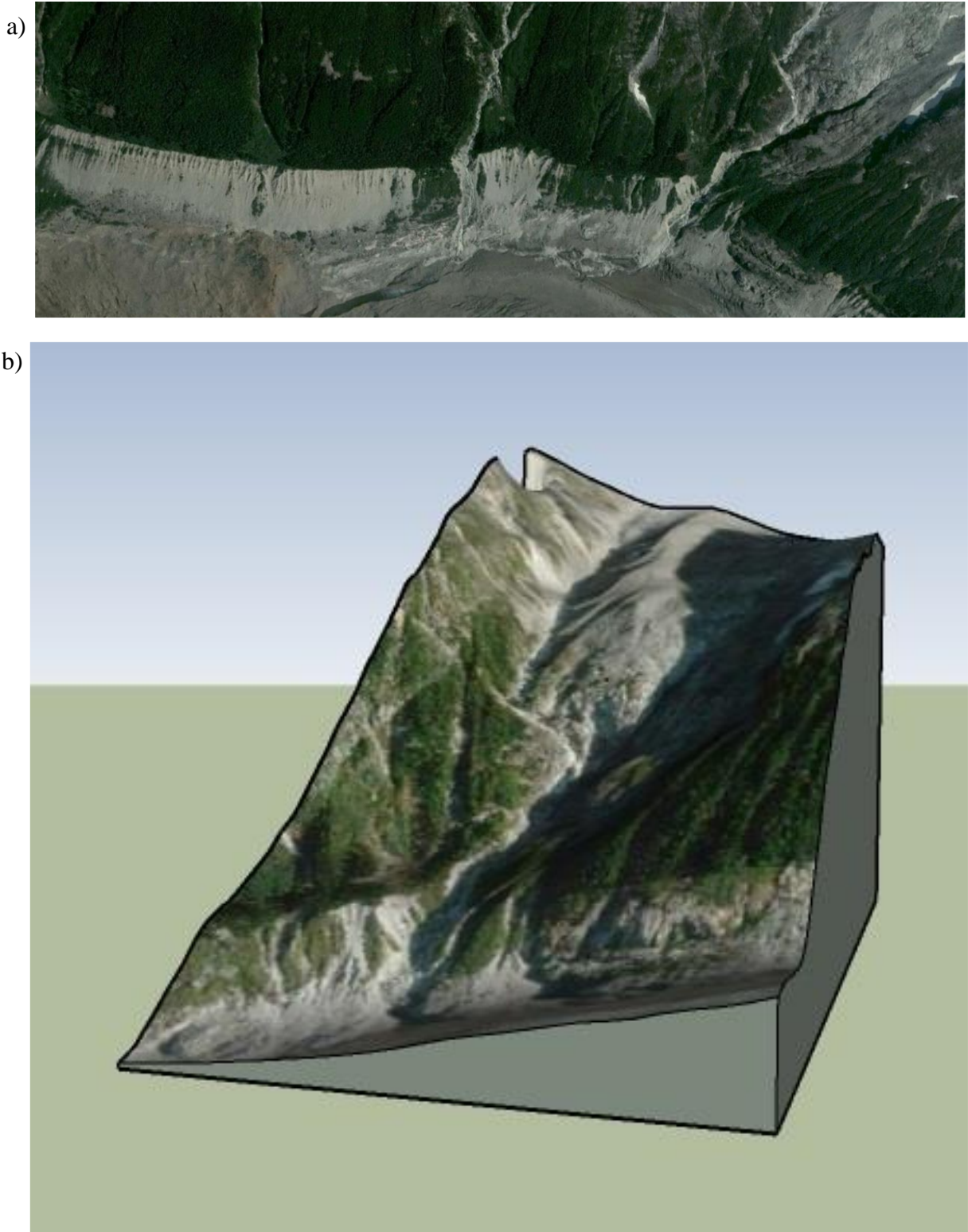


Figure A.11b: Study Site ID 028 (Bell Glacier) Terrain Model and Photo.

a) photo, retrieved from Google Earth, capturing the gullying of the lateral moraine in the mid-glacier section and in way of a fluvial debris flow, and b) Is a 2D graphic of the 3D terrain model of the fluvial debris supply.

Photo Retrieved November 23, 2019 from <https://goo.gl/maps/oGQ3MNyUk8dDBeKn6>.

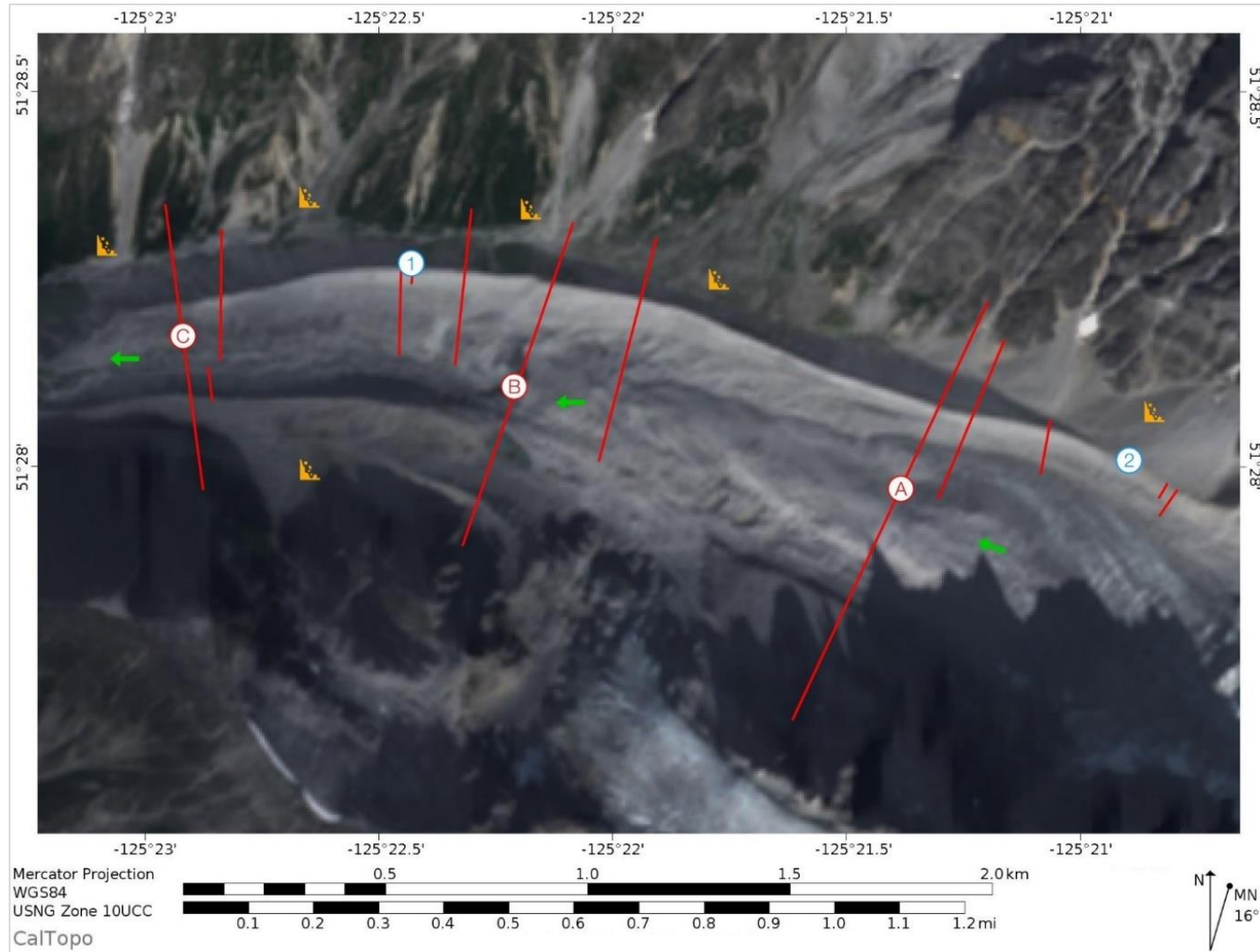


Figure A.12a: Study Site ID 029 (Roovers Glacier) Mercator Map.

The green arrow indicates the direction of the glacier flow path. The blue numbers identify the location of gullies. The orange icon identifies the location of debris fans. The red lines identify the locations where transit sections were taken; up-valley is identified by red letter A, mid-glacier is defined by the red letter B and down glacier is defined by the red letter C.

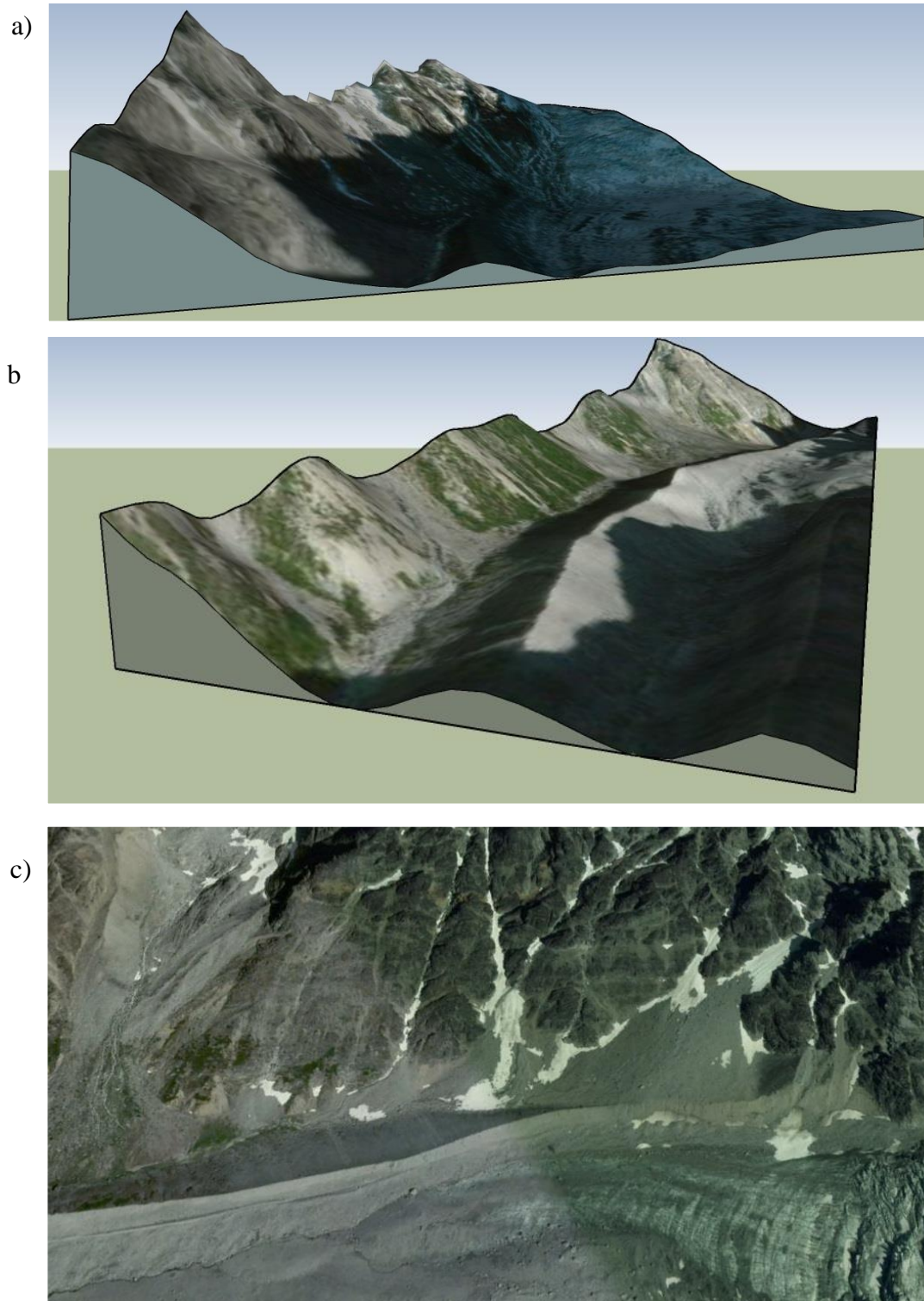


Figure A.12b: Study Site ID 029 (Roovers Glacier) Terrain Models and Photo.

a) and b) are 2D graphics of 3D terrain models of the north lateral moraine up-glacier in (a) and continuing down glacier in (b), c) is a photo, retrieved from Google Earth, capturing the debris fans buttressed by the north lateral moraine in up-glacier section.

Photo Retrieved November 23, 2019 from <https://goo.gl/maps/5rK8AQJnNM9apzci6>.

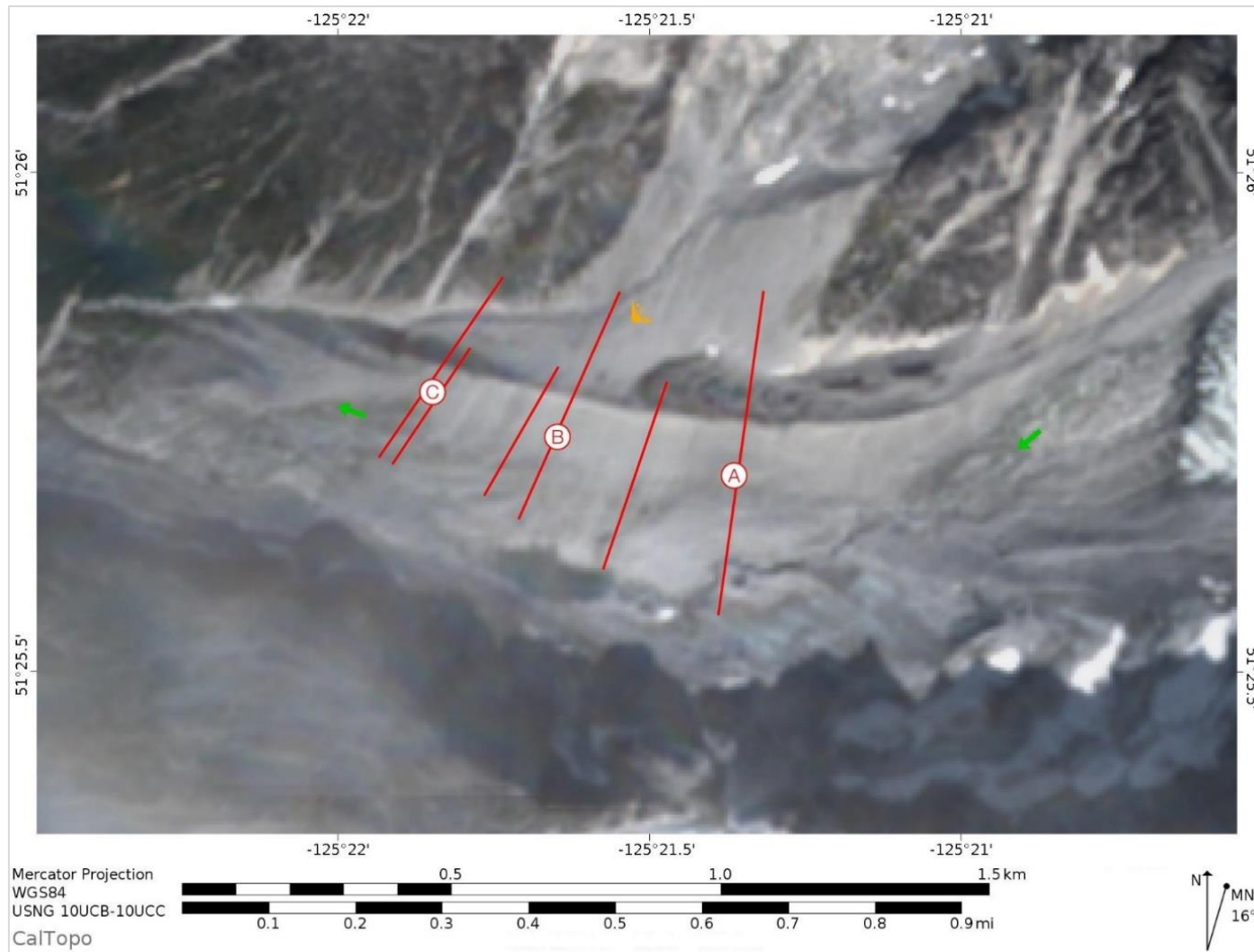


Figure A.13a: Study Site ID 030 (Geddes Glacier) Mercator Map.

The green arrow indicates the direction of the glacier flow path. The blue numbers identify the location of gullies. The orange icon identifies the location of debris fans. The red lines identify the locations where transit sections were taken; up-valley is identified by red letter A, mid-glacier is defined by the red letter B and down-glacier is defined by the red letter C.

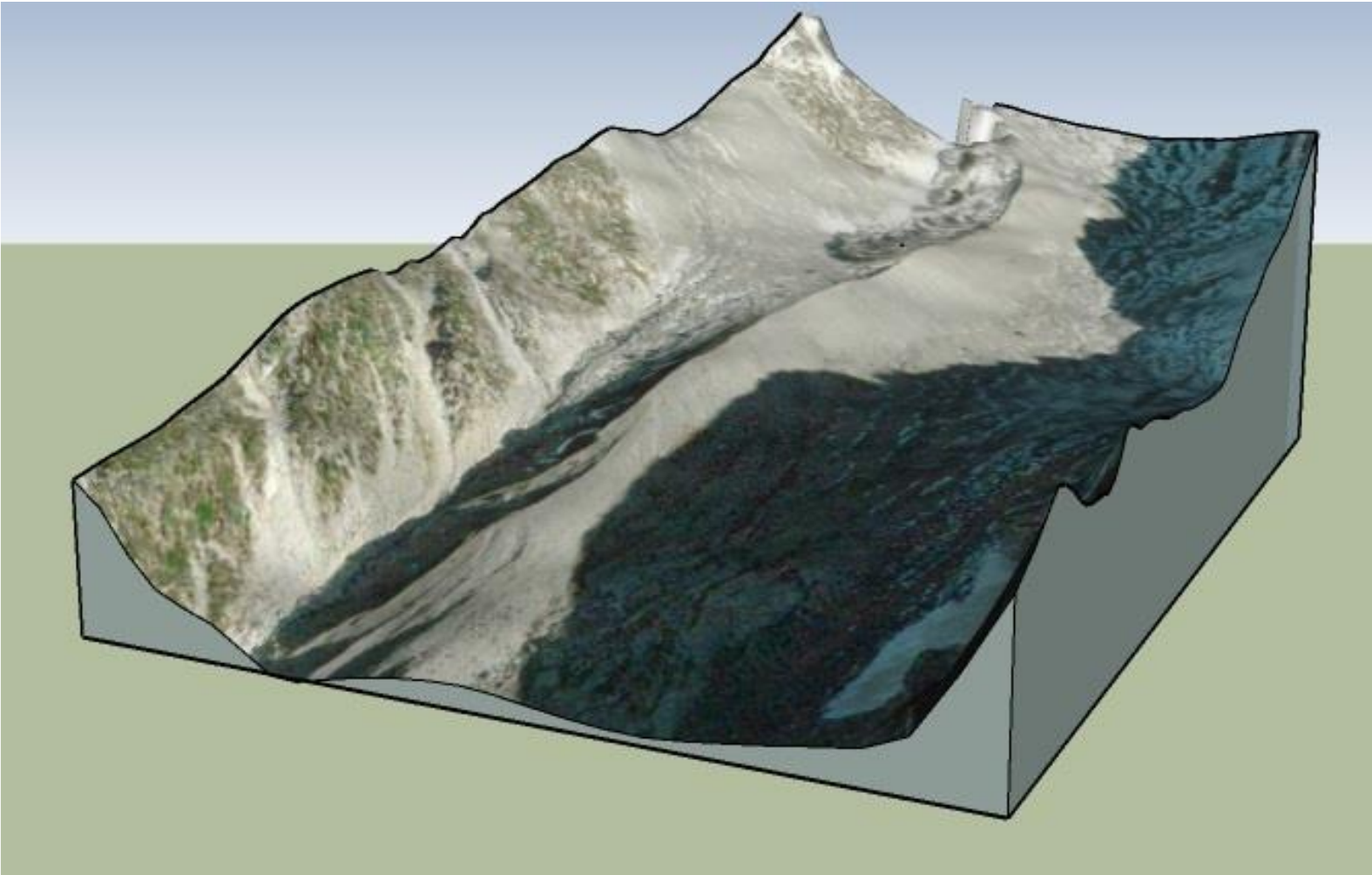


Figure A.13b: Figure M.2 Study Site ID 030 (Geddes Glacier) Terrain Model.
2D graphic of a 3D terrain model of the north lateral moraine with a debris fan buttressed by the moraine.

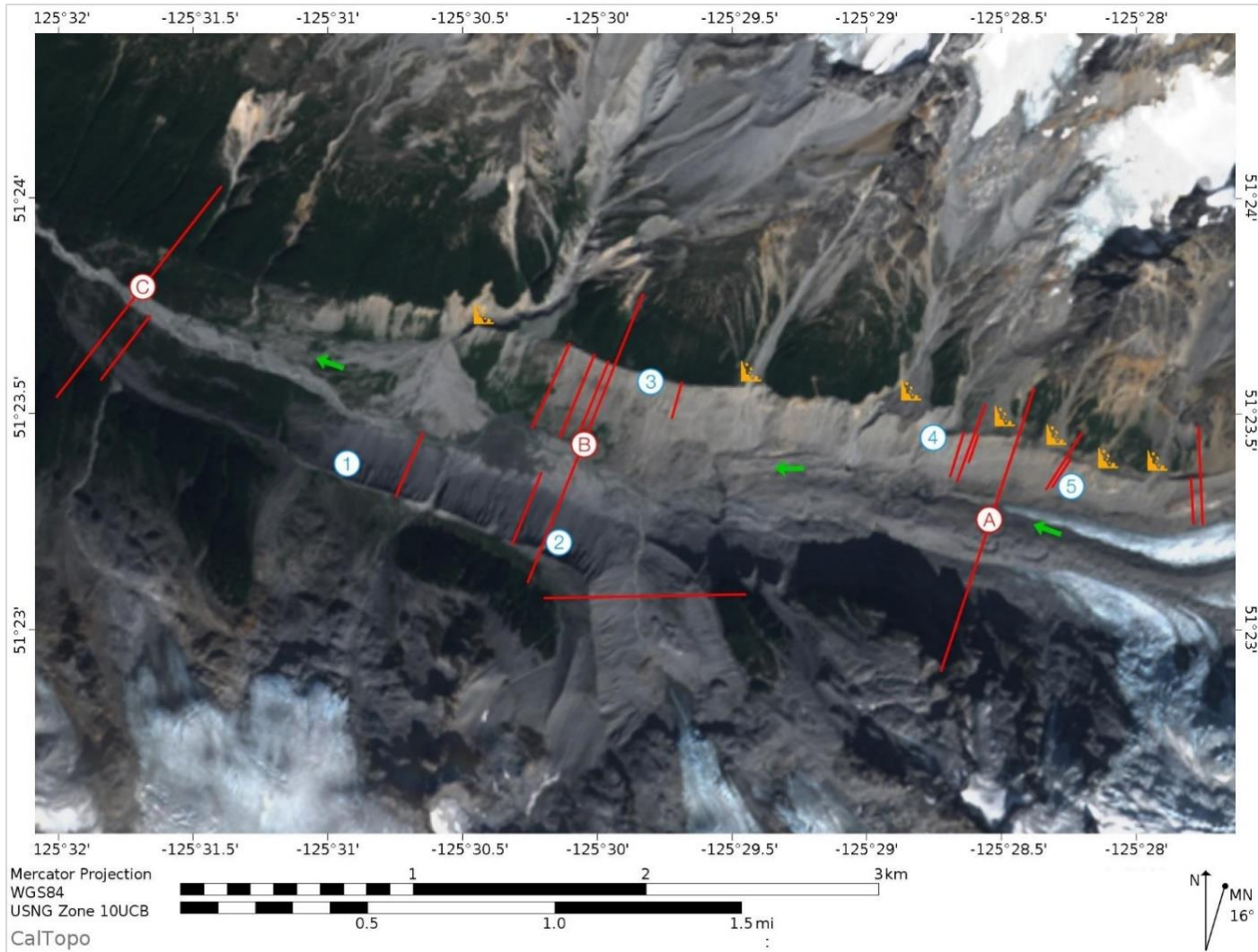


Figure A.14a: Study Site ID 032 (Dorothy Glacier) Mercator Map.

The green arrow indicates the direction of the glacier flow path. The blue numbers identify the location of gullies. The orange icon identifies the location of debris fans. The red lines identify the locations where transit sections were taken; up-valley is identified by red letter A, mid-glacier is defined by the red letter B and down glacier is defined by the red letter C.

a)

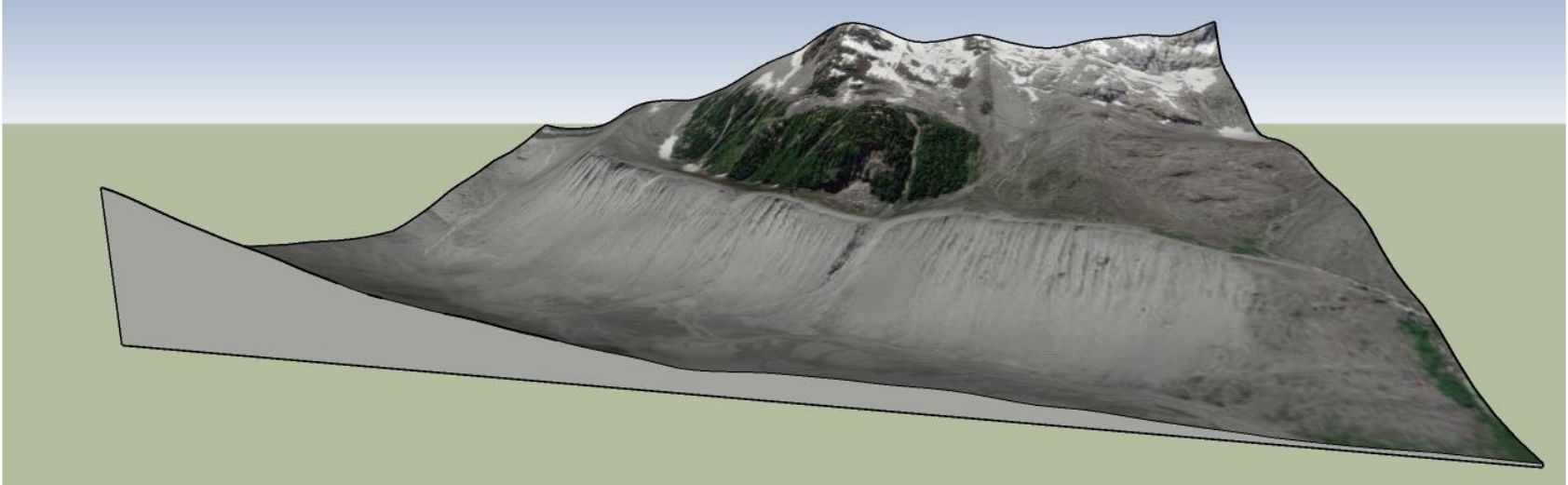


Figure A.14b: Study Site ID 032 (Dorothy Glacier) Terrain Model and Photo.

a) is a photo, retrieved from Google Earth, capturing the debris fans buttressed by the north lateral moraine. and b) is a 2D graphic of the 3D terrain model of the south lateral moraine with gullies (location 1 and 2) and a debris fan buttressed by the moraine.

Photo Retrieved November 23, 2019 from <https://goo.gl/maps/5rK8AQJnNM9apzci6>.

b)



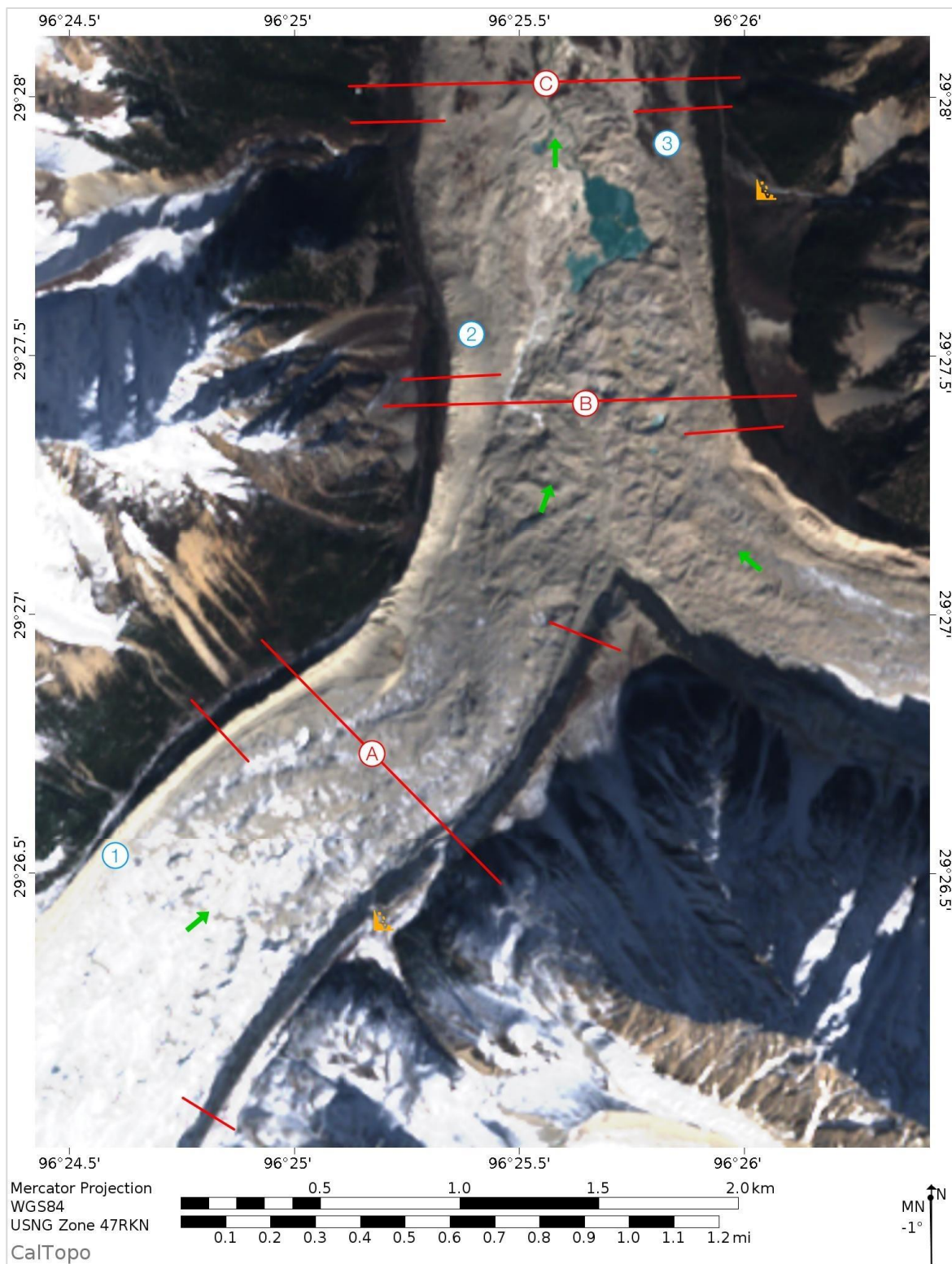


Figure A.15a: Study Site ID 048 (Nagong, China) Mercator Map. The green arrow indicates the direction of the glacier flow path. The blue numbers identify the location of gullies. The orange icon identifies the location of debris fans. The red lines identify the locations where transit sections were taken; up-valley is identified by red letter A, mid-glacier is defined by the red letter B and down-glacier is defined by the red letter C.

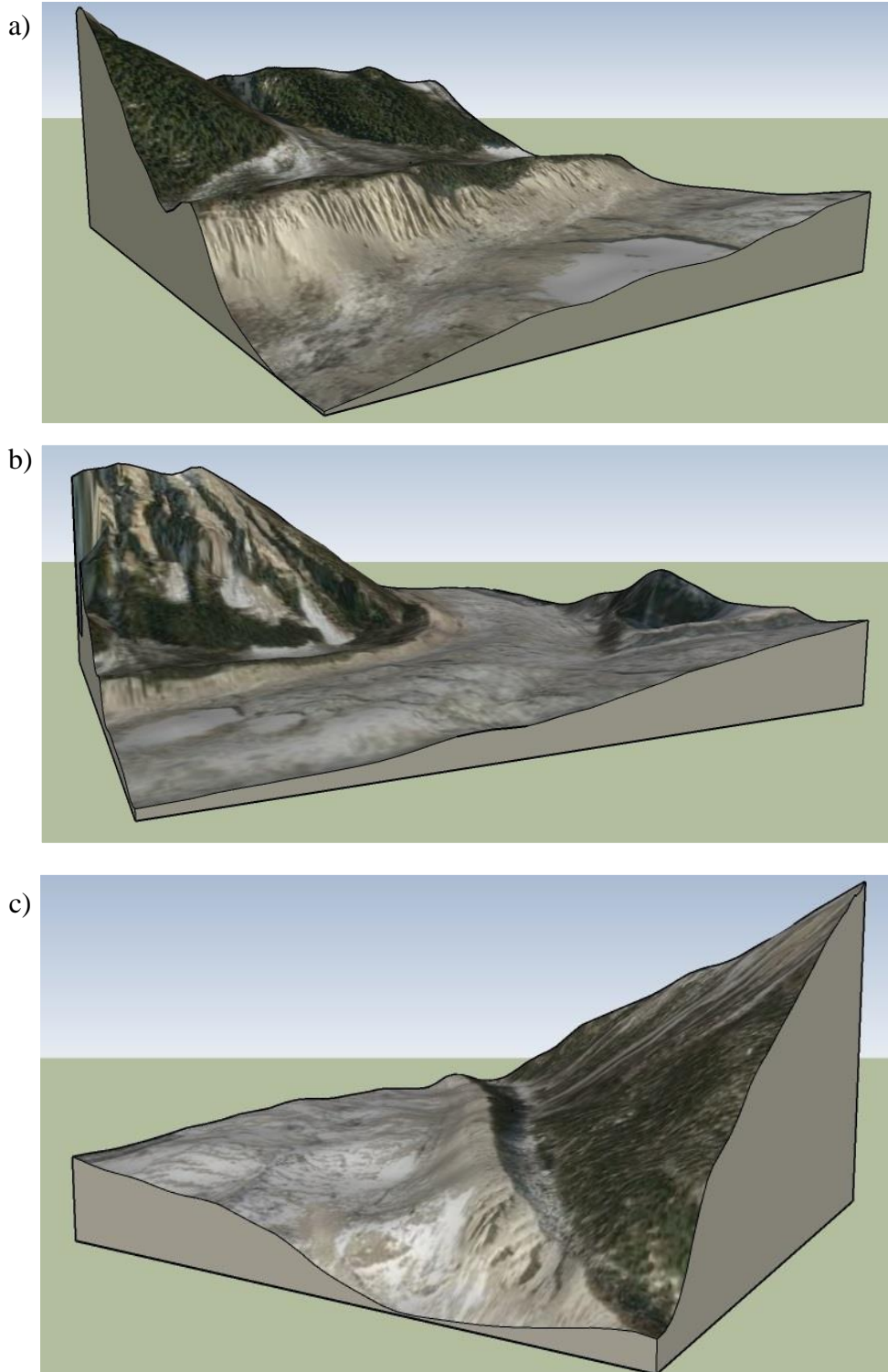


Figure A.15b: Study Site ID 048 (Nagong, China) Terrain Models.

a), b) and c) are 2D Graphics of 3D terrain models, (a) is a section of the reworked lateral moraine, in the down glacier section, where the debris fan buttresses the lateral moraine, (b) is the section of the valley where the two tributaries come together and (c) is an example of a the reworking of the lateral moraine by the fluvial runoff down the lateral morainic trough, located on the west moraine of the west tributary.

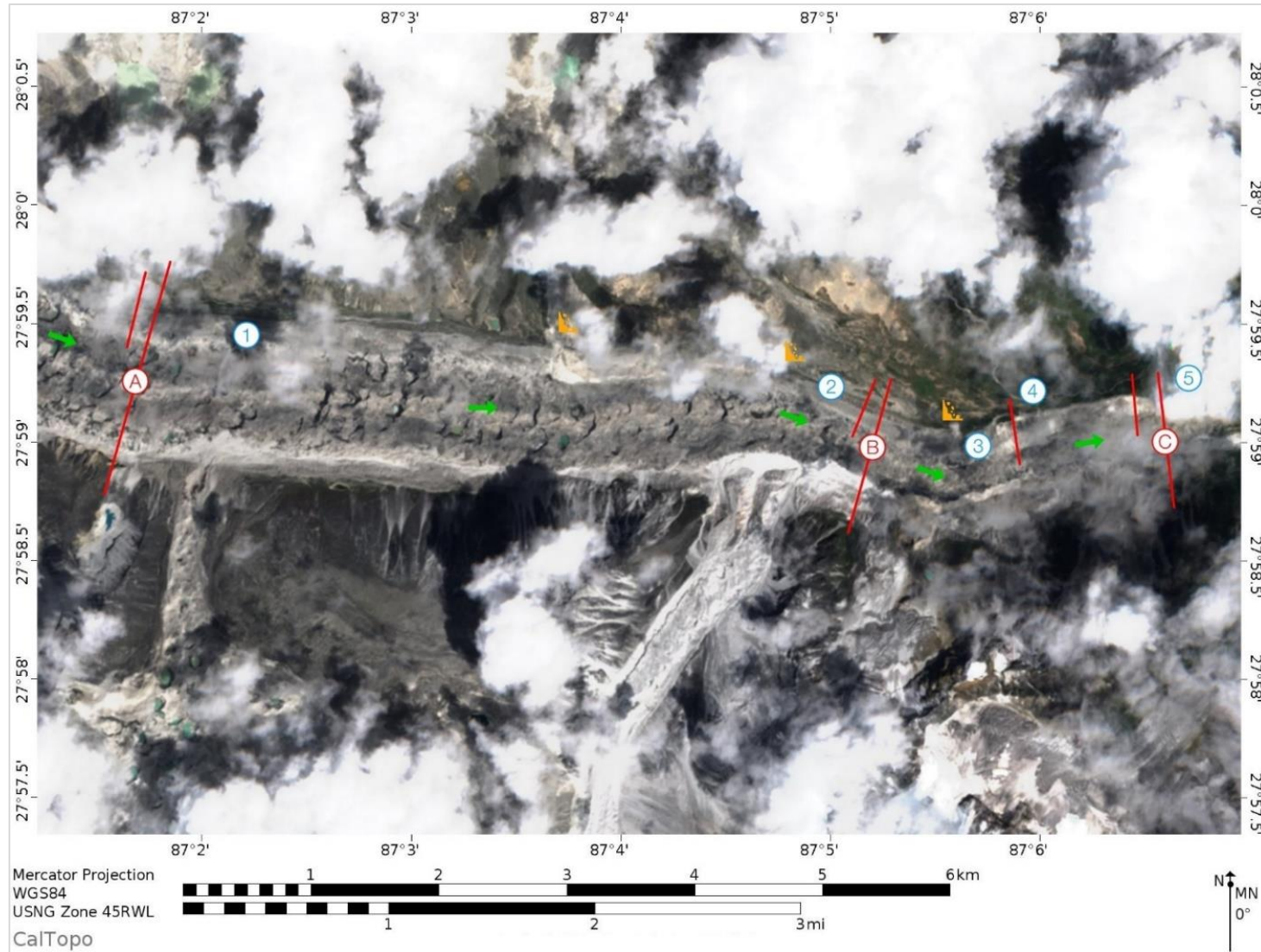


Figure A.16a: Study Site ID 034 (Mount Everest) Mercator Map.

The green arrow indicates the direction of the glacier flow path. The blue numbers identify the location of gullies. The orange icon identifies the location of debris fans. The red lines identify the locations where transit sections were taken; up-valley is identified by red letter A, mid-glacier is defined by the red letter B and down glacier is defined by the red letter C.

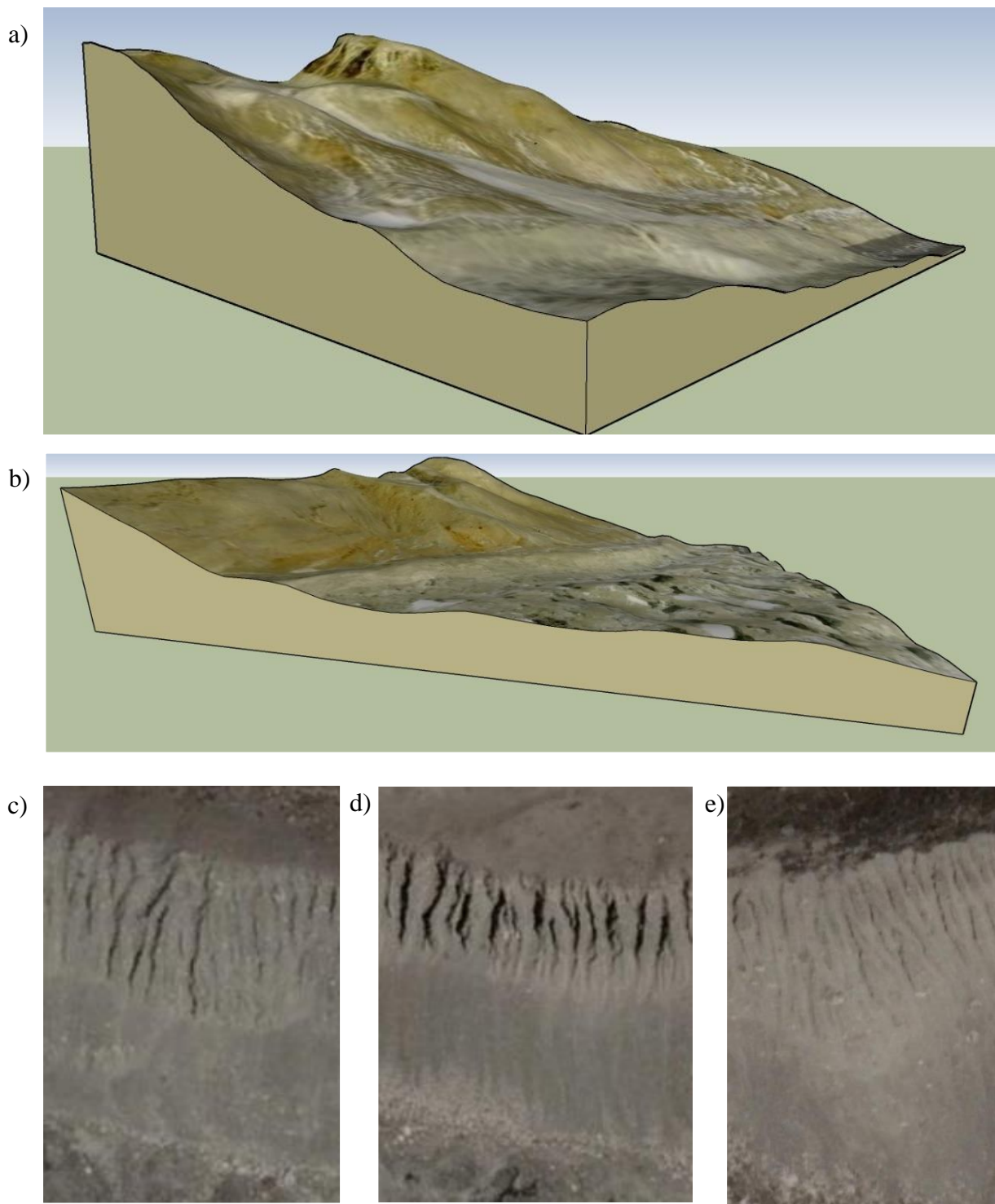


Figure A.16b: Study Site ID 034 (Mount Everest) Terrain Models and Photos.

a) and b) are 2D Graphics of 3D terrain models of the north lateral moraine with debris fans buttressed by the moraine in (a), c), d) and e) are photos, retrieved from Google Earth, capturing the lateral moraine gullies in the up-glacier, mid-glacier and down glacier positions respectively.

Photos Retrieved November 23, 2019 from <https://goo.gl/maps/44fD6vpexFriQr218>.

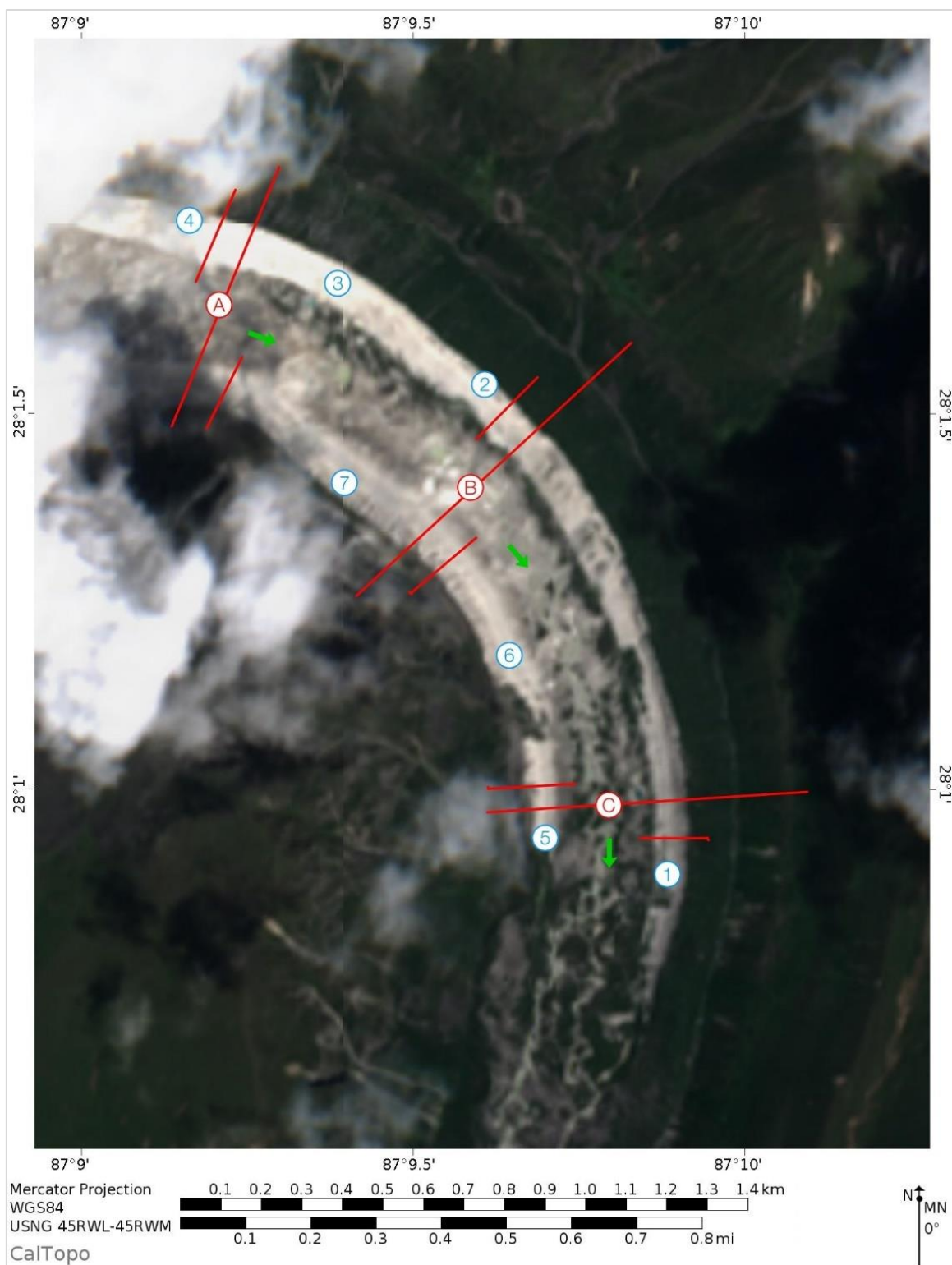


Figure A.17a: Study Site ID 056 (Mount Everest - 2) Mercator Map.

The green arrow indicates the direction of the glacier flow path. The blue numbers identify the location of gullies. The orange icon identifies the location of debris fans. The red lines identify the locations where transit sections were taken; up-valley is identified by the red letter A, mid-glacier is defined by the red letter B and down glacier is defined by the red letter C.

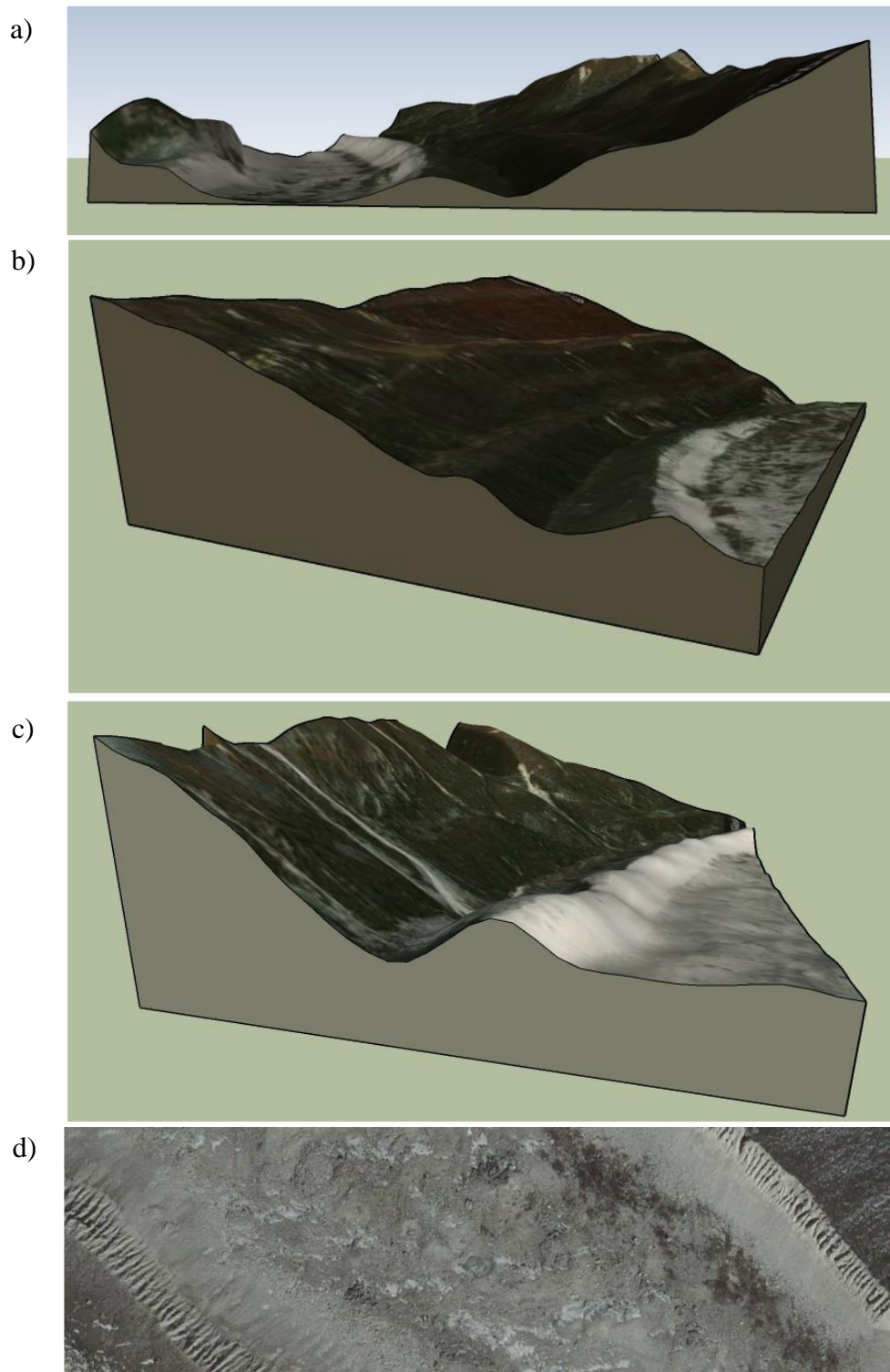


Figure A.17b: Study Site ID 056 (Mount Everest - 2) Terrain Models and Photo. a), b) and c) are 2D Graphics of 3D terrain models, (a) is a view up-glacier from the down glacier position (b) is a view down glacier of the east lateral moraine a mid-glacier and (c) is a view, up-glacier, of the east lateral moraine, and d) is a photo capture in Google Earth, of the gullied lateral moraines in the mid-glacier section. Photo Retrieved November 23, 2019 from <https://goo.gl/maps/K73VGxCfM865Ks3G8>.

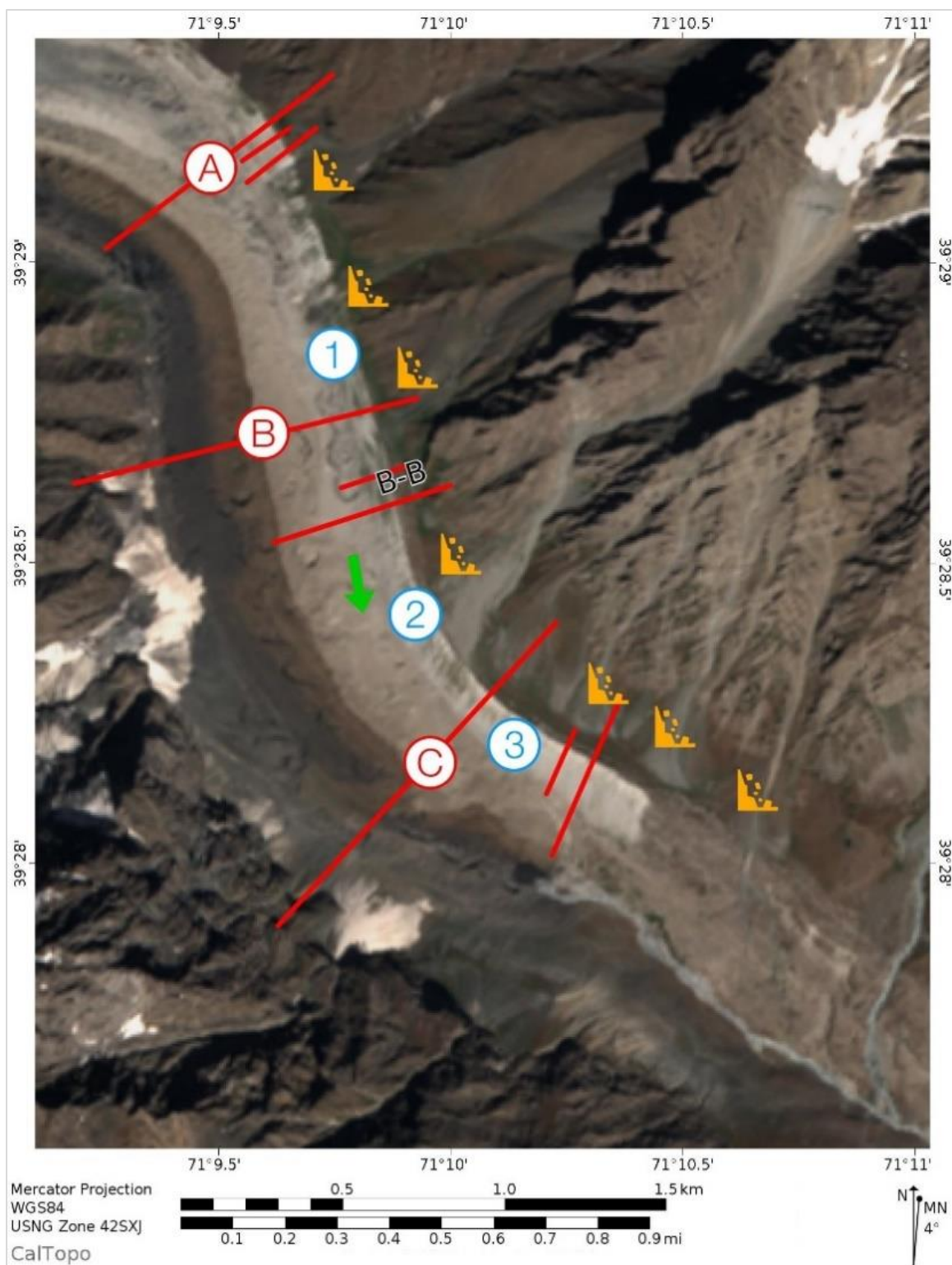


Figure A.18a: Study Site ID 012 (Tamdykul Mountain) Mercator Map.

The green arrow indicates the direction of the glacier flow path. The blue numbers identify the location of gullies. The orange icon identifies the location of debris fans. The red lines identify the locations where transit sections were taken; up-valley is identified by the red letter A, mid-glacier is defined by the red letter B and down glacier is defined by the red letter C.

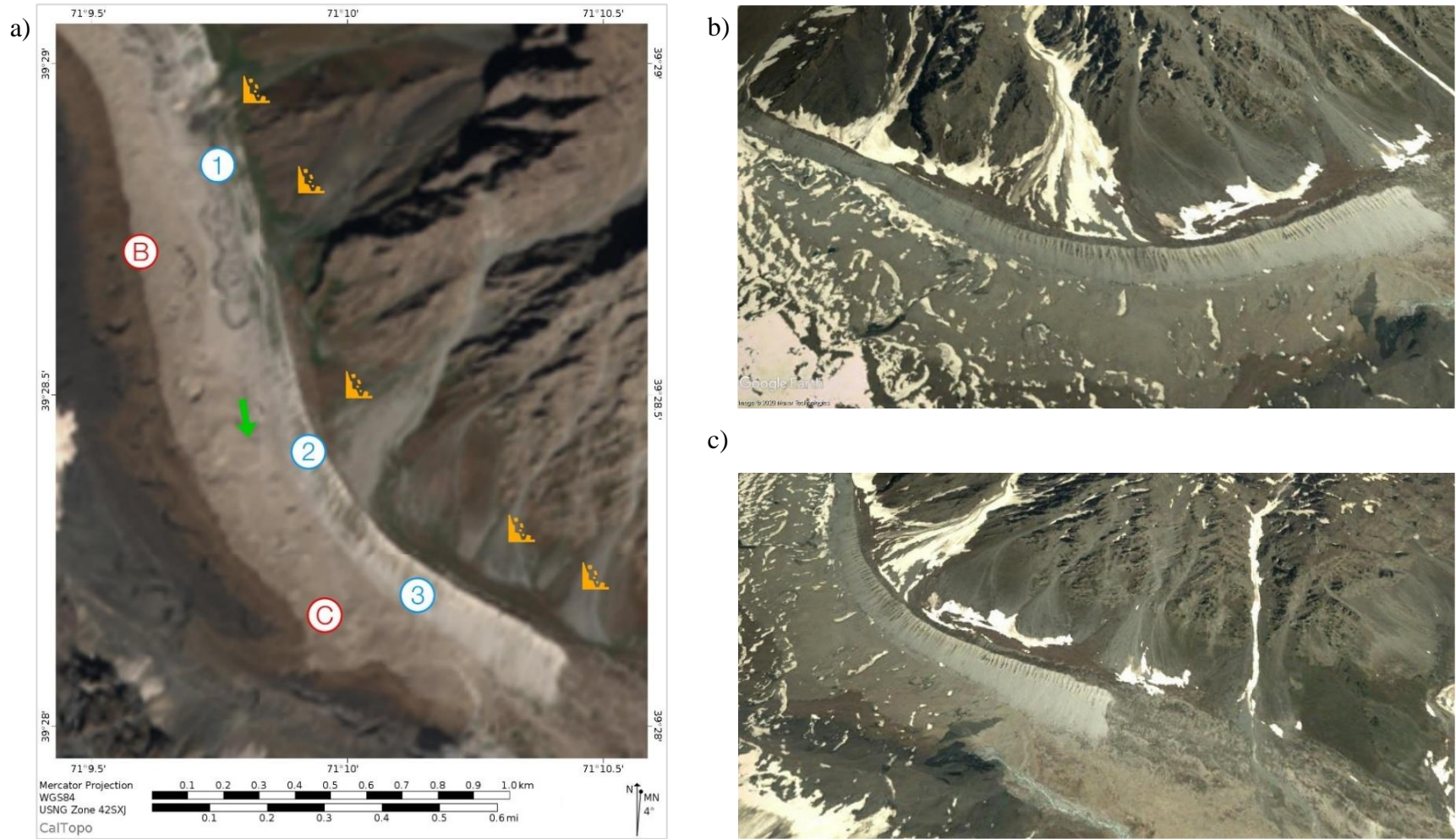


Figure A.18b: Study Site ID 012 (Tamdykul Mountain) Mercator Map and Photos.

a). A Mercator Map of the down glacier section, b) and c) Photos retrieved from Google Earth, capturing the debris fans buttressed by the lateral moraine, gulying of the moraine and the lateral morainic trough.

Photos Retrieved November 23, 2019 from <https://goo.gl/maps/73s8NXwCfxgD64Xy7>.

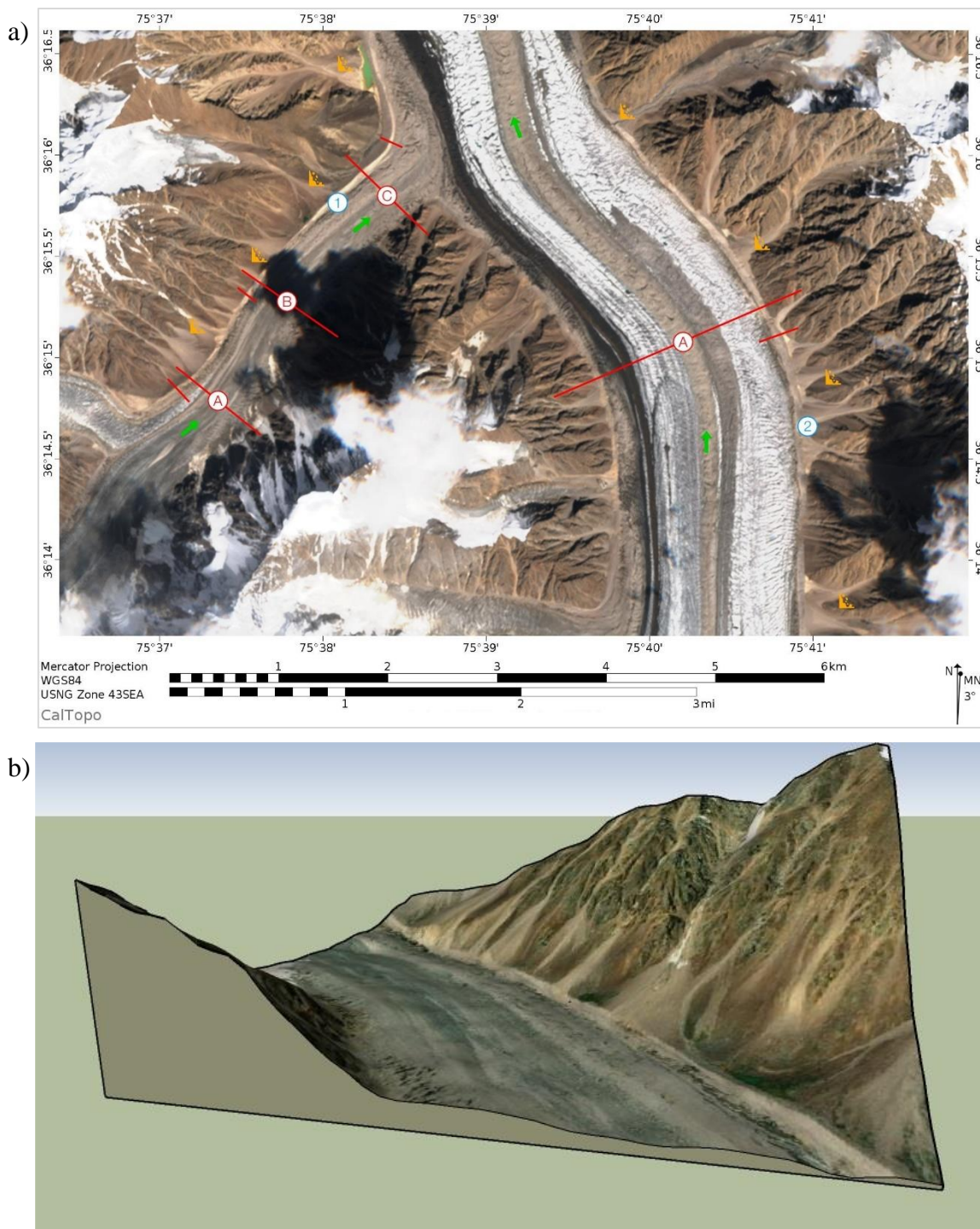


Figure A.19a: Study Site ID 041 (Afghanistan) Mercator Map and Terrain Model.

a) A Mercator Map of the Study Site. The green arrow indicates the direction of the glacier flow path. The blue numbers identify the location of gullies. The orange icon identifies the location of debris fans. The red lines identify the locations where transit sections were taken; up-valley is identified by red letter A, mid-glacier is defined by the red letter B and down glacier is defined by the red letter C and b) is a 2D graphic of a 3D terrain model of a portion of the deglaciating valley, looking down glacier from the up-glacier section of the trunk.

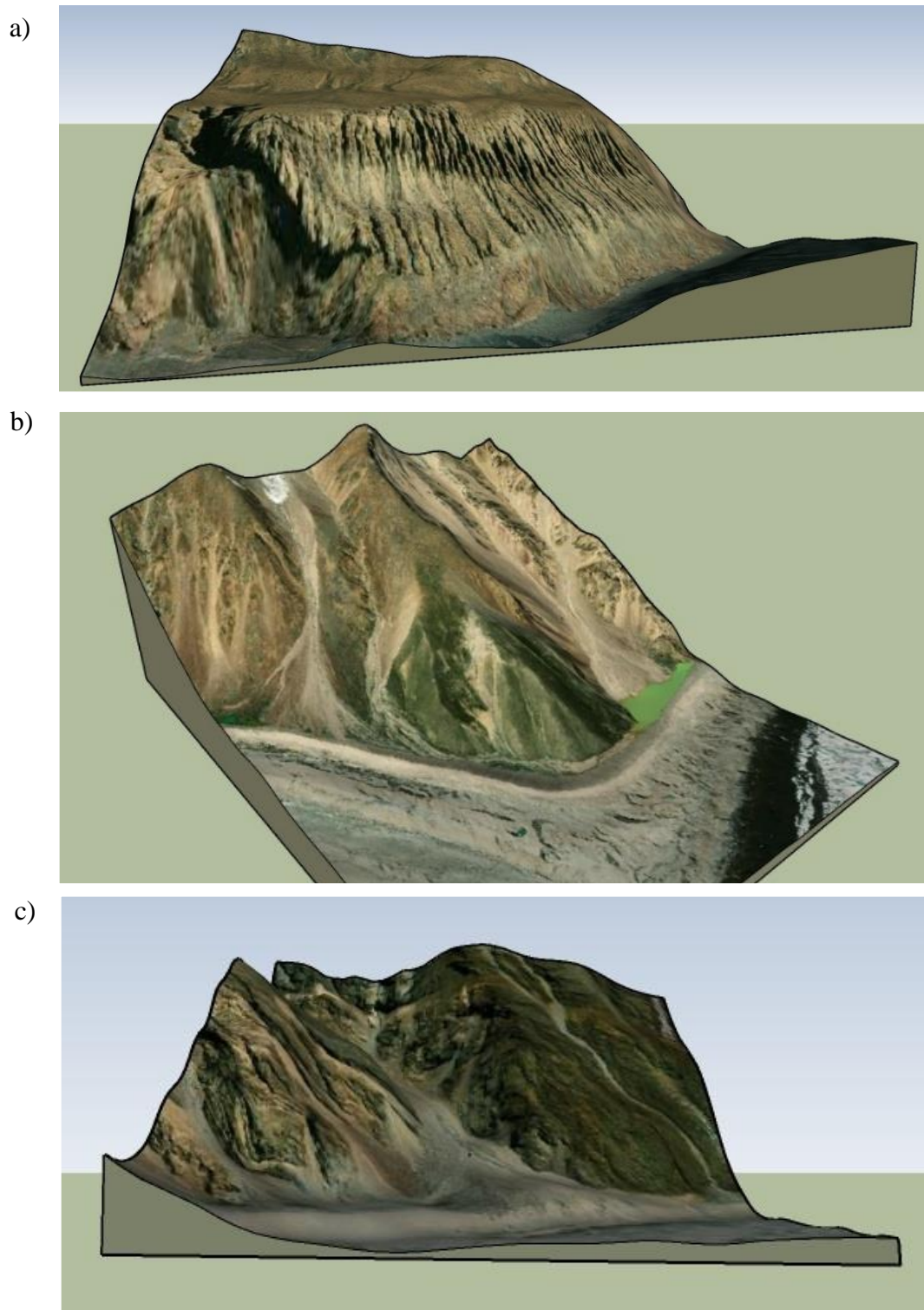


Figure A.19b: Study Site ID 041 (Afghanistan) Terrain Models.

a),b) and c) are 2D graphics of 3D terrain models, (a) is the gullied lateral moraine, (b) is a debris fans buttressed by the lateral moraine with a collection of water in one section of the lateral morainic trough and c) is a section of the lateral moraine where the lateral morainic trough has been completely infilled and the debris fan has breached the crest of the lateral moraine.

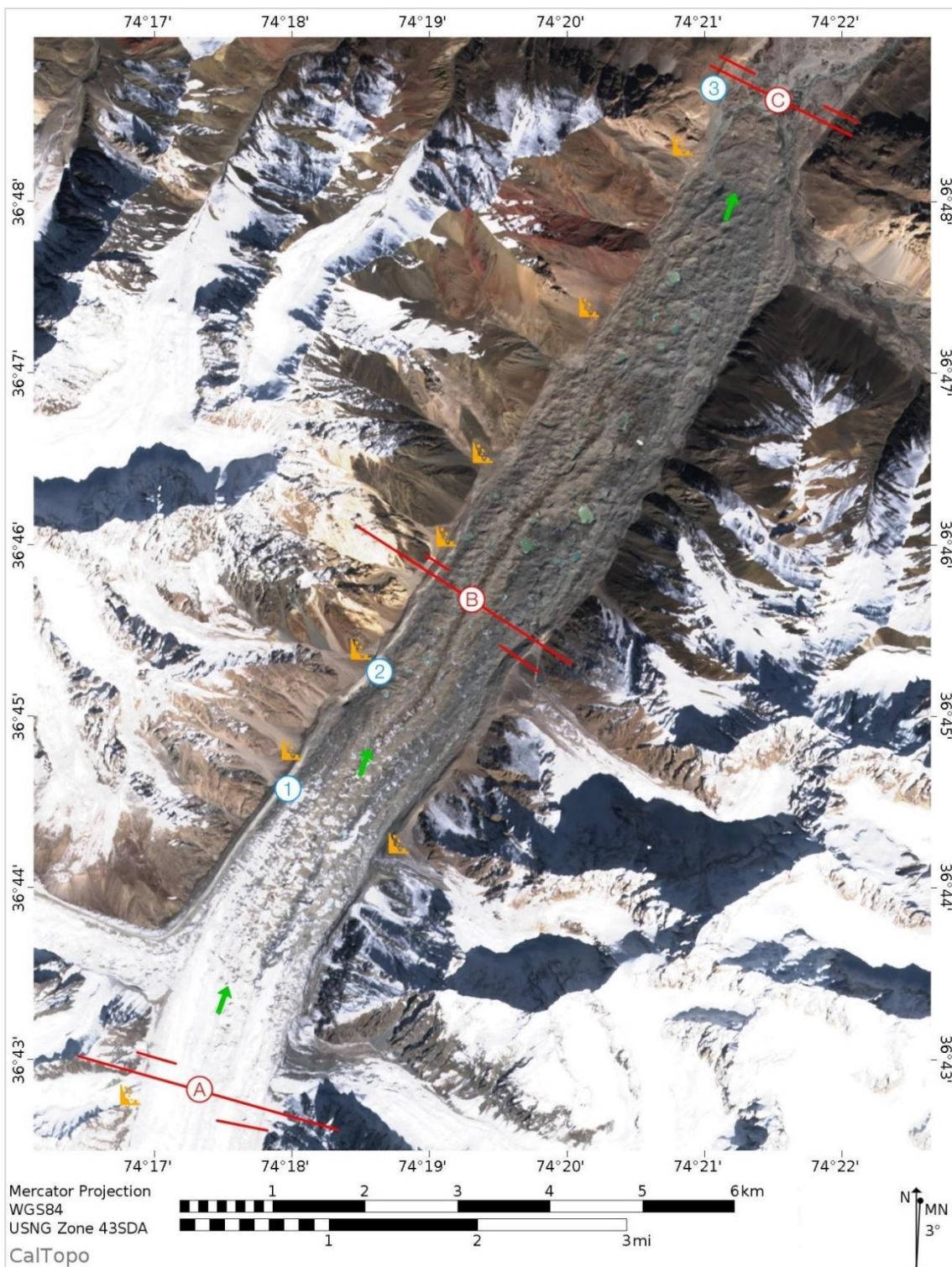


Figure A.20a: Study Site ID 046 (Shkuk Yoz Glacier) Mercator Map.

The green arrow indicates the direction of the glacier flow path. The blue numbers identify the location of gullies. The orange icon identifies the location of debris fans. The red lines identify the locations where transit sections were taken; up-valley is identified by the red letter A, mid-glacier is defined by the red letter B and down glacier is defined by the red letter C.

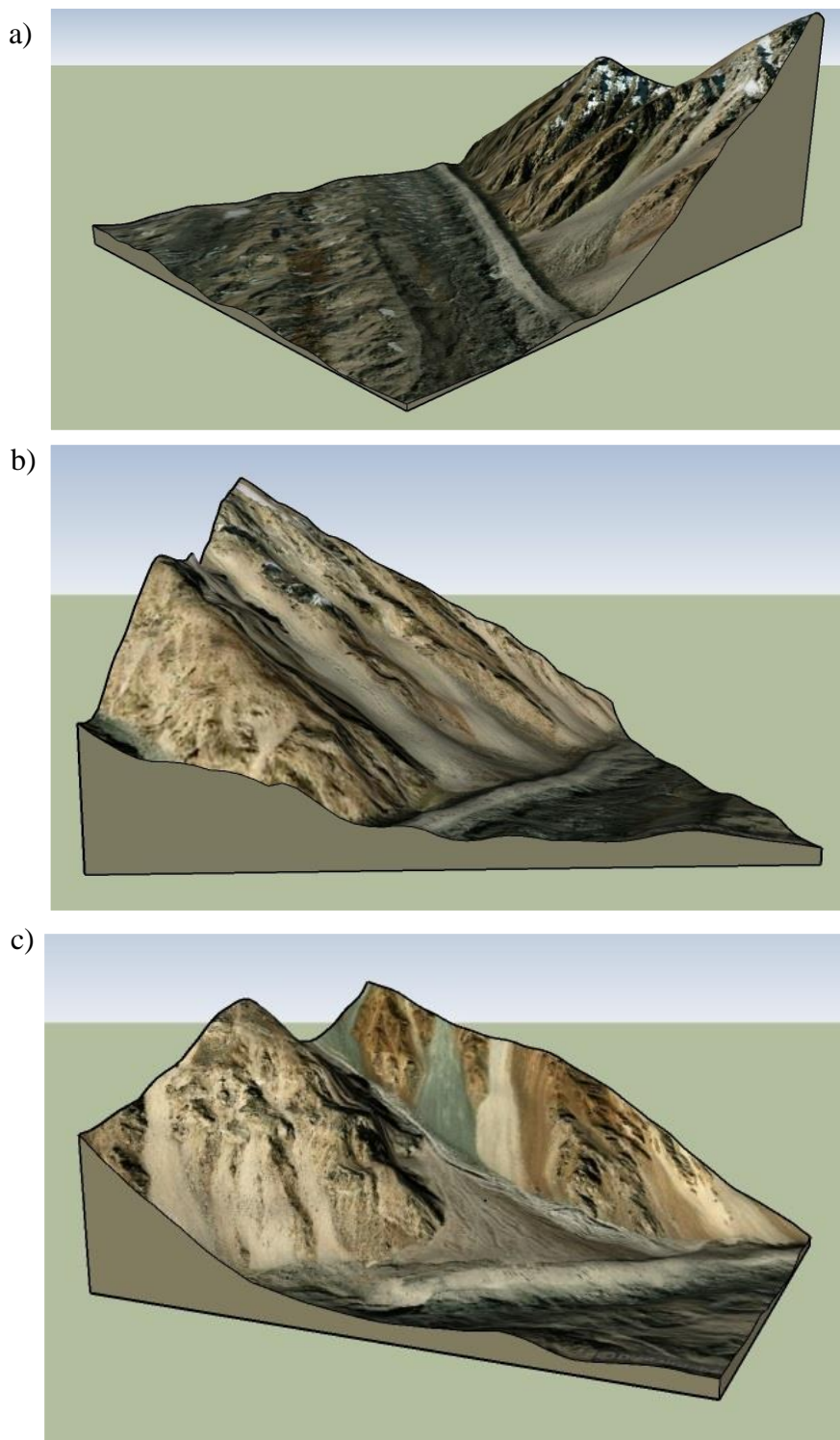


Figure A.20b: Study Site ID 046 (Shkuk Yoz Glacier) Terrain Models.

a), b) and c) are 2D graphics of 3D terrain models, along the west up-glacier lateral moraine, (a) is a section of the relatively unworked lateral moraine, (b) is a section of the are debris fans buttressed by the lateral moraine and (c) is an example of a more advance stage of the progression of infilling of the lateral morainic trough where the debris fan buttressed by the lateral moraine.

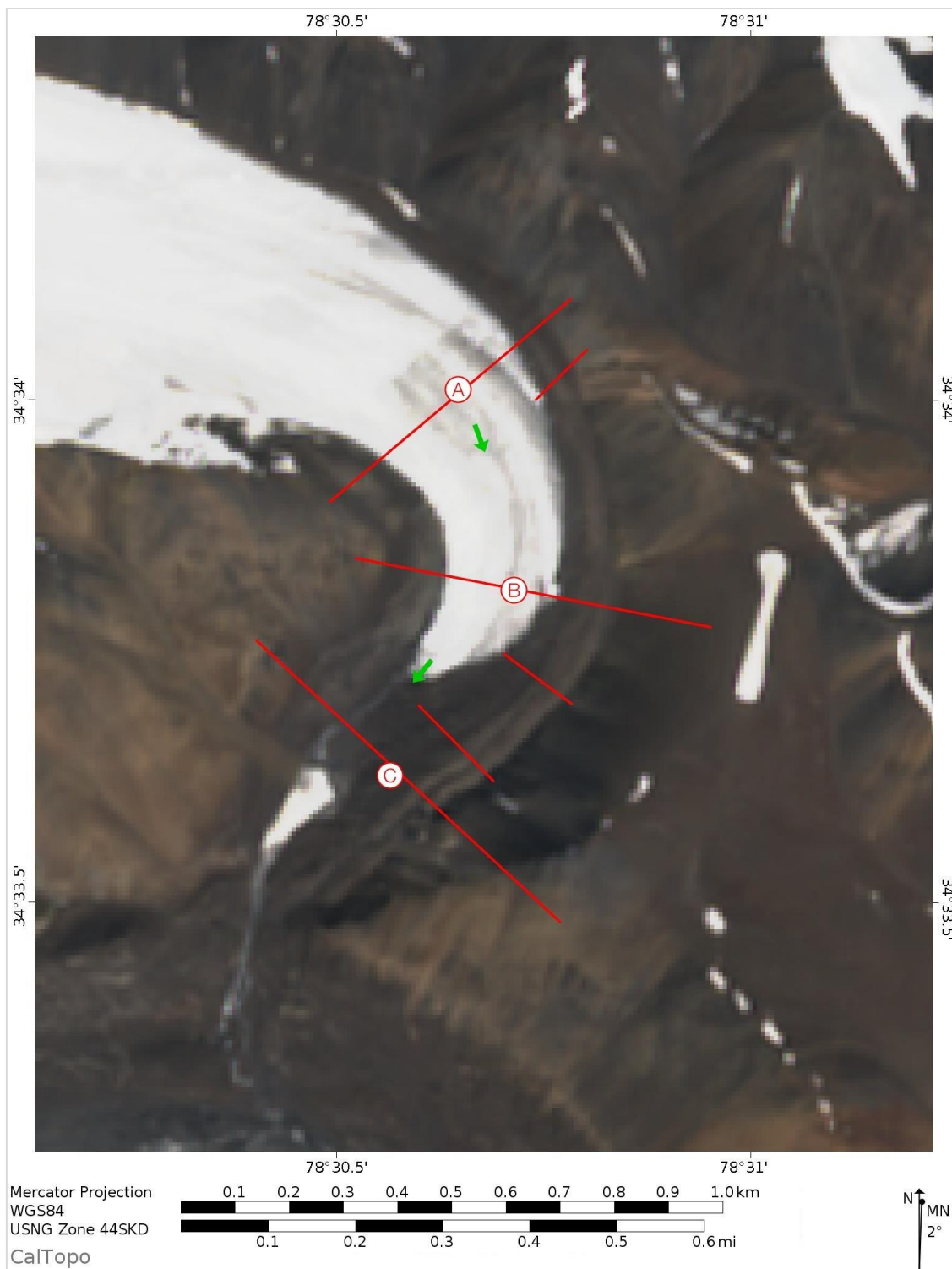


Figure A.21a: Study Site ID 036 (Karakoram Range) Mercator Map.

The green arrow indicates the direction of the glacier flow path. The blue numbers identify the location of gullies. The orange icon identifies the location of debris fans. The red lines identify the locations where transit sections were taken; up-valley is identified by red letter A, mid-glacier is defined by the red letter B and down glacier is defined by the red letter C.

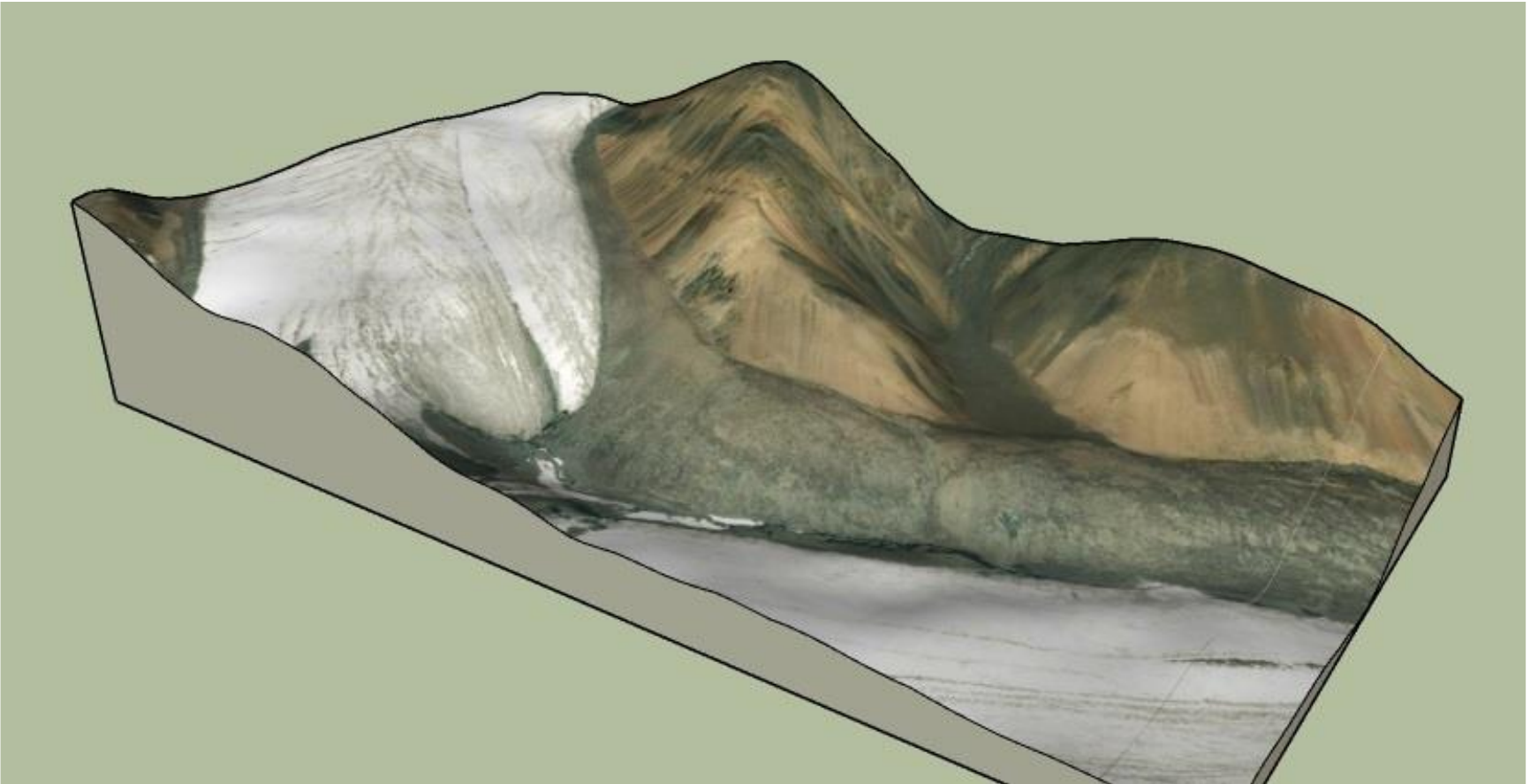


Figure A.21b: Study Site ID 036 (Karakoram Range) Terrain Model.

A 2D graphic of the 3D terrain model showing the intersection of the tributary lateral moraine terminus and the trunk lateral moraine.

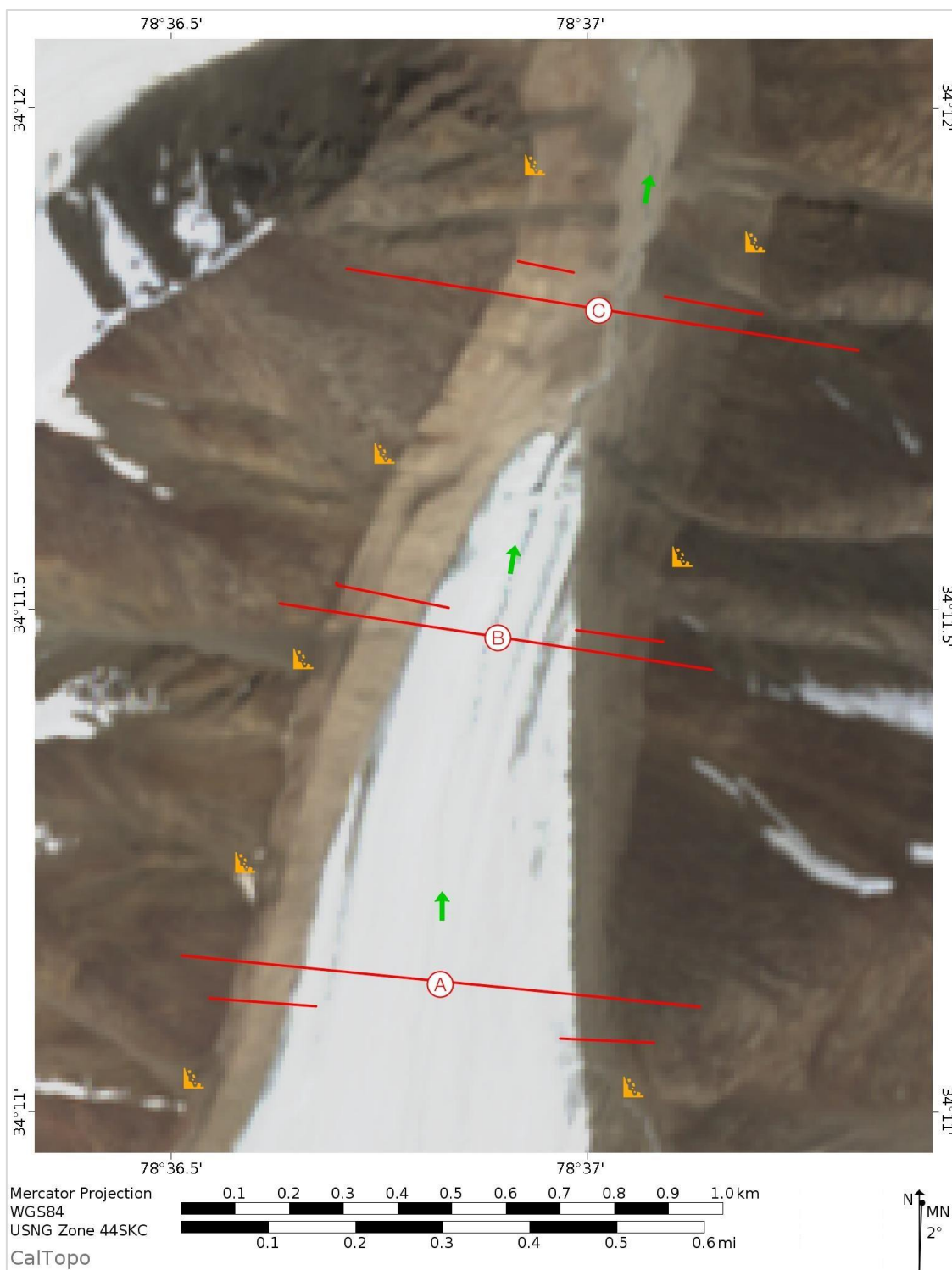


Figure A.22a: Study Site ID 040 (Karakoram Range - 2) Mercator Map.

The green arrow indicates the direction of the glacier flow path. The blue numbers identify the location of gullies. The orange icon identifies the location of debris fans. The red lines identify the locations where transit sections were taken; up-valley is identified by red letter A, mid-glacier is defined by the red letter B and down glacier is defined by the red letter C.

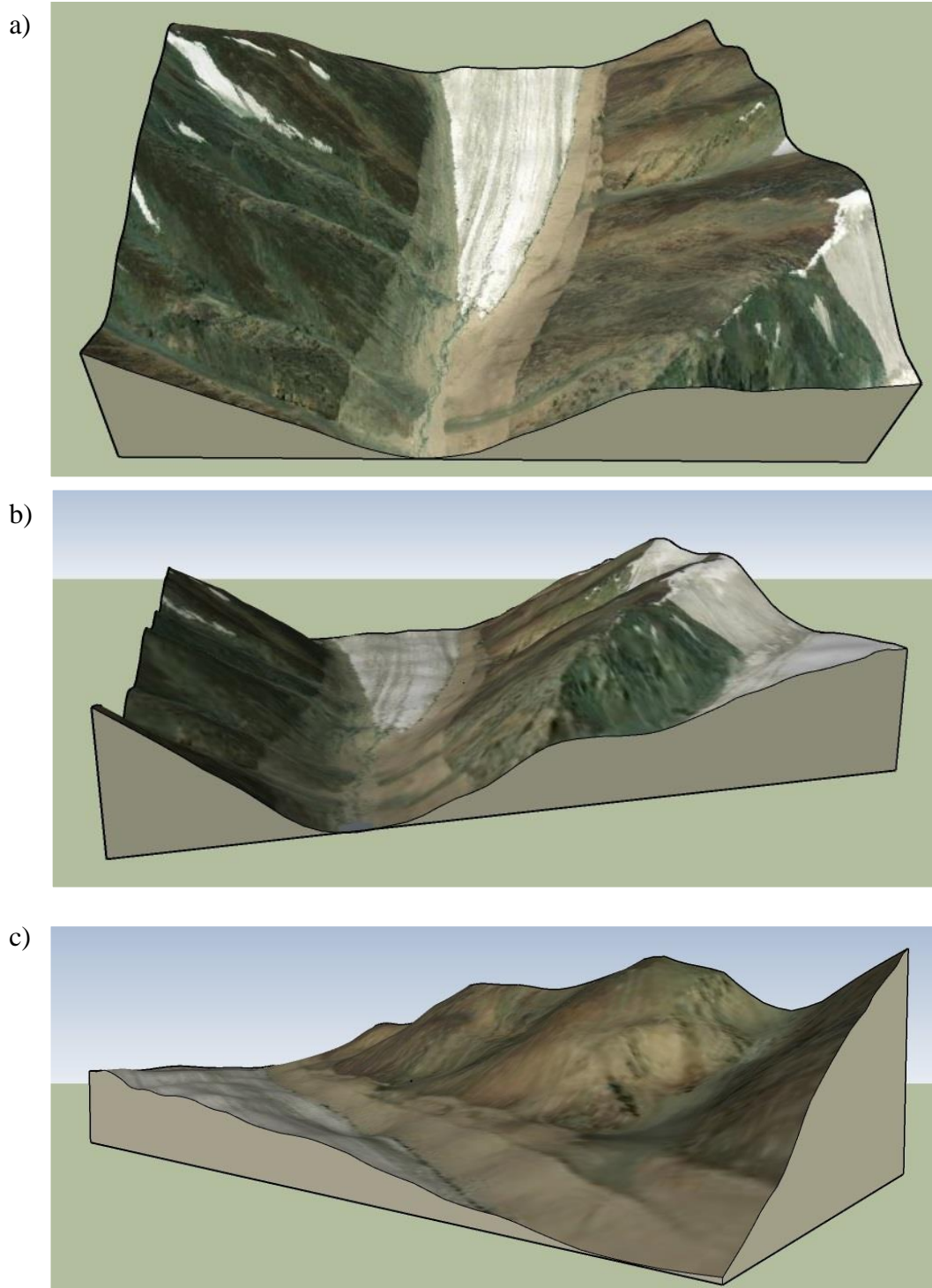


Figure A.22b: Study Site ID 040 (Karakoram Range -2) Terrain Models.

a), b) and c) are 2D graphics of 3D terrain models of the deglaciating valley, (a) is looking down on the valley from the down glacier position, (b) is looking up-glacier from the down glacier position and (c) is focused on the west lateral moraine and the debris fans buttressed by the lateral moraine.

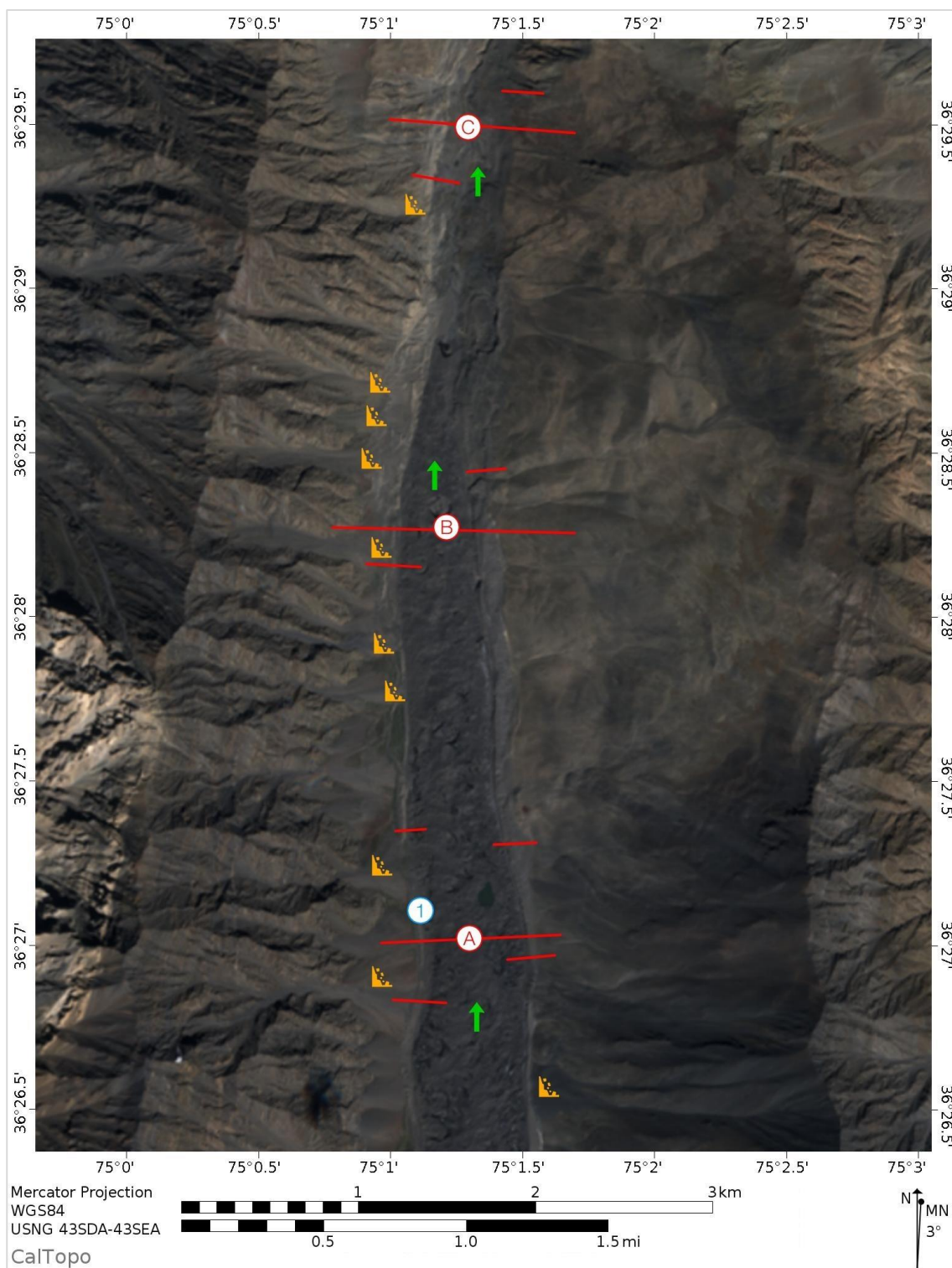


Figure A.23a: Study Site ID 045 (Lupghar Yaz Glacier) Mercator Map. The green arrow indicates the direction of the glacier flow path. The blue numbers identify the location of gullies. The orange icon identifies the location of debris fans. The red lines identify the locations where transit sections were taken; up-valley is identified by red letter A, mid-glacier is defined by the red letter B and down glacier is defined by the red letter C.

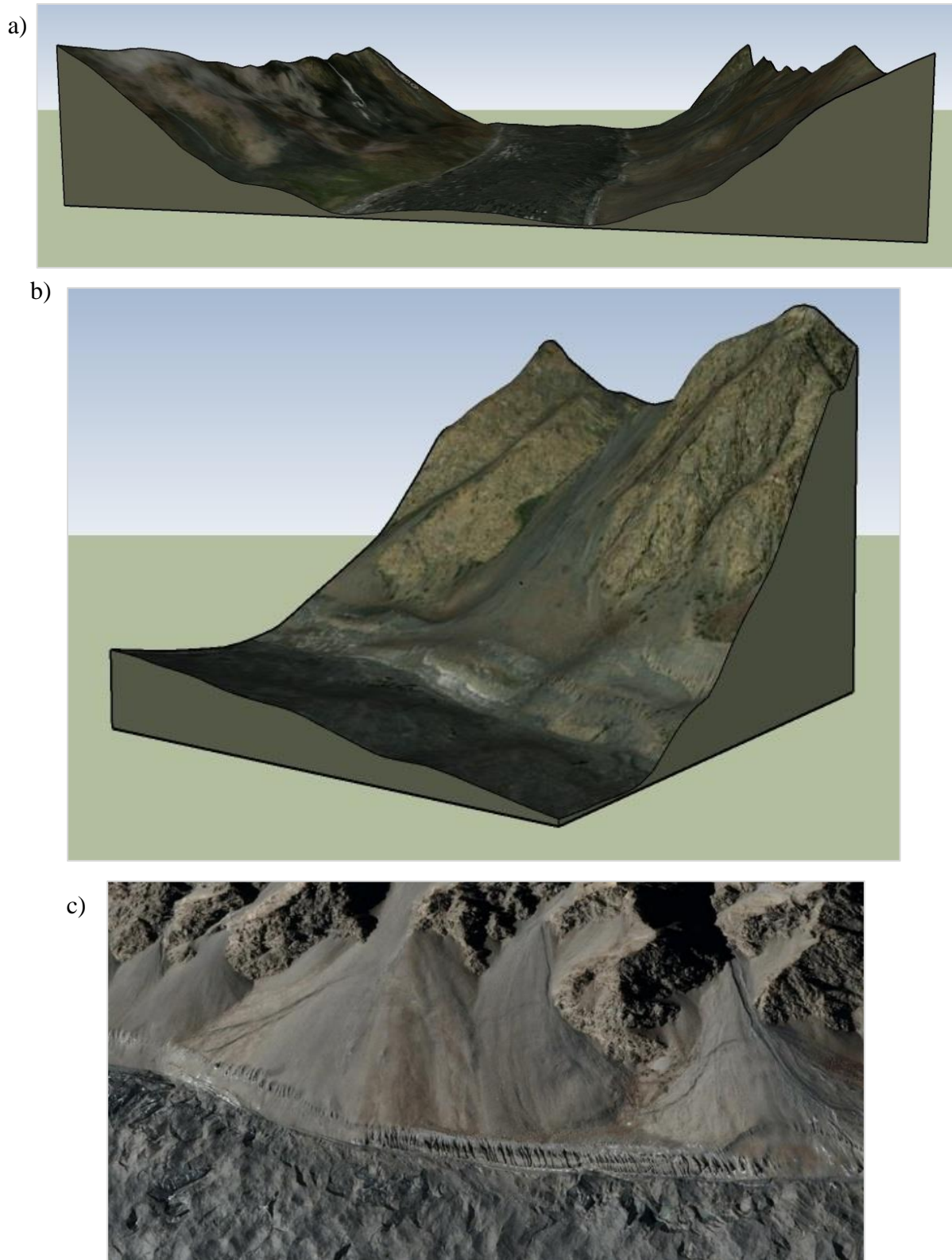


Figure A.23b: Study Site ID 045 (Lupghar Yaz Glacier) Terrain Models and Photo.
a) and b) are 2D graphics of 3D terrain models of up-glacier and down glacier valley respectively and c) is a photos capture in Google Earth of the debris fans in the down glacier section.

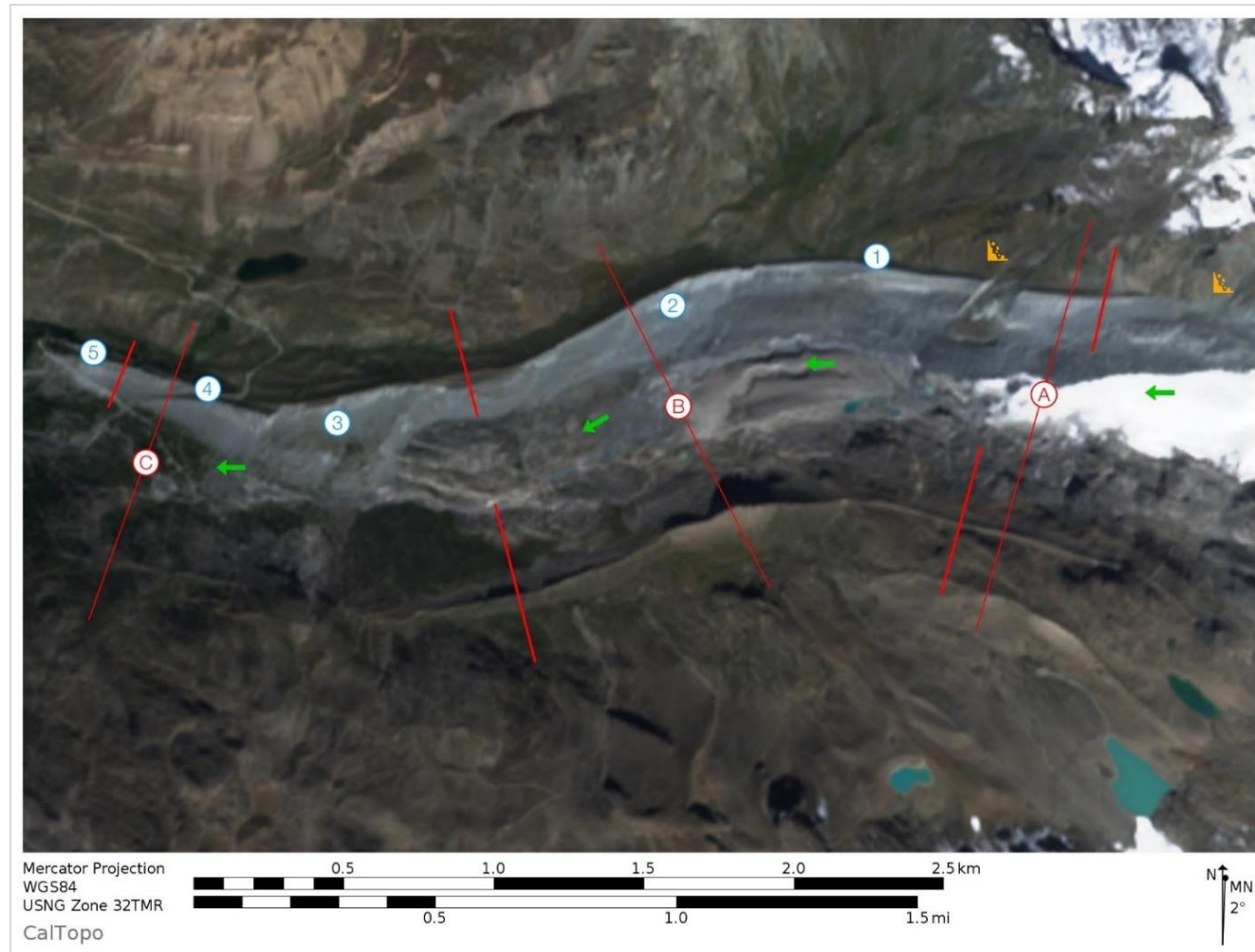


Figure A.24a: Study Site ID 054 (Findelengletscher Glacier) Mercator Map. The green arrow indicates the direction of the glacier flow path. The blue numbers identify the location of gullies. The orange icon identifies the location of debris fans. The red lines identify the locations where transit sections were taken; up-valley is identified by red letter A, mid-glacier is defined by the red letter B and down glacier is defined by the red letter C.

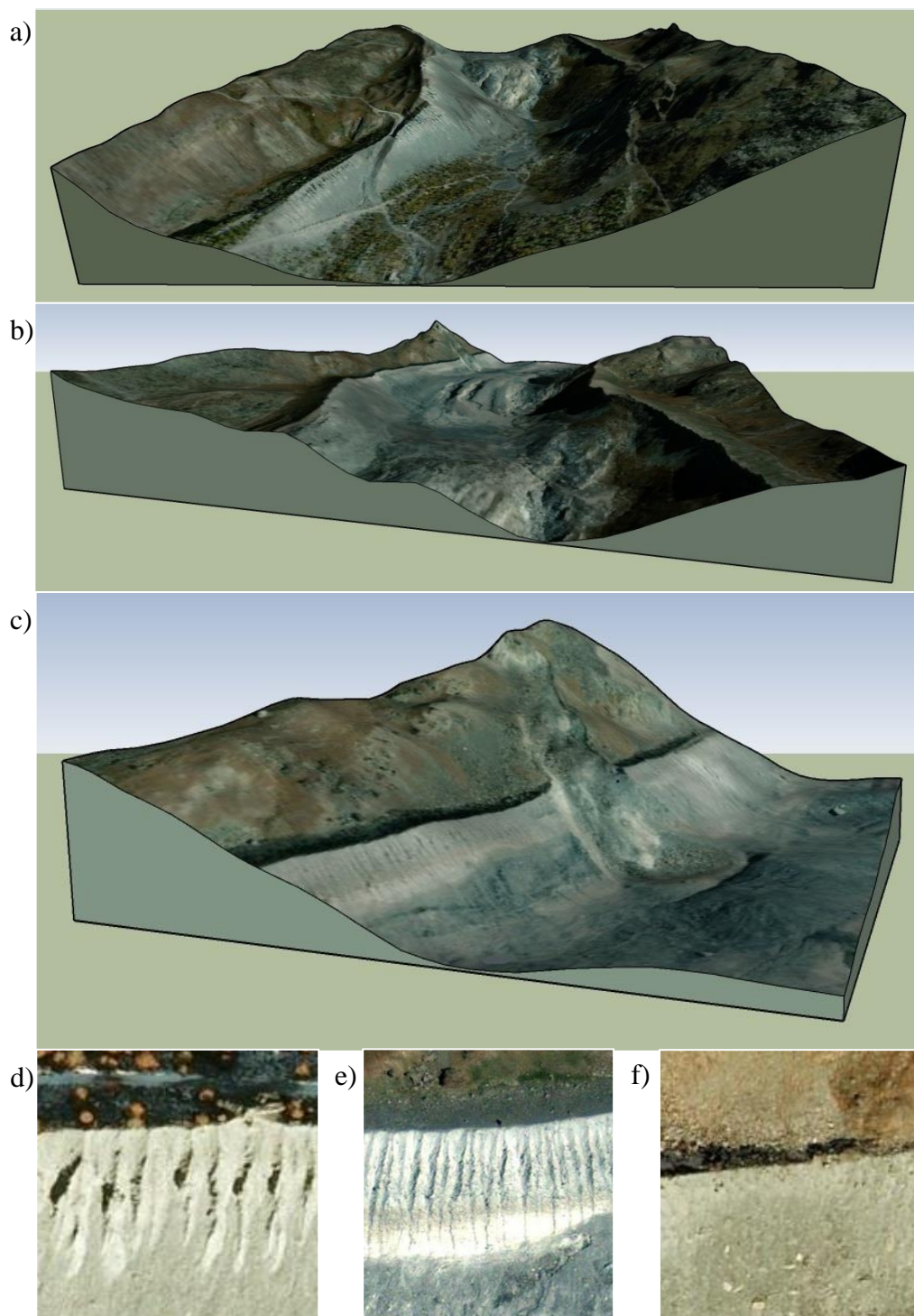


Figure A.24b: Study Site ID 054 (Findelengletscher Glacier) Terrain Models and Photos. a), b) and c) are 2D graphics of 3D terrain models, (a) is a view down glacier looking up-glacier and (b) is the continuation of (a), (c) is a debris fan buttressed by the lateral moraine, in the up-glacier, d), e) and f) are photos capture in Google Earth, of the gullied lateral moraine (d) is in the extreme down glacier position, (e) is in the mid-glacier position and (f) is in the extreme up-glacier section where no gullies are present. Photos Retrieved November 23, 2019 from <https://goo.gl/maps/LocBn7NNAg6wMfp4A>.

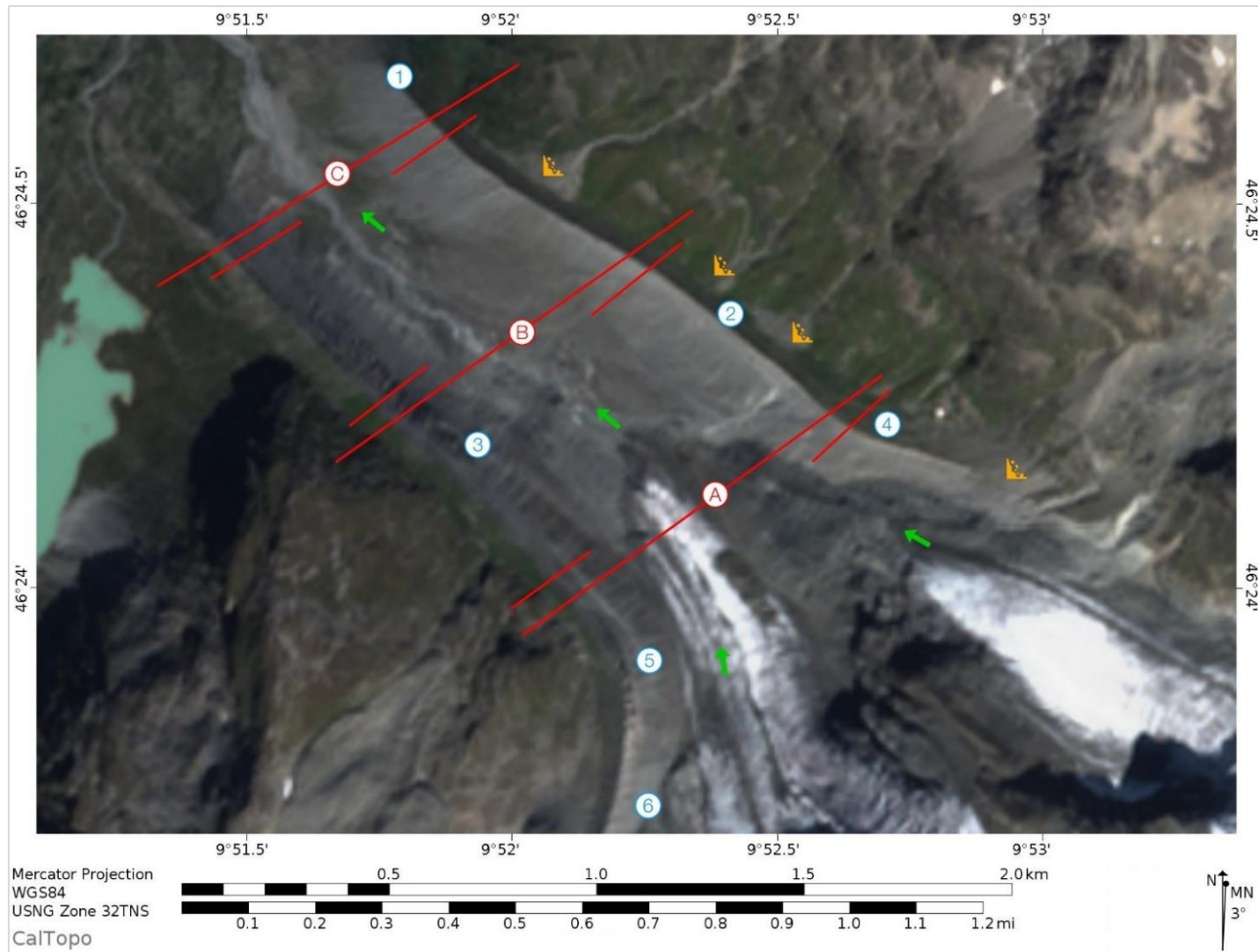


Figure A.25a: Study Site ID 057 (Vadret da Tschierva, Grisons) Mercator Map.

The green arrow indicates the direction of the glacier flow path. The blue numbers identify the location of gullies. The orange icon identifies the location of debris fans. The red lines identify the locations where transit sections were taken; up-valley is identified by red letter A, mid-glacier is defined by the red letter B and down glacier is defined by the red letter C.

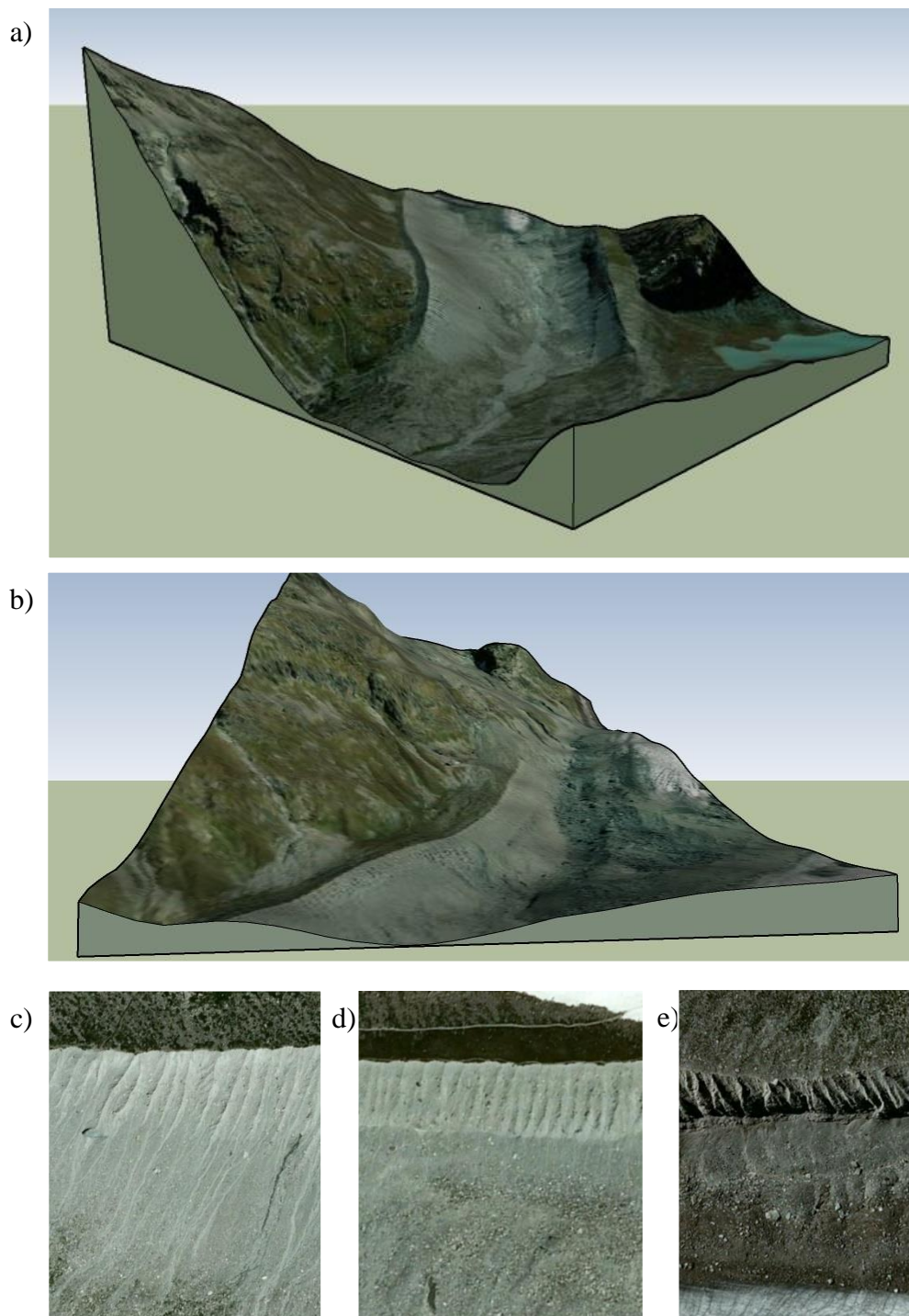


Figure A.25b: Study Site ID 057 (Vadret da Tschierva, Grisons) Terrain Models and Photos. a) and b) are 2D graphics of 3D terrain models, (a) is a view from down glacier looking up-glacier and (b) is view from down glacier looking up-glacier in way of the east lateral moraine where debris fans buttress by the lateral moraine, in the up-glacier section the lateral morainic trough has been infilled by the debris fan, (c), d) and e) are photos capture in Google Earth, of the gullied lateral moraine, (c) is in the extreme down glacier position, (d) is in the mid-glacier position and (e) is in the extreme up-glacier position. Photos Retrieved November 23, 2019 from <https://goo.gl/maps/FJvM9ahaczUezPHS6>.

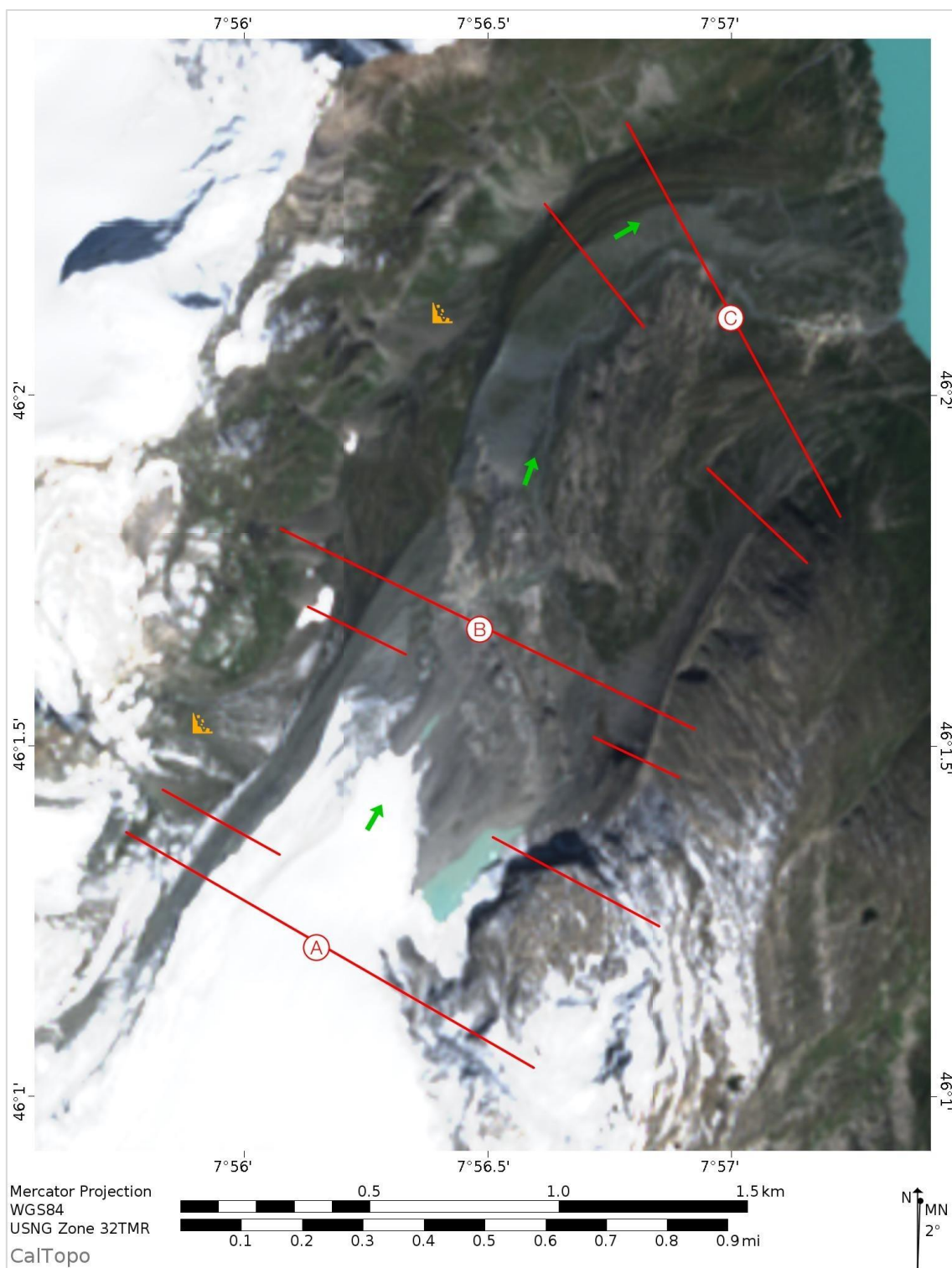


Figure A.26a: Study Site ID 052 (Fee Glacier) Mercator Map.

The green arrow indicates the direction of the glacier flow path. The blue numbers identify the location of gullies. The orange icon identifies the location of debris fans. The red lines identify the locations where transit sections were taken; up-valley is identified by the red letter A, mid-glacier is defined by the red letter B and down glacier is defined by the red letter C.

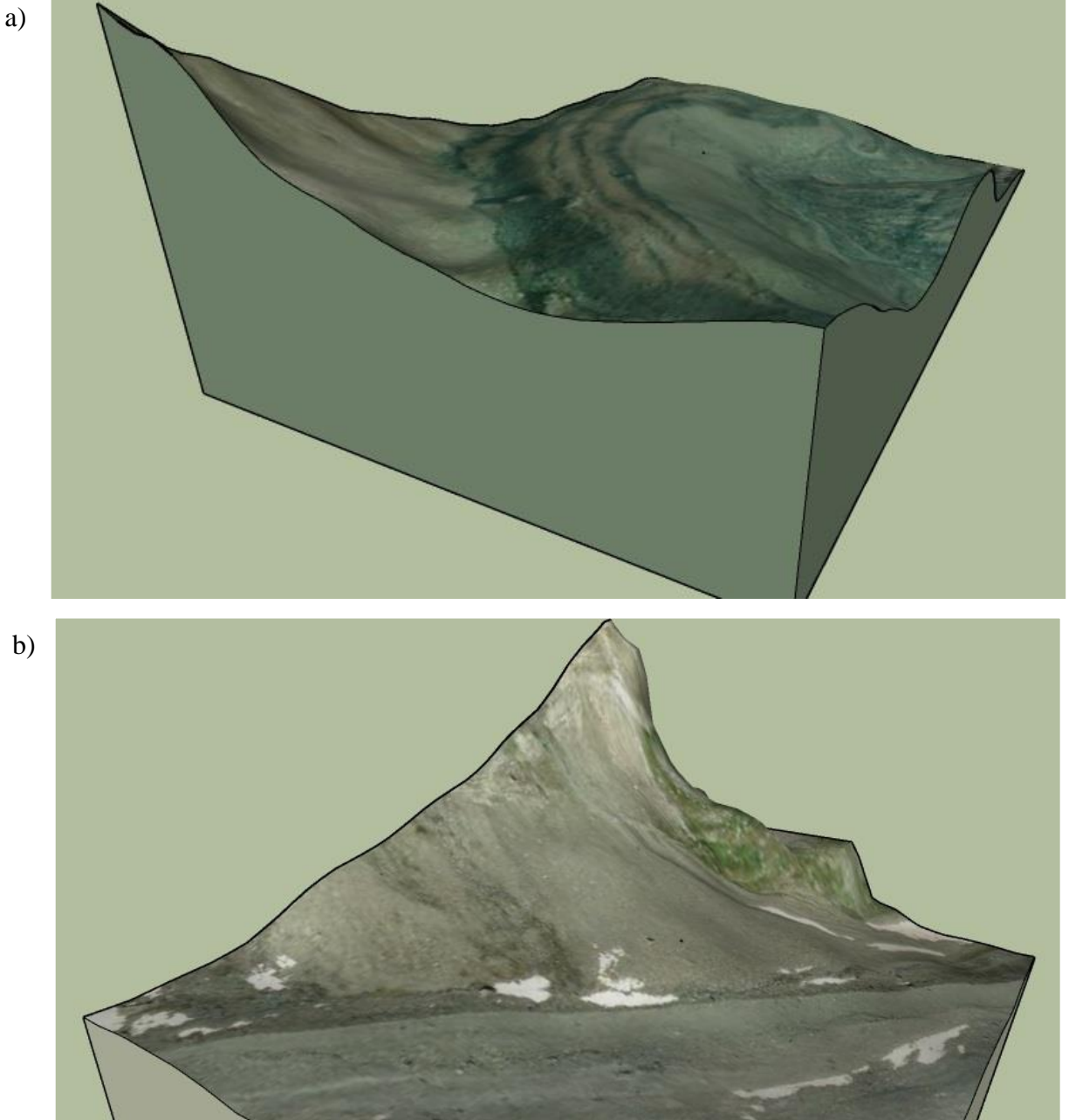


Figure A.26b: Study Site ID 052 (Fee Glacier) Terrain Models.

a) and b) are 2D graphics of 3D terrain models, (a) is a section showing, incremental plastering of till, in the down glacier section and (b) is an example of a debris fan buttressed by the lateral moraine in the up-glacier section.

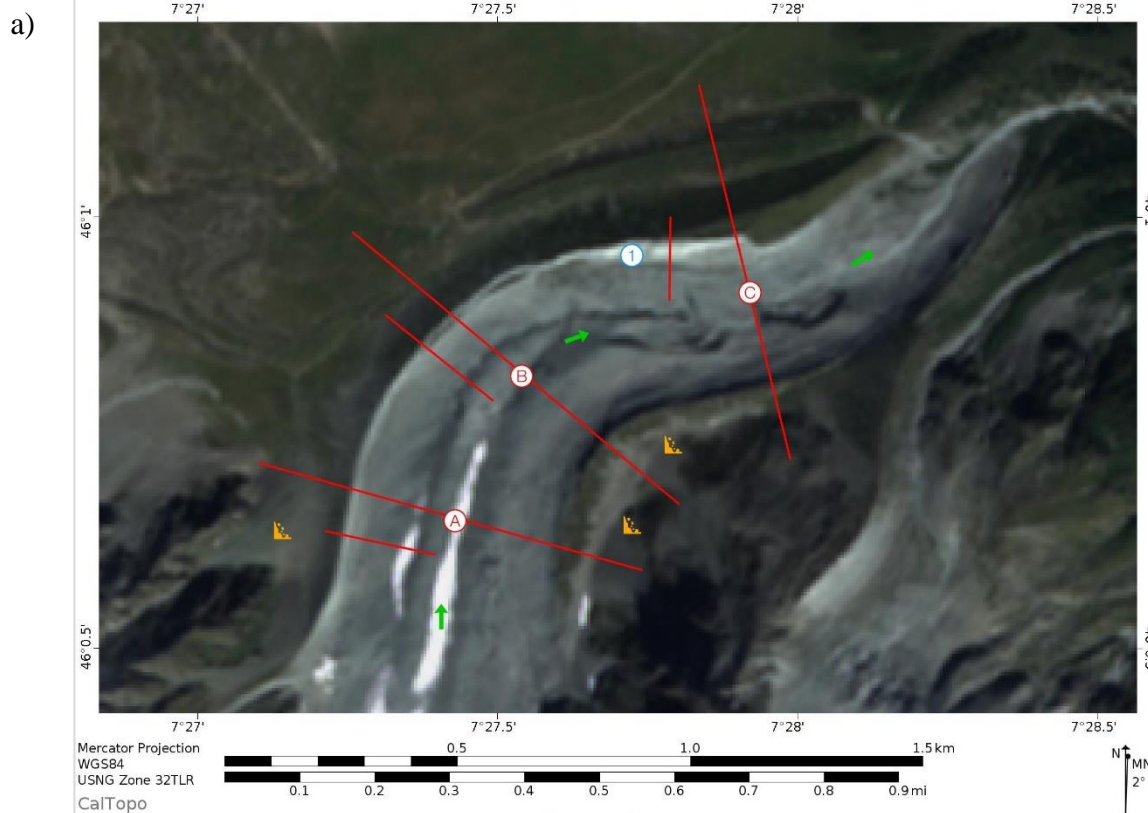


Figure A.27a: Study Site ID 053 (Tsidjiore Nouve). Mercator Map and Photo.

a) A Mercator Map of the Study Site. The green arrow indicates the direction of the glacier flow path. The blue numbers identify the location of gullies. The orange icon identifies the location of debris fans. The red lines identify the locations where transit sections were taken; up-valley is identified by the red letter A, mid-glacier is defined by the red letter B and down glacier is defined by the red letter C, and b) is a photo, retrieved from Google Earth, capturing the lateral moraine gullies in the down glacier position. Photo Retrieved November 23, 2019 from <https://goo.gl/maps/1PZ4UmHwV4qr9Eo88>.

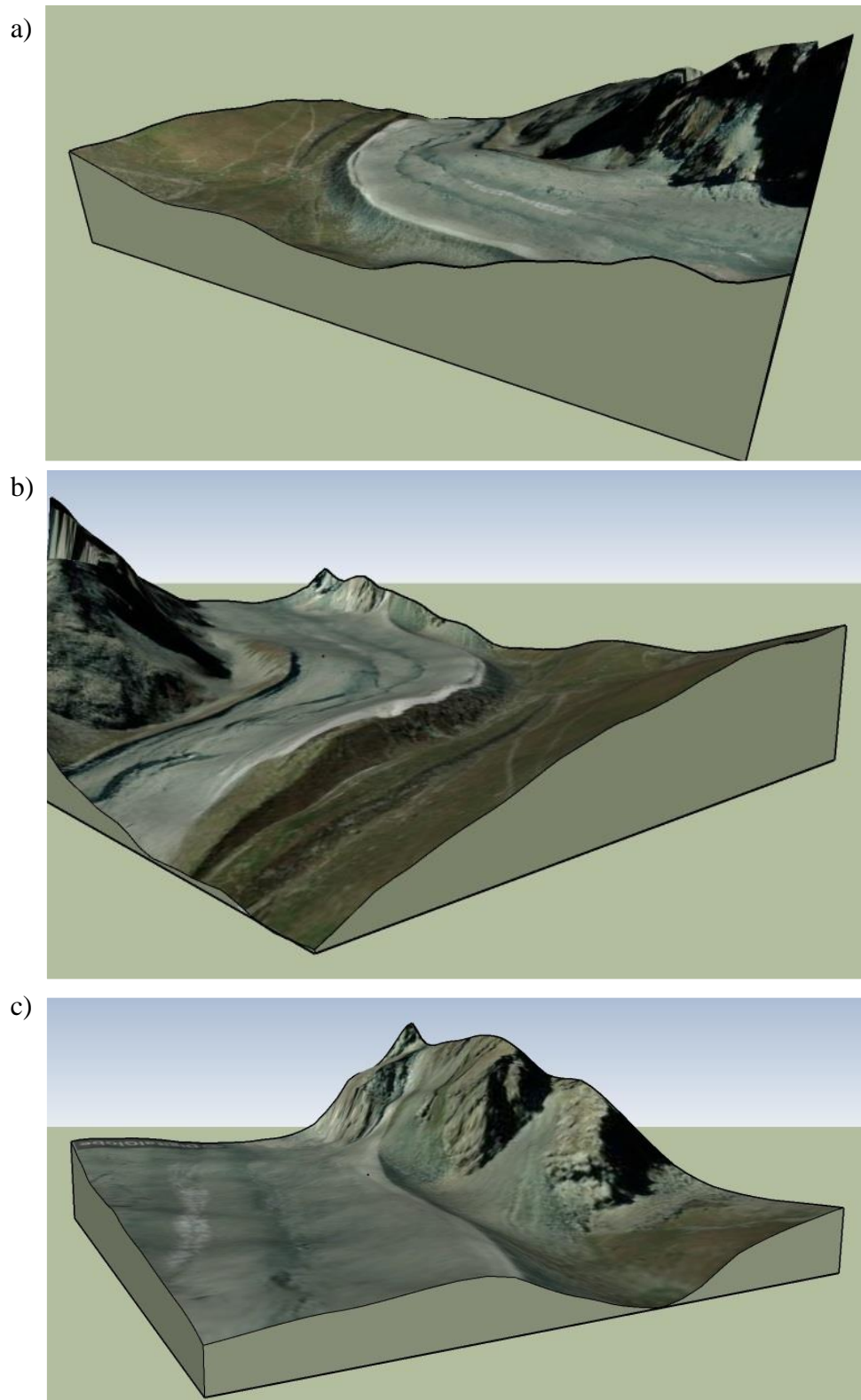


Figure A.27b: Study Site ID 053 (Tsidjiore Nouvelle) Terrain Models.

a), b) and c) are 2D graphics of 3D terrain models, (a) is a view down glacier, (b) is a view looking up-glacier and (c) is an example of a debris fans buttressed by the lateral moraine, in the up-glacier section.

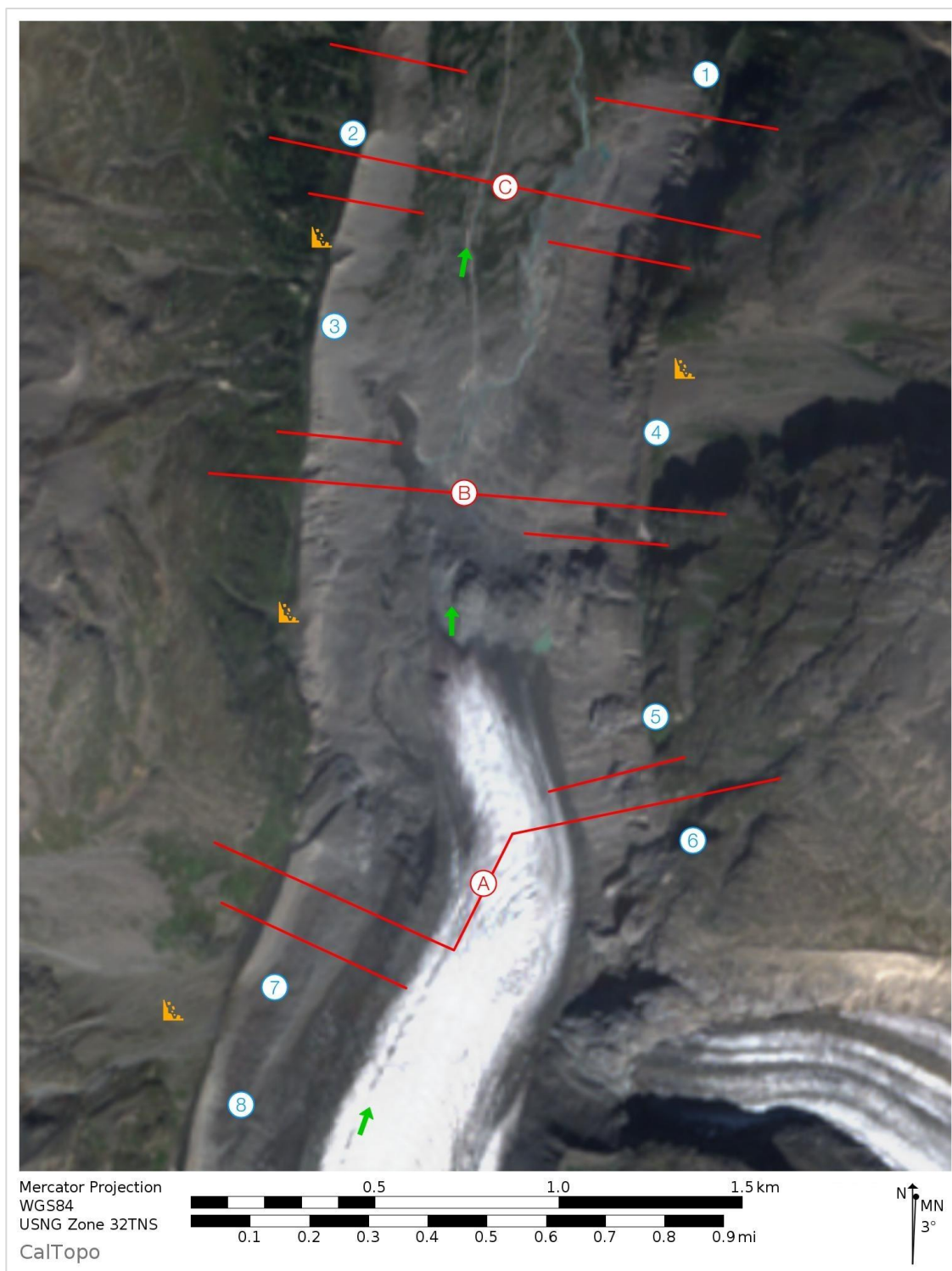


Figure A.28a: Study Site ID 058 (Vadret Pers dams) Mercator Map.

The green arrow indicates the direction of the glacier flow path. The blue numbers identify the location of gullies. The orange icon identifies the location of debris fans. The red lines identify the locations where transit sections were taken; up-valley is identified by red letter A, mid-glacier is defined by the red letter B and down glacier is defined by the red letter C.

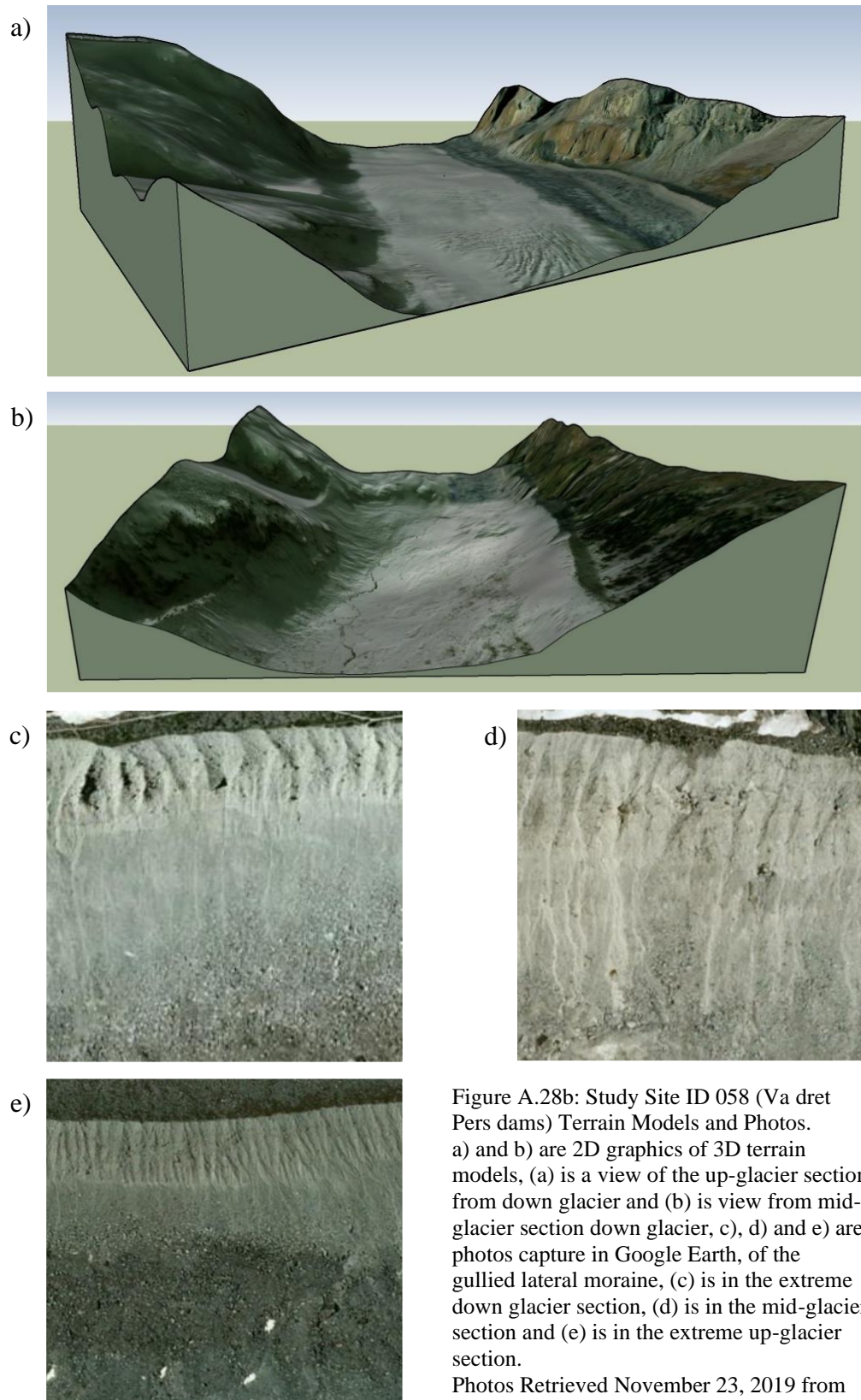


Figure A.28b: Study Site ID 058 (Va dret Pers dams) Terrain Models and Photos. a) and b) are 2D graphics of 3D terrain models, (a) is a view of the up-glacier section from down glacier and (b) is view from mid-glacier section down glacier, c), d) and e) are photos capture in Google Earth, of the gullied lateral moraine, (c) is in the extreme down glacier section, (d) is in the mid-glacier section and (e) is in the extreme up-glacier section.

Photos Retrieved November 23, 2019 from <https://goo.gl/maps/2Pc7VbmHdp1wucgz7>.

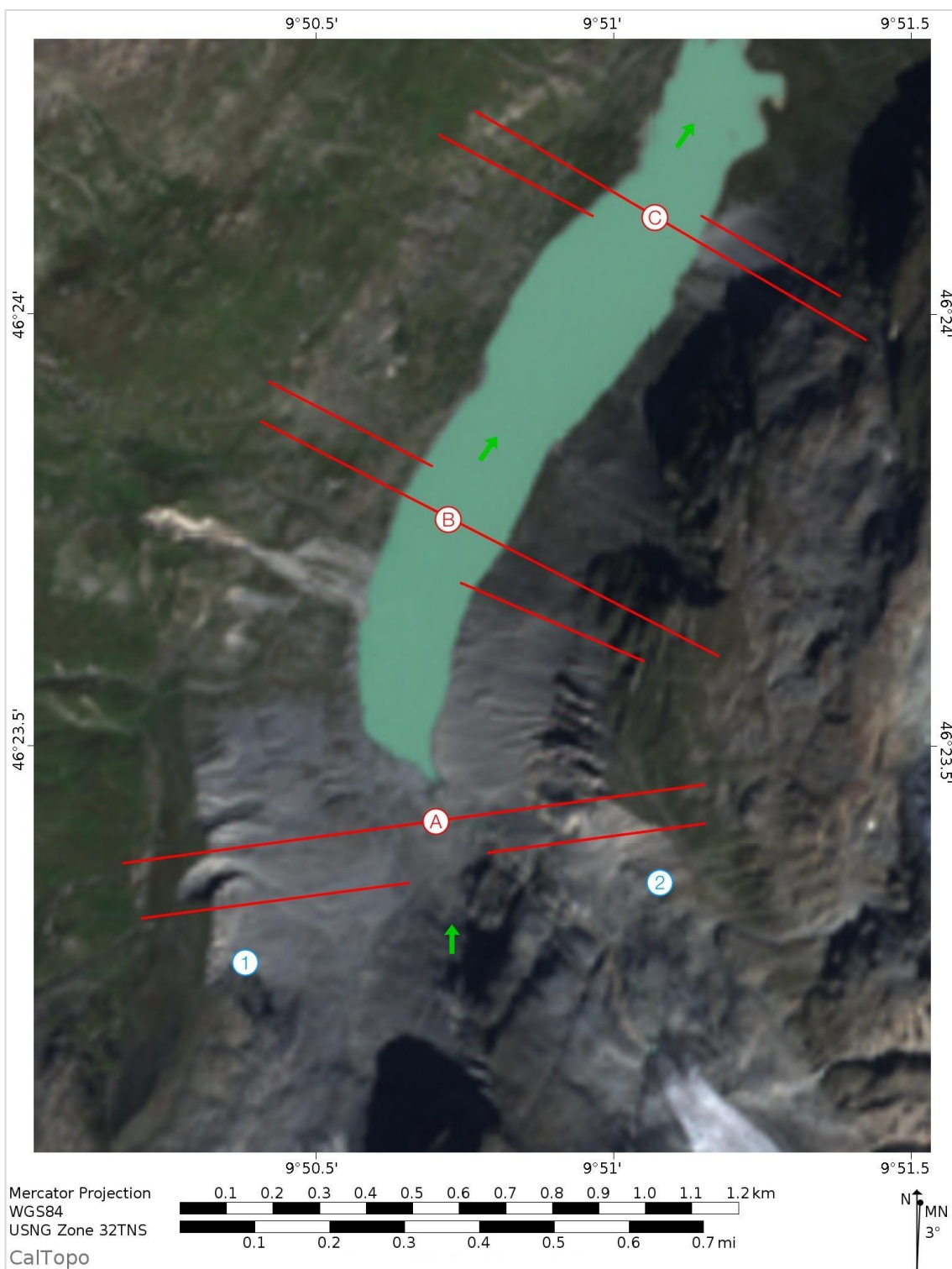


Figure A.29a: Study Site ID 059 (Vadret da Tschierva, Grisons) Mercator Map.

The green arrow indicates the direction of the glacier flow path. The blue numbers identify the location of gullies. The orange icon identifies the location of debris fans. The red lines identify the locations where transit sections were taken; up-valley is identified by the red letter A, mid-glacier is defined by the red letter B and down glacier is defined by the red letter C.

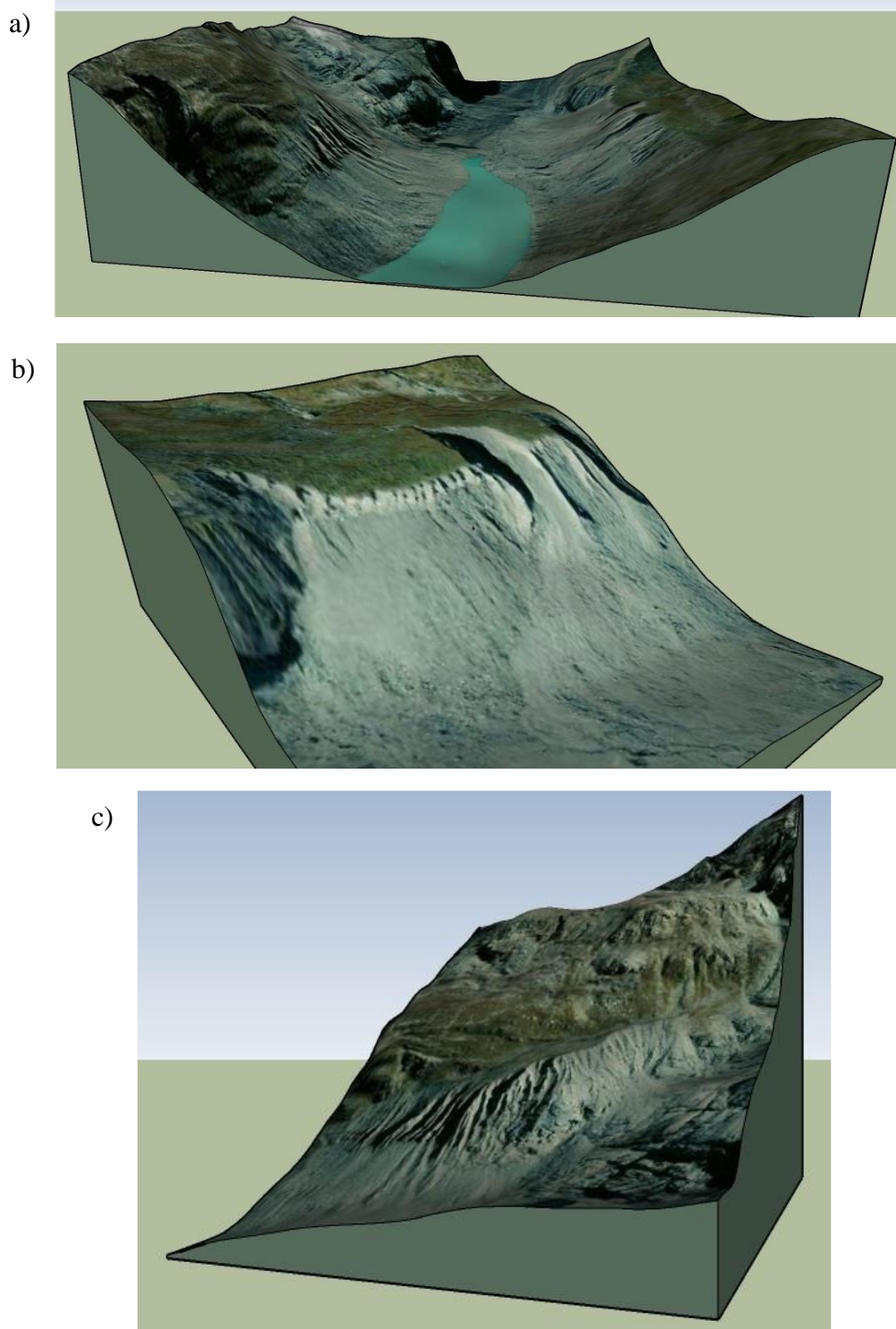


Figure A.29b: Study Site ID 059 (Vadret da Tschierva, Grisons) Terrain Models. a), b) and c) are 2D graphics of 3D terrain models, (a) is a view of the up-glacier section from down glacier and (b) is a view of the gullying on the west lateral moraine, up-glacier and (c) is a view of the gullying on the east lateral moraine, up-glacier.